THE ROLE OF MICRORNA AND SERINE PALMITOYLTRANSFERASE IN ALZHEIMER'S DISEASE

By

Hirosha Geekiyanage

A DISSERTATION

Submitted to
Michigan State University
In partial fulfillment of the requirements
For the degree of

DOCTOR OF PHILOSOPHY

Genetics

2012

ABSTACT

THE ROLE OF MICRORNA AND SERINE PALMITOYLTRANSFERASE IN ALZHEIMER'S DISEASE

By

Hirosha Geekiyanage

The mechanism by which early-on-set Alzheimer's disease (AD) manifests is well understood. However, little is known about the molecular mechanisms contributing to late-on-set AD, which accounts for >95% of AD cases. Research thus far invariably suggests that elevated ceramide, a sphingolipid, may be a risk factor for AD. Serine palmitoyltransferase (SPT) is not only the first rate limiting enzyme in the *de novo* synthesis of ceramide but varying SPT levels are consistently associated with varying ceramide levels. I observed that increased ceramide levels in AD are directly regulated by increased SPT levels. I also observed that SPT directly regulates amyloid beta (Aβ) levels through the post-transcriptional regulation of miR-137,-181c,-9 and -29a/b, suggesting SPT and the respective miRNAs are potential therapeutic targets for AD. Therefore, I investigated the use of SPT inhibition as a potential therapeutic strategy for AD. I administered a SPT inhibitor subcutaneously through surgically implanted osmotic pumps into an AD mouse model. I observed that the inhibition of SPT and thus ceramide, reduced cortical Aβ and hyperphosphorylated tau levels, major hallmarks of AD, with statistically significant correlations between SPT, ceramide and Aβ levels. With nominal toxic side effects observed, inhibition of SPT is suggested as a potentially safe therapeutic strategy to ameliorate the AD pathology. In addition, I have identified that the afore mentioned miRNAs are reduced in the blood sera of probable AD and amnestic mild cognitive impaired patients, suggesting a potential use for these circulating miRNAs as non-invasive diagnostic biomarkers.

In the AD mouse model studied, I observed that these miRNAs show positive correlations between their expressions in the brain cortices and presence in the sera, further suggesting a potential diagnostic role for these circulating miRNAs. A positive correlation was also observed between cortical and sera Aβ levels, providing further insights into the search of blood biomarkers.

In dedication of my family, Wijaya Geekiyanage, Chandani Geekiyanage and Oshan Geekiyanage

ACKNOWLEDGEMENT

I would like to thank my dissertation committee members Christina Chan, PhD (mentor); Karen Friderici, PhD; John Goudreau, DO, PhD, FACN; Debra Schutte, PhD and Hongbing Wang, PhD for their support throughout my PhD career.

I thank Peter Nelson, MD, PhD and the University of Kentucky, Alzheimer's Disease Center tissue bank -ADC NIA P30-AG0-28383 for providing the human autopsy brain samples and blood sera samples necessary for this study. I thank Daniel Jones, PhD and Lijun Chen from the MSU mass spectrometry facility for their support. I thank Amy S. Porter, HT (ASCP) QIHC and Kathleen A. Joseph, HT (ASCP) QIHC from the MSU Investigative Histopathology Laboratories for their assistance and support. I thank Melinda K. Frame, PhD from the MSU Center for Advanced Microscopy for her assistance and support. I thank Sue Sipkov from the MSU center for animal functional genomics core facility for her support. I would like to thank all the staff members of university laboratory animal resources (ULAR) and institutional animal care and use committee (IACUC). I extend a special thank to ULAR veterinary staff members Jean A. Gaymer, DVM and Danielle Ferguson, DVM for their support. I thank the undergraduate students, Aditi Upadhye, Dennis Corsi and Quoc Le for their assistance. I thank past and present Chan and Walton lab members for their support.

I would like to extend a special acknowledgement to the MSU Genetics Program, Barbara Sears, PhD (Director Genetics Program) and Jeannine Lee (Genetics Program secretary) for the support extended throughout my PhD career. I thank the Gen 800 seminar course “miRNA in development and disease” coordinated by Vilma Yuzbasiyan-Gurkan, PhD for providing an inspiration for the miRNA research conducted in this report.

I thank the funding sources the National Institute of Health (R01GM079688, R01GM089866, and R21RR024439), the National Science Foundation (CBET 0941055 and CBET-1049127), and the Michigan State University Foundation for funding my research.

Finally, I thank my father, Wijaya Geekiyanage, my mother, Chandani Geekiyanage, my brother Oshan Geekiyanage and my friends for their unconditional love and support.

TABLE OF CONTENT

LIST OF TABLES

LIST OF FIGURES

KEY TO SYMBOLS OR ABBREVIATIONS

AD	Alzheimer’s disease
Aβ	Amyloid beta
NFT	Neurofibrillary tangles
APP	Amyloid beta precursor protein
PSEN1	Presenilin 1
PSEN2	Presenilin 2
ApoE ε4	Apolipoprotein E isoform 4
GSK3β	Glycogen synthase kinase 3β
BACE1	Beta site amyloid beta precursor protein cleaving enzyme 1
PUFA	Polyunsaturated fatty acid
SPT	Serine palmitoyltransferase
SMase	Sphingomyelinase
SM	Sphingomyelin
LCS	L-cycloserine
SPTLC1	Serine palmitoyltransferase long chain 1
SPTLC2	Serine palmitoyltransferase long chain 2
SPTLC3	Serine palmitoyltransferase long chain 3
miRNA	MicroRNA
mRNA	Messenger RNA
CSF	Cerebrospinal fluid
hAPP	Human amyloid precursor protein

PrP	Prion protein
TgCRND8	Transgenic Center for Research in Neurodegenerative Disease
MMSE	Mini mental state examination
MCI	Mild cognitive impairment
NMDA	*N*-methyl-*D*-aspartate
DHA	Omega-3-fatty
PMI	Post-mortem interval
MRI	Magnetic resonance imaging
PET	Positron emission tomography
PiB	Pittsburgh compound B
PLP	Pyridoxal-5’-phosphate
T2DM	Type-2 diabetes mellitus

CHAPTER 1: INTRODUCTION

1.1 Alzheimer's disease

Alzheimer's disease (AD) is not only the principal cause of dementia in the United States but also one of the fastest growing diseases in developed countries (Huang, 2006). Currently there are over 5 million Americans diagnosed with AD and the number is estimated to double during the next 25 years (Migliore and Coppede, 2009). With a worldwide afflicted population of over 24 million, a number expected to double in the next 15 years (Ferri et al., 2005), AD is estimated to cost 20 trillion dollars to USA alone in the next 40 years (Alz.org, 2010). AD is a progressive neurodegenerative disorder characterized by amyloid beta (Aβ) plaques and neurofibrillary tangles (NFT). In an AD brain, the cortex shrivels damaging the areas of thinking, planning and memory while the hippocampus shrinks hindering formation of new memory. The amyloid cascade is responsible for triggering neuronal dysfunction and death in the brain. In the original hypothesis, it was believed that these toxic effects were imposed by the total amyloid load. With increased research, the central role of $A\beta_{42}$ oligomers in causing neurotoxicity is now evident (for review, see (Hardy, 2006)).

Early-on-set AD (< 65 years old), which accounts for less than 5% of AD cases, is an autosomal dominant disorder caused by mutations in amyloid precursor protein (*APP*), presenilin 1 (*PSEN1*) and presenilin 2 (*PSEN2*). The APP gene has been mapped to the centromeric region of chromosome 21. Over 20 pathogenic mutations responsible for early onset of AD have been identified within the APP gene (Blennow et al., 2006). The double mutations K670D/M671L, named Swedish mutation, increases cleavage by β-site APP cleaving enzyme 1 (BACE1) at the

β-secretase cleavage site and thus elevate both $A\beta_{40}$ and $A\beta_{42}$ levels (Citron et al., 1992; Suzuki et al., 1994), while the London, V717I, and Indiana, V717F, mutations at the γ-secretase cleavage site increases the production of $A\beta_{42}$ (Chartier-Harlin et al., 1991; Suzuki et al., 1994). PSEN1/2 are components of the γ secretase complex and the *PSEN1* gene is mapped to chromosome 14 while the *PSEN2* gene is located on chromosome 1 (Rocchi et al., 2003). While in the non-amyloidogeneic pathway APP is cleaved by α secretase and γ secretase does not produce Aβ , in the amyloidogeneic pathway Aβ is released as a result of proteolysis of APP by β-secretase and γ-secretase (Blennow et al., 2006). APP cleaved by BACE1 results in a C-terminal fragment and this is further cleaved by γ-secretase to generate $A\beta_{40}$ and $A\beta_{42}$. While $A\beta_{42}$ isoform is more fibriologenic and toxic than the more abundant $A\beta_{40}$ isoform (Rocchi et al., 2003), APP mutations within *Aβ*, Dutch (E693Q) and Arctic (E693G) mutations, increase fibrillogenesis (Nilsberth et al., 2001; Massi et al., 2002). While the core of Aβ plaques is comprised of Aβ fibrils, they are surrounded by dystrophic neurites and activated microglia (Stephan and Phillips, 2005). NFTs are comprised and triggered by hyperphosphorylated tau. Tau, a microtubule associated protein (Rockenstein et al., 2007) is mapped to chromosome 17 and is a phosphoprotein under physiological conditions. However, under pathological conditions tau is hyperphosphorylated and thus, tends to dissociate itself from microtubules (Gotz et al., 2004). Although the pathways linking Aβ and tau are poorly understood, the amyloid cascade hypothesis proposes that modifications in tau and the consequential NFTs are elicited by toxic concentrations of Aβ (Ballard et al., 2011).

The molecular cause of late-on-set AD (>65 years old), which accounts for more than 95% cases of AD, is not clearly understood. It is genetically associated with apolipoprotein E

isoform 4 (*ApoE ε4*) (for review, see (Rocchi et al., 2003)), glycogen synthase kinase 3β (*GSK3β*) (Kwok et al., 2008), dual specificity tyrosine-phosphorylation-regulated kinase 1A (*DYRK1A*) (Liu et al., 2008), tau, translocase of outer mitochondrial membrane 40 (*TOMM40*) (Roses, 2010), *CLU* and *PICALM* (Seshadri et al.; Harold et al., 2009). In addition to these genes, bridging integrator 1 *(BIN1)*, ATP-binding cassette, sub-family A (ABC1), member 7*(ABCA7)*, complement component (3b/4b) receptor 1 (knops blood group) *(CR1)*, menebrane-spanning 4-domains, subfamily A, member 6A *(MS4A6A)*, *CD33*, membrane-spanning 4-domains, subfamily A, member 4E *(MS4A4E)*, CD2-associated protein *(CD2AP)* have been ranked as top 10 genes associated with AD in AlzGene database. The AlzGene database includes 1395 studies and 320 meta-analyses which have identified 695 genes and 2973 polymorphisms (http://www.alzgene.org) (Bertram et al., 2007).

Alterations in AD related genes may not necessarily result in protein sequence changes. Gene duplications in the APP locus located on chromosome 21 causes early-on-set AD (Rovelet-Lecrux et al., 2006; McNaughton et al., 2012) and the extra copy of APP in Trisomy 21 (Down's syndrome) is associated with increased incidence of AD (Podlisny et al., 1987). Polyrmorphisms observed in the APP promoter which increases APP transcription are also associated with AD (Theuns et al., 2006) suggesting the importance of gene dosage and misregulation of protein expressions in AD pathogenesis. Therefore, understanding the regulation of genes could provide insights into the etiology and identification of novel therapeutic and diagnostic strategies for AD. In addition to genetic risk factors epidemiological studies have identified other risk factors that contribute to the etiology of AD.

1.2 Epidemiological risk factors for AD

Aging being the most blatant risk factor for AD with incidence increasing exponentially with age (Hebert et al., 1995; Zhu and Sano, 2006), population studies suggest that women are at higher risk than men with higher cognitive impairments and senile dementia of the AD type (Bachman et al., 1992; McPherson et al., 1999; Alberca et al., 2002). Epidemiological studies have suggested associations between AD and vascular diseases including hypercholesterolemia, hypertension, atherosclerosis, coronary heart disease, smoking, obesity and diabetes (for review, see (Mayeux, 2003)). In addition, traumatic brain injury is shown to be a risk factor; however, whether it initiates the pathogenic cascade or it simply diminishes the brain reserve capacity is unclear (for review, see (Jellinger, 2004)). In contrast, physical exercise and cognitive exercise have a protective effect on dementia incidence (Kramer et al., 1999; Ngandu et al., 2007; Solfrizzi et al., 2008). Evidence suggest that consumption of a Mediterranean diet, characterized by high intake of vegetables, fruits, nuts, legumes, cereals, fish, monounsaturated fatty acids, polyunsaturated fatty acid (PUFA), moderate intake of alcohol and a low intake of meat and dairy products, may have beneficial effects on the risk of dementia while saturated fatty acids may have harmful effects on cognitive function and the incident of dementia (for review, see (Solfrizzi et al., 2011)

1.3 High-fat diet and AD

Individuals of Japanese (Grant, 1999) and African (Hendrie et al., 1995) origins living in the USA have much higher incidences of AD, 4.1% and 6.24% respectively, than their counterparts, <2%, living in their native countries, supporting the theory that environmental

factors including diet and levels of exercise are also a vital component in the pathogenesis of AD. In support of this, a high cholesterol diet and high dietary fat intake, namely saturated fat, have increased the risk of cognitive decline in aged populations (Kalmijn et al., 1997; Sulkava, 1998; Luchsinger et al., 2002; Morris et al., 2004; Eskelinen et al., 2008). Furthermore, studies have shown high dietary intake of saturated fats may enhance cerebral deposition of Aβ (Sparks et al., 2000). Consumption of docosahexaenoic acid (DHA), the most abundant PUFA in the brain, have reduced the risk of AD in animals (Hooijmans and Kiliaan, 2008). Further, dietary restrictions have ameliorated AD in transgenic models of AD (Mattson, 2000). Conversely, Aβ levels have been shown to decrease (Howland et al., 1998; Van der Auwera et al., 2005) or be unchanged (George et al., 2004) with high-fat/high cholesterol diets in mouse models of AD. Concomitantly, other population based studies have shown no or weak associations between diet and cognitive impairment (Engelhart et al., 2002; Psaltopoulou et al., 2008). The risk of dietary fat intake has been utilized as a potential risk factor in chapters 2, 3 and 4 of this study. Concomitantly, a high-fat diet has been reported to increase plasma ceramide levels (Shah et al., 2008).

1.4 Ceramide and AD

Ceramides are sphingolipids, with over 50 distinct molecular species, contributing to sphingolipid signaling (Hannun and Obeid, 2008). In the *de novo* ceramide synthesis pathway that occurs in the endoplasmic reticulum (ER), serine palmitoyltransferse (SPT) condenses serine and palmitoyl-co-A to dihydrophingosine (Hannun and Obeid, 2008). Ceramide synthase (CerS) act on dihydrophingosine to produce dihydroceramide which undergoes desaturation to produce

ceramide. Ceramide may also be converted to ceramide-1- phosphate by ceramide kinase.(Linn et al., 2001; Hannun and Obeid, 2002) Both ceramide and ceramide-1-phosphate are bio-active. The *de novo* pathway is metabolically equipped to respond to variation in serine and palmitate concentrations as SPT exhibits K_m (0.2 mM) values that are in the physiological intracellular concentrations for the 2 substrates (Hannun and Obeid, 2008; Hu et al., 2009). Ceramide is also synthesized via sphingomyelinase (SMase) acting upon sphingomyelin (SM). Ceramide is converted to sphingosine by ceramidase (CDase) followed by the action of sphingosine kinase (SK) to produce sphingosin-1-phosphate (S-1-P). The *de novo* pathway could be induced by heat stress, UV radiation; chemotherapy and death receptors that bring about senescence, apoptosis and cell cycle arrest (Hannun and Obeid, 2008).

There is compelling evidence demonstrating an increase of ceramide levels (>3 folds) in the brains of AD patient, and suggesting its contribution to disease pathogenesis (Han et al., 2002; Cutler et al., 2004; Satoi et al., 2005; He et al., 2010). The primary location for amyloidogenic processing of APP are the lipid rafts (Sisodia, 1992; Cordy et al., 2003; Ehehalt et al., 2003; Wada et al., 2003; Won et al., 2008). Membrane ceramides are not only the major component of the lipid rafts but they also contribute to AD pathology by facilitating the mislocation of BACE1 and γ-secretase to lipid rafts, and thereby promoting Aβ formation (Lee et al., 1998; Vetrivel et al., 2004; Vetrivel et al., 2005; Hur et al., 2008; Haughey et al., 2010). Inactive BACE1 and γ-secretase resides outside of lipid rafts under non-pathological settings allowing non-amyloidogenic processing of APP while under disease state ceramide facilitate the trafficking of these pathogenic secretases to lipid rafts where they become active to produce Aβ (Cordy et al., 2003; Vetrivel et al., 2005; Ebina et al., 2009). Inhibiting the *de novo* ceramide synthesis decreases the production of Aβ, while exogenous addition of ceramide increases Aβ

production by stabilizing BACE1 (Puglielli et al., 2003; Costantini et al., 2007) . Multiple *in vitro* and *in vivo* studies suggest a connection between ceramides and Aβ and thereby indicating increased ceramide levels could be an important risk factor for late on-set AD (Cutler et al., 2002; Gulbins and Kolesnick, 2003; Puglielli et al., 2003; Kalvodova et al., 2005; Mattson et al., 2005). Ceramide synthesis through the catalysis of SPT is further explored in this report.

1.5 Regulation of SPT

SPT is the first rate limiting enzyme in the *de novo* ceramide synthesis pathway (Merrill et al., 1985; Hanada et al., 1997; Hannun and Obeid, 2008). Activation of SPT elevates ceramide levels (Perry et al., 2000) and inhibition of SPT with ISP-1 or L-cycloserine (LCS) decreases ceramide levels, both *in vitro* and *in vivo* (Hojjati et al., 2005b; Holland et al., 2007; Patil et al., 2007; Strettoi et al., 2010), suggesting SPT is a potent regulator of ceramide. Further, inhibition of SPT with ISP-1 decreases neuronal cell death by Aβ (Cutler et al., 2004) and induces the non-amyloidogenic processing of APP (Sawamura et al., 2004). These studies highlight the importance of SPT in AD. SPT is a heterodimer composed of serine palmitoyltransferase long chain 1 (SPTLC1) and either serine palmitoyltransferase long chain 2 (SPTLC2) (Hanada, 2003) or serine palmitoyltransferase long chain 3 (SPTLC3) (Hornemann et al., 2006). Mutations in *SPTLC1* (Bejaoui et al., 2001; Dawkins et al., 2001; Rotthier et al., 2009) and *SPTLC2* (Rotthier et al., 2010), the major subunits in the brain (Altura et al.; Hornemann et al., 2006) cause hereditary sensory and autonomic neuropathy type 1 (HSAN-1). No mutations as yet have been identified in *SPTLC3* (Rotthier et al., 2010). In the human genome, *SPTLC1* is comprised of 15 exons spanning ~85 kbp in chromosome 9q21-q22 region, while *SPTLC2* is comprised of 12

exons spanning ~110 kbps in chromosome 14q24.3-q31 region (Hanada, 2003). The mammalian *SPTLC1* and *SPTLC2* encode proteins of 53 kDa and 63 kDa respectively, with ~20% similarity and neither subunit submitted to glycosylation (Hanada et al., 1997; Weiss and Stoffel, 1997). Affinity-peptide chromatography assays have demonstrated that SPT consists of SPTLC1 and SPTLC2 at a 1:1 ratio (Hanada et al., 2000). Both SPTLC1 and SPTLC2 are essential for embryonic development since complete knockout (homozygous) of *Sptlc1* or *Sptlc2* are embryonic lethal (Hojjati et al., 2005a). However, the regulation of these subunits and in turn SPT is not well understood. Cell culture studies demonstrate that SPT activity increases in response to stimuli (i.e. etoposide or retinoic acid or resveratrol), but without concomitant changes in *SPTLC1* and *SPTLC2* mRNA levels (Herget et al., 2000; Perry et al., 2000; Scarlatti et al., 2003), which have led researchers to hypothesize that SPT is post-transcriptionally regulated.

1.6 Post-transcriptional regulation by miRNA

Gene expression may be post-transcriptionally regulated through microRNAs (miRNA) (Ambros, 2004; Bartel, 2004). MiRNAs are endogenous small RNAs of 21–25 nucleotides that negatively regulate gene expression at the post-transcriptional level (Lagos-Quintana et al., 2001). There are over 1000 miRNAs identified (Griffiths-Jones et al., 2008; mirbase.org, 2012) and 1/3 of the miRNA genes are located within protein coding messenger RNAs (mRNA) while the others are intergenic (Delay et al., 2012). In animals two processing events direct the formation of mature miRNA. The nascent miRNA transcripts (pri-miRNA) are processed into ~70-nucleotide precursors (pre-miRNA) followed by a second process where the pre-miRNA is

cleaved to generate ~21–25 nucleotide mature miRNAs. These chronological cleavages of miRNA maturation are catalysed by RNase-III enzymes, Drosha and Dicer (He and Hannon, 2004). MiRNAs bind to 3'UTR of the target mRNA to cause translational repression or degradation of the targeted mRNA by feeding into the RNA interference (RNAi) pathway (He and Hannon, 2004; Chekulaeva and Filipowicz, 2009).

In mammals more than 30% of all protein-coding genes (Nilsen, 2007; Filipowicz et al., 2008) and more than 90% of the human genes (Barbato et al., 2009) are predicted to be regulated by miRNAs. A miRNA "family", defined as a group of miRNAs having the same seed sequence, in most cases, but not all, target the same gene. Conversely, a single miRNA may target several genes, potentially regulating multiple pathways (Baek et al., 2008; Selbach et al., 2008). Reduction of total brain miRNAs have resulted in progressive neurodegeneration with knock-out of *Dicer* resulting in neuronal loss, brain shrinkage and inflammation. Moreover, dicer-deficient mice have demonstrated changes in APP levels and tau hyperphosphorylation (Kim et al., 2007; Schaefer et al., 2007; Cuellar et al., 2008; Davis et al., 2008; Hebert et al., 2010; Kawase-Koga et al., 2010; Tao et al., 2011) suggesting a contribution of the miRNA regulating pathways to the pathogenesis of AD. The first indication of changes in miRNA profiles in AD was reported in a small-scale study in 2007 (Lukiw, 2007), and since then many researchers, using large-scale genome wide studies have demonstrated alterations in miRNA patterns in AD brains, blood and cerebrospinal fluid (CSF) (Schipper et al., 2007; Cogswell et al., 2008; Hebert et al., 2008; Nelson and Wang, 2010; Nunez-Iglesias et al., 2010; Shioya et al., 2010).

Other gene regulatory mechanisms include cell signaling, mRNA splicing, polyadenylation and localization, chromatin modifications; and mechanisms of protein localization, modification and degradation (Chen and Rajewsky, 2007).

In order to study gene regulations and thus alterations in biomarkers and investigate their potential therapeutic applications researchers incorporate animal models in their studies.

1.7 Mouse models of AD

There is no existing mouse model that recapitulates all the clinical and pathological features of AD, including cognitive and behavioral deficits, amyloid plaque, NFTs, gliosis, synapse loss, axonopathy, neuronal loss and neurodegeneration, raising concerns regarding the use of mouse models for preclinical testing (Hall and Roberson, 2012) with many disease modifying treatments that show promise in mouse models failing in clinical trials (Mangialasche et al., 2010). Nevertheless, AD mouse models can be used as a reductionist tool for understanding the effects on the brain, genes and proteins associated with AD, and identifying strategies to block the effects (Hall and Roberson, 2012).

Transgenic expression of the human APP (hAPP) is the basis of most of the widely used mouse models of AD. While autosomal dominant AD only accounts for a limited number of AD cases and thus may cause limitations in these models, clinicians report the similarities between early-on-set and late on-set AD are more significant than their differences (Hall and Roberson, 2012). The 3 isoforms of APP include APP695, APP751 and APP770. APP695 has been incorporated into PDAPP (Chen et al., 2000), J20 (Mucke et al., 2000) and Tg2576 (Arendash and King, 2002). APP751 has been incorporated into APP23 (Calhoun et al., 1998) and TASD-41 (Rockenstein et al., 2001). APP770 has been incorporated into PDAPP (Chen et al., 2000) and J20 (Mucke et al., 2000). In addition, Swedish mutation has been incorporated into Tg2576 (Arendash and King, 2002) and APP23 (Calhoun et al., 1998), while Indiana mutation has been

incorporated into PDAPP (Chen et al., 2000), and both Indiana and Swedish mutations have been incorporated into J20 (Mucke et al., 2000), and London and Swedish mutations have been incorporated into TASD-41 (Rockenstein et al., 2001). The expression of these genes are driven by numerous promoters that include platelet-derived growth factor B-chain (PDGF-B) (e.g. PDAPP (Chen et al., 2000), J20 (Mucke et al., 2000)), thymocyte differentiation antigen 1 (Thy-1) (e.g. APP23 (Calhoun et al., 1998), TASD-41 (Rockenstein et al., 2001)), and prion protein (PrP) (e.g. Tg2576 (Arendash and King, 2002)), to express the genes at different levels and spatial patterns under a variety of background strains that modulate the phenotype. These mouse models initiate the development of symptoms and hallmarks, cognitive deficits and plaques, at different times of development, ranging from 3 to17 months. Other transgenic mouse models include Aβ (e.g. BRI-Aβ42A (McGowan et al., 2005)), presenilin and hAPP (e.g. PSAPP (Arendash et al., 2001), Tg2576xPS1 (Jankowsky et al., 2004), 5xFAD (Kimura and Ohno, 2009)) and human tau (e.g. TAPP (Lewis et al., 2001), 3xTg (Billings et al., 2005), vhtau (Andorfer et al., 2003)).

Non-transgenic animal models include diabetes, obesity and traumatic brain injury models. Streptozotic (STZ), a betacytotoxic drug, injection model that selectively destroys insulin-secreting pancreatic β cells and thereby causing type-1 diabetes mellitus has shown to increase tau hyperphosphorylation (Planel et al., 2007; Kim et al., 2009). Type-2 diabetes mellitus (T2DM) spontaneous models include bio-breeding Zucker diabetic rat/Wor rats and db/db mice (Li et al., 2007; Kim et al., 2009) with prominent neurodegernative changes, neuronal loss, gliosis and synaptic loss (Park). In addition, long term ingestion of a high-fat diet leads to obesity and T2DM. This phenomenon has been incorporated in to transgenic models of AD to induce Aβ generation (Ho et al., 2004; Kohjima et al., 2010). Further, cross-mated double-

transgenic animals with APP23-ob/ob (leptin deficient) and APP23-NSY (polygenic T2DM) show severe congnitive imapairement (Takeda et al., 2010). In humans diffuse Aβ deposits have been reported to occure between 4 hours to 2.5 years after traumatic brain injury (Roberts et al., 1994). This anomaly has been modeled by controlled cortical impact in combination with transgenic models to enhance the pathologies (Tran et al., 2011).

For the studies described in this report, TgCRND8 (Centre for Research in Neurodegenerative Diseases) transgenic mice, containing the hAPP 695-cDNA with both the Indiana and the Swedish mutations, in a hybrid C3H/He-C57BL/6 background were used. TgCRND8 mice express the APP transgene at 5 folds higher than the endogenous APP under the control of the Syrian hamster PrP promoter. Due to the regulation of the PrP promoter these mice may express hAPP up to 15-folds above the endogenous levels but with less spatial selectivity, allowing expressions in neurons, astrocytes, oligodendrocytes, microglia (Boy et al., 2006), liver, kidney, spleen and other organs (Asante et al., 2002). Further, they develop cognitive deficits and Aβ deposits as early as 3 months (Chishti et al., 2001). The early pathogenesis was a vital component in selecting the TgCRND8 model for this research. With the use of TgCRND8 and wild-type risk factor mouse models, this study aims to identify potential diagnosis biomarkers and and therapeutic targets in AD.

1.8 Diagnosis and biomarkers

At present, AD can only be conclusively diagnosed at autopsy. The risk assessment criteria that are discussed in round table meetings include epidemiological risk factors, age, insulin resistance/ diabetes, genetic risk factors, vascular risk factors, and amyloid and tau

pathologies. The Cambridge Neuropsychologucal Test Automated Battery (CAN-TAB), a prodromal AD test based on paired associative learning (PAL) and the cognitive testing performed by Cog-state are used as computerized screening tools. In CANTAB PAL test, AD participants have expressed deteriorating scores over time along with some who have been screened with memeory complaints and patients with questionable dementia could convert to probable AD (Carrillo et al., 2009). Currently the most common method of screening for AD is to assess the cognitive decline. The mini mental state examination (MMSE) is the most widely used and is considered an index for the severity of cognitive decline (Ashford, 2008). However, MMSE not only provides minimal information on the mild impairment range but also lacks discriminative power against other forms of dementia (Ashford, 2008). It creates diagnostic uncertainty during the earlier phases of dementia, failing to distinguish between normal and pathological conditions. In addition, MMSE score variations have been observed with respect to age, education levels (Crum et al., 1993), and ethnicity (Ng et al., 2007).

Other methods of diagnosis include computed tomography (CT) and magnetic resonance imaging (MRI), which are used to detect intracranial lesions (Waldemar et al., 2007) or cortical thinning (Mungas et al., 2002). However, the sensitivity of these imaging techniques does not afford sufficient demarcations in the medical temporal atrophy between AD and non-AD dementia to provide clear and decisive diagnosis (Wahlund et al., 2000; Scheltens et al., 2002). Functional neuro-imaging techniques such as radio-isotopic scans have been developed for probable diagnosis (Ballard et al., 2011), but again with insufficient clinical accuracy in discriminating between AD and control individuals (Dougall et al., 2004). Even though positron emission tomography (PET) imaging in conjunction with the Pittsburgh Compound B (PiB) has

been able to distinguish cases with probable AD from normal and non-AD cases, wide variations in sensitivity and specificity have been reported (Patwardhan et al., 2004).

Aβ (Sjogren et al., 2002) and hyperphosphorylated tau (de Souza et al., 2011) levels in the CSF have also been suggested as diagnostic markers for AD. However these CSF markers may not be able to distinguish between mild cognitive impairment (MCI), non-progressive deficits and healthy older adults since similar patterns have been observed in these cases. Further, their high inter-laboratory variations (Forlenza et al., 2010) and invasive procedures in sample acquisition limits their wide application. Therefore, the ability to identify biomarkers through less invasive procedures, such as in blood would be significant. However, attempts to measure Aβ levels in blood, thus far, have led to inconsistent results (Ballard et al., 2011).

The current screening/selection criteria that AD centers utilized is based on National Institute of Neurological and Communicative Disorders and Stroke; Alzheimer's ddisease and Related Disorders Association (NINCDS-ADRDA) (McKhann et al., 1984). The diagnosis for AD and other dementia consists of 3 steps that include the clinical diagnosis of dementia, the exclusion of other causes of dementia and diagnostic classification of dementia subtypes. This diagnosis is based on careful evaluation of the history of clinical neurological examinations, technical and laboratory methods which included MMSE, brain imaging modalities (MRI or/and emission tomography based techniques) and Aβ, tau, hyperphosporylated tau and proteomics of the CSF. Other causes of dementia that are particularly excluded are infections of the CNS (HIV, syphilis) or Creutzfeld-Jacob disease, subdural haematoma, communicative hydrocephalus, brain tumors, drug intoxication, alcohol intoxication, thyroid disease, parathyroid disease, and vitamine or other deficiencies (European Medicines Agenecy guidelines, 2008). The disease

centers discuss their selection and elimination criterias for the respective patients in a round table panel that include certified neurologists.

Early and accurate diagnosis is crucial, enabling early treatments to slow or delay the progression of the disease and provide patients and family members with information to plan for the future.

1.9 Therapeutic strategies

Symptomatic treatments for AD include cholinesterase inhibitors and NMDA receptor antagonists. Donepezil, rivastigmine and galatamine are cholinesterase inhibitors that are licensed for the treatment of mild to moderate AD. Moderate improvements in cognition, apathy and social interactions are reported with the use of cholinesterase inhibitors in randomized controlled trials (Loy and Schneider, 2006; Birks et al., 2009; Waldemar et al., 2011). However, the outcome measured in these clinical trials fails to translate well into practice (Rockwood et al., 2006). Memantine, an NMDA receptor antagonist, is licensed for moderate to severe AD and have improved cognitive performance (McShane et al., 2006).

Treatments strategies for neuropsychiatric symptoms of AD include atypical antipsychotics (risperidone, quetiapine, olanzapine and aripiprazole) (Ballard and Howard, 2006), antidepressants (citalopram and sertraline) (Weintraub et al., 2010) and anticonvulsants (carbamazepine) (Ballard et al., 2009b). While risperidone is licensed for short-term treatment of severe aggression in AD, other neuropsychiatric drugs are used off-license with severe adverse side effects including sedation, parkinsonism, chest infections, stoke and death (Ballard et al., 2009a).

With minimal improvements observed with symptomatic treatments, the necessity for disease modifying treatments is evident. Proposed treatments under clinical trials to treat the etiology of AD include immunotherapy (bapineuzumab), sectretase inhibitors (tarenflurbil and semagacestat), Cu or Zn modulators (PBTS), tau aggregation inhibitors (Methylthioninium chloride), GSK3 inhibitors (Lithium) and natural products and vitamins (vitamin E, ginkgo biloba, omega-3-fatty acids and DHA). Immunotherapy to clear Aβ has been effective in transgenic mice (Schenk et al., 1999) however the clinical benefits are less apparent (Holmes et al., 2008). With only a limited number of antibodies crossing the blood-brain-barrier, immunotherapy is subjected to skepticism (Ballard et al., 2011). Potential therapies to inhibit β-secretase or modulate γ-secretase that increase $A\beta_{40}$ and reduce $A\beta_{42}$ levels although shows promise in phase 2 trials failed in large randomized controlled trials (Green et al., 2009). PBT2 and tau aggregation inhibitors have shown promise in phase 2 trials and await phase 3 trials (Lannfelt et al., 2008). While GSK3 inhibitors reduce tau hyperphosphorylation in animal models and are subjected to early stage clinical trials (Leroy et al., 2010), natural products (Weinmann et al., 2010) and vitamins (Petersen et al., 2005) have been unsuccessful in randomized controlled trials; however omega-3-fatty acids show possible benefits on neuropsychiatric symptoms in a subgroup of the patients (Freund-Levi et al., 2006) and DHA currently under a phase 3 trial (Ballard et al., 2011). With several promising drugs failing in randomized controlled trials there is an urgent need to identify new drugs and drug targets to treat the etiology of the disease.

1.10 Summary to introduction

The manifestation of early-on-set AD is due to autosomal dominant mutations in APP, PSEN 1 and PSEN 2. However, molecular mechanisms leading to late-on-set AD is unclear. Many researchers have identified that ceramide levels, a sphingolipid, are increased in late-on-set AD autopsy brain samples. The *de novo* synthesis of ceramide is catalyzed by the enzyme SPT. However, the regulation of SPT was not understood. Therefore, chapter 2 of this report seeks to understand the regulation of SPT in respect to AD with emphasis given on the regulation of Aβ by SPT. In addition, with no conclusive current diagnostic methodology available and many biomarkers and imaging techniques failing to provide an accurate diagnosis, there is an essential need to identify early diagnostic biomarkers to provide a comprehensive diagnosis and prognosis for AD. Thus, Chapter 3 of this dissertation inquires the potential use of blood sera miRNAs as non-invasive biomarkers for AD. With many drugs failing in clinical trials, there is a pressing need to identify new drugs and drug targets to treat the etiology of AD. Therefore, chapter 4 endeavors to identify the potential therapeutic application of SPT inhibition in AD with the use of a transgenic AD mouse model, TgCRND8. The specific aims in this research include

Chapter 2

1. Understand the regulation of SPT

   Hypothesis: SPT is post-transcriptionally regulated by miRNAs

2. Study the effects of miRNA and in turn SPT on Aβ levels

   Hypothesis: miR-137/181c and in turn SPTLC1 regulates Aβ levels

Chapter 3

3. Inquire the use of blood sera miRNAs as potential diagnostic biomarkers

Hypothesis: miR-137, -181c, -9 and -29a/b are down regulated in probable AD and probable early AD blood sera samples

Chapter 4

4. Investigate the inhibition of SPT/ceramide as a potential therapeutic target to ameliorate the Aβ burden, *in vivo*

   Hypothesis: The inhibition of SPT could reduce Aβ and hyperphosphorylated tau levels in an AD mouse model

Finally, chapter 5 discusses the concluding remarks and identifies potential future applications/studies that can be derived from this research.

CHAPTER 2: MIR-137/181C REGULATES SPT AND IN TURN AB, NOVEL TARGETS IN SPORADIC ALZHEIMER'S DISEASE

Publication: **Geekiyanage, H**. and Chan, C., 2011. MiR-137/181c regulates SPT and in turn Aβ, novel targets in sporadic Alzheimer's disease. ***Journal of Neuroscience*** 31(41): 14820-30

ABSTRACT

The contribution of mutations in *APP* and *PSEN* to familial Alzheimer's disease is well established. However, little is known about the molecular mechanisms leading to Aβ generation in sporadic AD. Increased brain ceramide levels have been associated with sporadic AD, and are a suggested risk factor. SPT is the first rate limiting enzyme in the *de novo* ceramide synthesis. However, the regulation of SPT is not yet understood. Evidence suggests that it may be post-transcriptionally regulated. Therefore, I investigated the role of miRNAs in the regulation of SPT and Aβ generation. I show that SPT is upregulated in a subgroup of sporadic AD patient brains. This is further confirmed in AD mouse risk factor model studies. I identified that the loss of miR-137, -181c, -9 and -29a/b-1 increases SPT and in turn Aβ levels, and provides a mechanism for the elevated risk of AD associated with age, high-fat diet and gender. Finally, these results suggest SPT and the respective miRNAs may be potential therapeutic targets for sporadic AD.

Keywords: Alzheimer's disease, amyloid beta, serine palmitoyltransferase, microRNA

2.1 Introduction

It is well established that Aβ accumulation in familial Alzheimer's disease is due to mutations in *APP* and *PSEN* genes (reviewed in ref. (Cruts and Van Broeckhoven, 1998)). However, the mechanisms contributing to Aβ accumulation in sporadic AD is less well understood. Research thus far, consistently demonstrates that ceramide, a sphingolipid, is increased in AD patients (Cutler et al., 2004; He et al., 2010) and may contribute to the disease pathogenesis. Membrane ceramides are not only the major component of lipid rafts but they also contribute to AD pathology by facilitating the mislocation of BACE1 and γ-secretase to lipid rafts, and thereby promoting Aβ formation (Lee et al., 1998; Vetrivel et al., 2005). Inhibiting *de novo* ceramide synthesis has been shown to decrease the production of Aβ while exogenous addition of ceramide increased Aβ production (Puglielli et al., 2003; Patil et al., 2007). Numerous studies suggest a connection between ceramides and Aβ, and indicate increased ceramide levels may be an important risk factor for sporadic AD (Puglielli et al., 2003; Mattson et al., 2005).

SPT is the first rate limiting enzyme in the *de novo* ceramide synthesis pathway (Hannun and Obeid, 2008). Activation of SPT elevates ceramide levels (Perry et al., 2000) and inhibition of SPT decreases ceramide levels (Hojjati et al., 2005b; Patil et al., 2007) and neuronal cell death by Aβ (Cutler et al., 2004), supporting SPT as an important regulator of ceramide. SPT is a heterodimer composed of SPTLC1 and either SPTLC2 or SPTLC3 (Rotthier et al., 2010). In the brain, *SPTLC3* is lowly expressed while SPTLC1 and SPTLC2 are the major subunits (Hornemann et al., 2006). However, the regulation of these subunits and in turn SPT is not well understood. Cell culture studies demonstrate that SPT activity increases in response to various

stimuli (i.e. etoposide or resveratrol), but without concomitant changes in *SPTLC1* and *SPTLC2* mRNA levels (Perry et al., 2000; Scarlatti et al., 2003), which have led researchers to hypothesize that SPT may be post-transcriptionally regulated.

Gene expression may be post-transcriptionally regulated through miRNAs, endogenous small RNAs of 21–25 nucleotides, that bind to 3′UTR of the target mRNA to cause translational repression or degradation of the mRNAs (He and Hannon, 2004). MiRNAs have been associated with neuronal differentiation, synaptic plasticity and memory formation (Sempere et al., 2004; Mehler and Mattick, 2006; Schratt et al., 2006). From miRNA expression profiles, several miRNAs are differentially expressed in AD patients (Lukiw, 2007; Cogswell et al., 2008; Hebert et al., 2008; Wang et al., 2008) and several have been reported to be specific or enriched in the brain (Sempere et al., 2004). Indeed a recent study reported altered expressions of several miRNAs in response to Aβ (Schonrock et al., 2010), suggesting the involvement of miRNA in sporadic AD. Therefore, I investigated whether miRNAs mediated the post-transcriptional regulation of SPT with respect to sporadic AD.

2.2 Material and Methods

Patient information. The AD (n=7) and control (n=7) neocortical brain samples were from the University of Kentucky (UK) Alzheimer's disease center tissue bank (ADC) as frozen tissues. The samples have been clinically diagnosed by neurologists, neuropathologists, neuropsychologists, and other staff members in the ADC clinic. Most samples have been obtained in <4hrs post-mortem interval (PMI). All individuals were between the ages of 88-99 years. The reference number (ref. #), gender, Braak stage, mini mental state exam scores, frontal

neuritic plaque numbers (NP), NFT and ApoE genotype of the individuals are listed in Table 1. The cause of death of these individuals is multifactorial or unclear with pneumonia being the classical cause of death. The above information was provided by the University of Kentucky (UK) Alzheimer's disease center tissue bank (ADC).

Animals. Wild type male C57BL/6 mice purchased from Jackson laboratories were used in the developmental study. Wild type mice on a hybrid background, C3H/He (Charles River) x C57BL/6 were used in the diet (all male) and gender specific studies (7 males, 7 females). All procedures conducted were approved by the Institutional Animal Care and Use Committee at Michigan State University.

Primary cell culture. Primary astrocytes were isolated and cultured from <24hr old wild type Sprague-Dawley rat pups and 3 week old TgCRND8 (Centre for Research in Neurodegenerative Diseases) transgenic mouse pups, containing the APP 695-cDNA with both the Indiana and the Swedish mutations, in a hybrid C3H/He x C57BL/6 background (Chishti et al., 2001) as described (Patil et al., 2007). The TgCRND8 mice express the APP transgene at 5-folds higher than the endogenous APP under the control of the Syrian hamster prion promoter (Chishti et al., 2001).

Protein extraction and western blot analysis. Cells, mouse brain cortices and human brain neocortices (homogenized) were lysed in buffer: 1% (v / v) Triton, 0.1% (w / v) sodium dodecyl sulfate, 0.5% (w / v) deoxycholate, 20 mm Tris, pH 7.4, 150 mm, NaCl, 100 mm NaF, 1 mm Na3VO4, 1 mm EDTA, 1 mm EGTA ,1 mm phenylmethylsulfonyl fluoride and protease

inhibitor cocktail (all chemicals from Sigma). The lysis was spun at 10,000 rpm for 10 min then the total protein concentration of the supernatant was measured by Bradford's assays and was mixed with reducing loading buffer and heated at 94^{o}C for 5 min. Immunoblot analysis was performed as described (Patil et al., 2007). Protein quantifications were conducted by normalizing to GAPDH or β-Actin. Western blots were quantified using Quantity One (BioRad) version 4.5.

ELISA. Protein was extracted from human autopsy brain samples and ELISA was performed for human $A\beta_{42}$ using KHB3441 (Invitrogen) according to the manufacturer's instruction. The $A\beta_{42}$ levels were calculated by normalizing to the total protein levels measured by Bradford's assay.

Transfections, plasmids and luciferase assays. Primary wild type and transgenic astrocytes were plated in 12 well plates and transfected for 24 – 72 hrs with 100-150nM of Syn-miRNA miScript miRNA mimic or anti-miR-RNA miScript miRNA inhibitor (Qiagen) or 500 ng – 2 µg of human *SPTLC1* cDNA or 1.5 – 2 µg of luciferase vector construct using Lipofectamine RNAi/MAX or Lipofectamine 2000 following manufacturer's instructions. The *SPTLC1* cDNA plasmid and *SPTLC1* and *SPTLC2* luciferase 3'UTR expression clones, containing the luciferase reporter gene and Renilla tracking gene and driven by the SV40 promoter, were purchased from Genecopoeia. The luciferase assay was conducted with dual luciferase assay kit (Luc-Pair™ miR Luciferase Assay Kit) (Genecopoeia). The Luciferase expression levels were normalized to Renilla expression levels.

Quantitative RT-PCR (qRT-PCR). Total mRNA was extracted using RNeasy Plus Mini Kit (Qiagen) and total RNA was quantified using ND-1000 nanodrop spectrophotometer. RNA quality control was performed by assessing OD 260/280 ratio. RNA quality control of the control and human AD brain samples were performed using the Agilent Bioanalyzer 2100. In addition the PCR products were run on agarose gels. qRT-PCR was conducted using iQSYBR Green Supermix (BioRad) and MyiQ real-time PCR detection system following reverse transcription using iScript™ cDNA Synthesis Kit according to manufacturer's instructions. Primers include human *SPTLC1*: 5' TGGAAGAGAGCACTGGGTCT 3' and 5' GCTACCTCCTTGATGGTGGA 3'; human *SPTLC2*: 5' GAGACGCCTGAAAGAGATGG 3' and 5' TGGTATGAGCTGCTGACAGG 3'; human *GAPDH*: 5'GAGTCAACGGATTTGGTCGT 3' and 5' TTGATTTTGGAGGGATCTCG 3'; mouse *Sptlc1*:5' AGTGGTGGGAGAGTCCCTTT 3' and 5' CAGTGACCACAACCCTGATG 3'; mouse *Sptlc2*: 5' CCTGTCAGCAGCTCATACCA 3' and 5' CACACTGTCCTGGGAGGAAT 3'; mouse *Gapdh*: 5' AACTTTGGCATTGTGGAAGG 3' and 5' ACACATTGGGGGTAGGAACA 3'; rat *Sptlc1*: 5' ACCTGGAGCGACTGCTAAAA 3' and 5' ATCCCATAGTGCTCGGTGAC 3'; rat *Sptlc2*: 5' TTGAGACTCACTGGCCCTCT 3' and 5' GGCCAGGAGGAGTCACATAA 3'; rat *Gapdh*: 5' AGACAGCCGCATCTTCTTGT 3' and 5' CTTGCCGTGGGTAGAGTCAT 3'. Relative human, mouse and rat *SPTLC1* and *SPTLC2* expressions were calculated using the comparative CT method normalizing to their corresponding *GAPDH* expressions.

Total miRNAs were extracted using miRNeasy Mini Kit (Qiagen) and RNeasy MinElute Cleanup Kit (Qiagen) total RNA was quantified using ND-1000 nanodrop spectrophotometer. RNA quality control was performed by assessing OD 260/280 ratio. In addition the PCR

products were run on agarose gels. qRT-PCR was conducted using miScript SYBR Green PCR Kit (Qiagen) and MyiQ real time PCR detection system following reverse transcription using miScript Reverse Transcription Kit (Qiagen) according to manufacturer's instructions. All miRNA primers were purchased from Qiagen and the relative expressions were calculated using the comparative CT method using RNU6B as the normalizing control.

Ceramide quantification. Lipids were extracted from homogenized human brain neocortices and mouse brain cortices according to Bligh and Dyer (Bligh and Dyer, 1959). Tandem mass spectrometry (MS/MS) was performed using Quattro Premier XE (Waters), Acquity ultra performance liquid chromatography (Waters) (LC-MS/MS) and Mass Lynx 4.1 software. External ceramide standards were purchased from Matreya and Avanti, Polar Lipids Inc. C12:0 (Avanti, Polar Lipids Inc.) was used as the internal standard.

Antibodies. LCB1 (BD Transduction Laboratories™), SPTLC1 (proteintech), SPTLC2 (abcam), GAPDH (cell signaling), β-Actin (Sigma), β-Amyloid (cell signaling), β-Amyloid -4G8 clone (Covance).

Statistical analysis. Statistical significances were determined by using 2 tailed *t* tests and Spearman correlation (2 tailed-T distribution test).

2.3 Results

Elevated ceramide and SPT expression in a subgroup of sporadic AD patients

The levels of ceramide and SPT protein expression were measured in the frontal brain cortices of 7 sporadic AD patients and 7 controls (see Table 1 for information on the patients). Of the vast number of distinct ceramide species (over 50 species), d18:1;18:0 and d18:1;16:0 are reported to be the major sphingolipid species in rat neurons (Valsecchi et al., 2007) and human brain (Ladisch et al., 1994). Consistent with previous reports (Cutler et al., 2004; He et al., 2010), ceramide levels, d18:1; 16:0 (P=0.037, student's t test) and d18:1; 18:0 (P=0.033), were significantly increased in this subgroup of AD patients (Figure 1A) (see Appendix A, Figure 21 for a representation of gender differentiated expression of ceramide). Several reports have shown that the sphingomyelin levels either increased (Pettegrew et al., 2001; Bandaru et al., 2009) or remained unchanged (Han et al., 2002) in AD brains. In contrast, other researchers have shown that the sphingomyelin levels decreased (Cutler et al., 2004; He et al., 2010) in AD brain. I found that the sphingomyelin 18:1, 16:0 levels increased (P=0.045) while the 18:1, 18:0 levels remained unchanged in the subgroup of AD patient brain cortices studied (Figure 1B). This suggests that the increased ceramide levels in these patients are from the *de novo* synthesis pathway. Accordingly, SPTLC1 (P=0.004) and SPTLC2 (P=0.007) protein expression were significantly elevated in the autopsy AD brain samples (Figure 1C and D). However, *SPTLC1* and *SPTLC2* mRNA levels remained predominantly unchanged in the AD samples as measured by quantitative RT-PCR (qRT-PCR) (Figure 1E).

Previously, our group found that palmitate (a saturated fatty acid) increased *de novo* ceramide synthesis in astrocytes through SPT (Patil et al., 2007). Thus I treated wild-type

primary rat astrocytes with palmitate for 24 hrs and found that the SPTLC1 (P=0.032) and SPTLC2 (P=0.015) protein levels (Figure 1F) increased without a concomitant change in their mRNA levels (Figure 1G), which is consistent with previous reports (Perry et al., 2000; Scarlatti et al., 2003). Overall, these results support that increased SPTLC1 and SPTLC2 expressions may be post-transcriptionally regulated in a subgroup of sporadic AD patients and in primary astrocytes cultured with palmitate. Thus, I proceeded to further elucidate the potential regulation of SPT by miRNAs.

SPTLC1 and *SPTLC2* are miRNA targeted genes

Prediction algorithms miRbase (Griffiths-Jones et al., 2008), Targetscan (Lewis et al., 2005), Pictar (Krek et al., 2005) and miRanda (Betel et al., 2008) were used to select potential miRNAs that bind the human 3'UTR of *SPTLC1* or *SPTLC2* with strongly conserved (in mammals) target sites. Likely miRNA candidates were filtered according to the following criteria, it must be 1) predicted by at least 2 algorithms, and 2) down-regulated in AD patients or enriched in the brain. Of the miRNAs predicted by 2 or more algorithms to bind the 3'UTR of *SPTLC1*, miR-15a and miR-181c (Hebert et al., 2008) are reported to be down regulated in sporadic AD patients, while miR-137 and miR-124 (Sempere et al., 2004) are reported to be enriched in the brain. Of the miRNAs predicted by 2 or more algorithms to bind the 3'UTR of *SPTLC2*, miR-29a, miR-29b-1 and miR-9 are reported to be down-regulated in sporadic AD patients while miR-9 is also reported to be enriched in the brain.

Two luciferase reporter constructs were generated containing the 3'UTR of human *SPTLC1* or *SPTLC2*. The miRNAs (sense) were co-transfected with the constructs and the luciferase expression was detected in wild-type primary rat astrocytes. While miR-137

(*P*=0.000016, student's *t* test) and miR-181c (*P*=0.0003) significantly decreased the luciferase expression of the construct containing the 3'UTR of *SPTLC1*, miR-15a and miR-124 did not (Figure 2A). The luciferase expression of the construct containing the 3'UTR of *SPTLC2* decreased significantly upon co-transfection with miR-9 (*P*=1.023E-08), miR-29a (*P*=1.2E-07) or miR-29b-1(*P*=0.007) (Figure 2B). These results were confirmed by transfecting primary rat astrocytes with either the sense-miRs or anti-miRs (anti-sense) of their respective miRNAs following analysis of the endogenous miRNA expression levels in primary rat astrocytes (Figure 2I). MiR-137 and miR-181c significantly suppressed the endogenous SPTLC1 expression and cellular ceramide levels while anti-miR-137 and anti-miR-181c significantly enhanced the endogenous SPTLC1 (Figure 2C and 2E) and cellular ceramide (Figure 2G) levels upon transient tranfection. Similarly, miR-9, miR-29a and miR-29b-1 significantly suppressed the endogenous SPTLC2 and cellular ceramide levels while anti-miR-9 and anti-miRs-29a/b-1 significantly enhanced the endogenous SPTLC2 (Figure 2D and 2F) and cellular ceramide (Figure 2H) levels upon transient transfection (see Appendix A, Figure 22-23 for sphingomyelin levels)

Changes in miRNA correlate with SPT expression in AD

The expression levels of miR-137 (*P*=0.006, student's *t* test), miR-181c (*P*=0.006), miR-9 (*P*=0.045), miR-29a (*P*=0.03) and miR-29b-1 (*P*=0.03) (Figure 3A-C), miR-15 (*P*=0.048) and miR-124 (*P*=0.002) (see Appendix A, Figure 24) were significantly down-regulated in the frontal cortices of the subgroup of sporadic AD patient.

Statistically significant negative correlations were observed between SPTLC1 and miR-137 (*r*=–0.807, *P*=0.0005, Spearman's correlation) (Figure 3D), miR-181c (*r*=-0.569, *P*=0.034) (Figure 3E), miR-15a (*r*=–0.59, *P*=0.026) and miR-124 (*r*=–0.67, *P*=0.009) (see Appendix A,

Figure 22) in the subgroups of control and AD patients. Significant negative correlations were also observed between SPTLC2 and miR-9 (r=–0.675, P=0.008) (Figure 3F), miR-29a (r=–0.603, P=0.023) (Figure 3G) and miR-29b-1 (r=–0.714, P=0.004) (Figure 3H) in the subgroup of AD patients. This negative correlation between the subunits of SPT and their corresponding miRNA expressions, coupled with the transient transfection results, suggest the possibility that changes in miR-137 or miR-181c, and miR-9, miR-29a or miR-29b-1 contribute, at least in part, to the overall protein expressions of SPTLC1 and SPTLC2, respectively, in AD.

Developmental coregulation of miRNA and SPT in brain

Given that AD is an age related disorder (Bachman et al., 1992) I assessed the expressions of SPTLC1 (Figure 4A and B), SPTLC2 (Figure 4A and C) and their corresponding miRNAs (Figure 4D-F) with development. The protein, mRNA and miRNA expressions were evaluated in wild-type mice brain cortices from post-natal day 0 (P0) up to 18 months. This provided an independent confirmation of the correlation between SPTLC1, SPTLC2 and their respective miRNAs under non-pathological settings. During development, the expression levels of miR-137, miR-181c (Figure 4D) and miR-124 (see Appendix A, Figure 25) increased while SPTLC1 expression levels decreased with age (Figure 4A and B). Consistent with previous reports (Hebert et al., 2008), expression levels of miR-29a and miR-29b-1 were found to increase (Figure 4E) with development, while the expression levels of SPTLC2 decreased with age (Figure 4A and 4C). The *Sptlc1* and *Sptlc2* mRNA expression levels remained unchanged (stable) over the period analyzed (Figure 4F), a signature of miRNA regulation. These results suggest that miR-137, miR-181c, miR-29a and miR-29b-1 are developmentally regulated, with the highest expressions in adult mice. Concomitantly, protein analyses indicate that SPTLC1 and

SPTLC2 have lower expression levels in adult mice, thereby further supporting a negative relationship between SPTLC1/2 and their corresponding miRNAs.

High-fat diet increases SPT expression with decreased miRNA expression

Increasing evidence in animal models suggest that a high-fat diet aggravates the Aβ burden and thereby the AD pathology (Julien et al., 2010). Indeed, high-fat/ high cholesterol diets have been found to increase plasma ceramide levels in rodents (Shah et al., 2008). Moreover, prior research in our lab demonstrated that palmitate, a saturated fatty acid, increases ceramide levels and induces AD-like pathology in primary neuronal cell culture mediated by astrocytes (Patil et al., 2007). Therefore, the expression levels of ceramide, SPTLC1 and SPTLC2 and their corresponding miRNAs were measured in brain cortices of wild-type male mice fed a 60% kcal high-fat diet for a period of 5 months (starting at 4 months of age). While ceramide (Figure 5A), SPTLC1 and SPTLC2 (Figure 5B) expression levels increased in mice fed a high-fat diet, *Sptlc1* and *Sptlc2* mRNA levels remained unchanged (Figure 5C), supporting our hypothesis that SPTLC1/2 may be post-transcriptiponally regulated by miRNAs. Indeed, miR-137 (P=0.005, student's t test) (Figure 5D), miR-181c (P=0.026) (Figure 5D), miR-15a (P=0.01) (see Appendix A, Figure 26) and miR-9 (P=0.0027) (Figure 5E) expression levels were down-regulated in mice fed a high-fat diet. In agreement with our *in vivo* results miR-137 (P=5.6E-05) (Figure 5F), miR-181c (P=2.2E-06) (Figure 5F), and miR-9 (P=1.9E-05) (Figure 5G) expression levels were down-regulated in wild-type primary rat astrocytes treated with palmitate, whereas SPTLC1/2 protein expression levels were upregulated (Figure 1F). However, miR-29a and miR-29b-1 expressions did not change with either a high-fat diet (*in vivo*) or palmitate treatment (*in vitro*).

SPT and miRNA are differentially expressed with respect to gender

Evidence suggests that AD pathology may be more prevalent in females than in males (Bachman et al., 1992). Therefore, I evaluated the SPTLC1, SPTLC2 and miRNA expression levels in the brain cortices of female and male wild-type mice (9 months of age). Ceramide species, d18:1; 18:0 (P=0.0042, student's t test), d18:1; 16:0 (P=0.0045, student's t test) (Figure 6A), SPTLC1 (P=0.018) and SPTLC2 (P=0.014) (Figure 6B and 6C) protein expression levels were higher in females as compared to males, while the *Sptlc1* and *Sptlc2* mRNA levels remained unchanged (Figure 6D), further indicating that SPTLC1/2 may be post-transcriptionally regulated by miRNAs. Concomittantly, miR-137 (P=0.011), miR-181c (P=0.038) (Figure 6E), miR-124 (see Appendix A, Figure 27) miR-29a (P=0.031) and miR-29b-1 (P=0.004) (Figure 6F) expression levels are downregulated, but not miR-9, in female mice, while SPTLC1/2 protein expression levels are increased, further supporting a negative relationship between SPTLC1/2 and their target miRNAs.

miRNA modulates SPT and Aβ

A casual relationship between miR-29a/b-1, BACE1 activity and Aβ has been established by (Hebert et al., 2008). Therefore, I assessed whether a relationship exists between miR-137/181c and Aβ, mediated by SPTLC1. Statistically significant positive correlations were observed between SPTLC1 (western blot) and $A\beta_{42}$ protein levels (from ELISA) (r=0.76, P=0.002, Spearman's correlation) (Figure 7A), and SPTLC2 (western blot) and $A\beta_{42}$ protein levels (r=0.67, P=0.007) (Figure 7B) in the subgroups of control and AD patients. Additionally, statistically significant negative correlations were observed between $A\beta_{42}$ and miR-137 (r=-0.75,

P=0.003), miR-181c (*r*=–0.57, *P*=0.037), miR-9 (*r*=–0.7, *P*=0.007), miR-29a (*r*=–0.64, *P*=0.01) and miR-29b-1 (*r*=–0.569, *P*=0.037) in the subgroups of control and AD patients. Furthermore, I performed gain- and loss-of-function experiments in primary astrocytes derived from transgenic mice expressing the human APP Swedish mutation. In these cells, over-expressing miR-137 or miR-181c down-regulated the endogenous expression levels of SPTLC1 (*P*=0.001) and Aβ (*P*=0.01) (Figure 7D and F). The functional affects were reversed upon transfection with the complementary anti-miRs-137 and -181c (Figure 7C and E). Thus, the loss of the suppressing activity of miR-137 and miR-181c led to increased Aβ production in cell culture. Additionally, transient overexpression of SPTLC1 (*P*=0.033) restored/increased Aβ expression levels in cells co-transfected with miR-137/-181c (*P*=0.005) (Figure 7D and F). In order to assess the direct role of miR-137, miR-181c, and thus SPTLC1 on Aβ expression, "target protectors" were designed against the targeted site on SPTLC1 for miR-137 and miR-181c. Primary astrocytes expressing the human APP Swedish mutation were transiently transfected with miR-137 or miR-181c along with their respective "target protectors" (Figure 7G, H, I and J). Both SPTLC1 and Aβ expression levels decreased significantly upon transfection with miR-137 (Figure 7G and I) or miR-181c (Figure 7H and J) along with a negative target protector. SPTLC1 and Aβ expression levels remained unchanged upon transfection with miR-137 (Figure 7G and I) or miR-181c (Figure 7H and J) along with their respective target protectors. Additionally, the transfection of anti-miR-137 (Figure 7G and I) or anti-miR-181c (Figure 7H and J) significantly increased Aβ and SPTLC1 expression levels.

2.4 DISCUSSION

I found a subgroup of sporadic AD patients exhibited increased levels of ceramides (this study and refs. (Cutler et al., 2004; He et al., 2010)) suggesting that ceramide may be a potential target for the treatment of AD. Increased ceramide levels have been associated with increased neutral SMase (N-SMase) levels in AD where Aβ induced N-SMase (Jana and Pahan, 2010). In this study I observed that the Aβ levels increased with overexpression of SPTLC1. Therefore, ceramide rise through the *de novo* synthesis pathway upregulates Aβ levels, and the Aβ in turn may induce N-SMase activity to reinforce the production of ceramide, and thereby propagate a continual cycle of ceramide-Aβ generation.

I identified that a subgroup of sporadic AD patients exhibit increased levels of ceramides with concomitant increase in SPTLC1 and SPTLC2 protein expression levels in their brain cortices. This coupled with our animal and cell culture studies suggests that SPT may be a novel target for the treatment of AD. Further, *SPTLC1/2* mRNA levels in these AD patient samples did not differ significantly from the levels in the control samples. This in combination with the luciferase assays and primary cell culture data suggests SPTLC1/2 may be post-transcriptionally regulated through miRNAs. Along these lines, I found negative correlations/relationships between the expression levels of miR-137/-181c and SPTLC1, and between miR-9/-29a/b-1 and SPTLC2 protein expressions, in sporadic AD brains, and developing, diet and gender specific mouse brains.

Apart from changes in miRNA expressions, binding sites for the transcription factor NFκB have been identified in the promoter region of *Sptlc2* (Chang et al., 2011). However, this regulation may be tissue- and stimuli-specific as the tested experimental conditions did not

impact brain SPT activity (Memon et al., 2001). Further, a significant increase in SPTLC2 protein levels was observed in human glioma tissue with only a slight increase in *SPTLC2* mRNA (An et al., 2009). Interestingly, miR-29b is downregulated in glioblastomas (Cortez et al., 2010) suggesting miR-29b could be involved in elevating the SPTLC2 protein levels. In this present study I observed that *SPTLC1* and *SPTLC2* mRNA expression levels remained unchanged in the brain cortices of AD patients, as well as in primary astrocytes treated with palmitate and in mice fed a high-fat diet. This was also observed with development and in both genders of mice. Further, correlation analyses coupled with the transfection studies in cells suggest changes in the miRNA levels, miR-137, -181c, -9 and 29a/b-1, could contribute to altered SPTLC1 and SPTLC2 expression levels in this subgroup of sporadic AD patient samples. Of the miRNAs identified to regulate SPT expression, increased expression levels of miR-137 has been shown to induce neurogenesis in hippocampus (Szulwach et al., 2010) while miR-9 is involved in neurogenesis and differentiation (Gao; Coolen and Bally-Cuif, 2009). In addition, (Hebert et al., 2008) and (Cogswell et al., 2008) observed down-regulated miR-9 levels in AD patient brains, whereas (Lukiw, 2007) detected an up-regulation in AD. In contrast, miR-29a/b-1 was observed to be consistently down-regulated by (Hebert et al., 2008), (Wang et al., 2008) and (Shioya et al., 2010) in AD brains. Similarly, (Hebert et al., 2008) also detected down-regulated miR-181c expression levels in these patients. Consistent with these reports I found miR-181c, -9 and 29a/b-1 levels are down-regulated in the frontal cortex of the sub-group of AD patients in this study. In addition, I observed that miR-137 was also down-regulated in the frontal cortex of these 7 AD patients. In support of this, chromosome 1p13.3-q31.1 region which includes the map location of miR-137, chromosome 1p21, has been linked to late-onset-AD (Butler et al., 2009). The map location of miR-181c, chromosome 19p13.13, has also been linked to late-onset-AD

(Butler et al., 2009). I observed the suppression of SPTLC1 by miR-137 and miR-181c reduced Aβ expression levels in a target specific manner while over-expression of *SPTLC1* and inhibition of miR-137 and miR-181c increased Aβ expression levels. This coupled with the fact that over-expression of BACE1 did not increase Aβ levels even though it increased β-CTF levels (Hebert et al., 2008), leaves open a possible role of ceramide, mediated by SPT, in transporting BACE1 and γ-secretase to the lipid rafts for amyloidogenic processing of APP. Inactive BACE1 and γ-secretase resides outside of the lipid rafts under non-pathological settings allowing non-amyloidogenic processing of APP, while under disease state the ceramides facilitate the trafficking of these pathogenic secretases to lipid rafts where they become active to produce Aβ (Cordy et al., 2003; Vetrivel et al., 2005; Ebina et al., 2009). Ceramide also increases Aβ production by stabilizing BACE1 (Puglielli et al., 2003; Costantini et al., 2007; Patil et al., 2007) through increased acetylation (Ko and Puglielli, 2009). MiR-9 and miR-29a/b previously have been identified as potential suppressors of BACE1 and thus associated with sporadic AD (Hebert et al., 2008). Given that SPT is also regulated by miR-9 and miR-29a/b-1, it further strengthens the contribution of SPT to the etiology of sporadic AD.

Of the miRNAs identified to regulate SPTLC1 expression, miR-137 was shown to be negatively regulated in adult neural stem cells, epigenetically and transcriptionally by MeCP2 and Sox2 through direct binding to the 5' regulatory region (Szulwach et al., 2010). Research conducted to treat Rett syndrome, a disease caused by mutations in MeCP2, indicates that a high-fat diet may increase MeCP2 levels (Haas et al., 1986; Liebhaber et al., 2003), providing a potential explanation for the reduced miR-137 levels in mice fed a high-fat diet. The other miRNA identified to regulate SPTLC1, miR-181c, is positively regulated by Akt1 at the transcriptional level (Androulidaki et al., 2009). Akt activity is reduced in response to high-fat

diet (Tremblay et al., 2001), providing a possible mechanism for our observations that miR-181c expression levels are reduced in mice fed a high-fat diet. Of the miRNAs identified to regulate SPTLC2 expression, miR-9 is negatively regulated by RE1-silencing transcription factor (REST) but positively regulated by cAMP-response element binding protein (CREB) (Laneve et al., 2010). High-fat has been shown to suppresses CREB protein expression in the liver (Inoue et al., 2005) providing a possible explanantion for the reduced miR-9 expression levels observed in high-fat diet fed mice.

Many studies suggest that dysregulation of miRNA expression is aging-associated, and contributes to AD (Niwa et al., 2008). Additionally, increased DNA methylation have led to down-regulated expressions of miR-137 (Langevin et al., 2010) and miR-29 family (Koturbash et al., 2011) in females, indicative of differential expression of miRNA in a gender-specific manner and further supporting our observations in the mice study. Furthermore, maternal high-fat diet has been shown to influence differential expression of mouse hepatic miRNAs in offsprings including down-regulation of miR-29a (Zhang et al., 2009). I observed a reduction of miR-137, -181 and -29a/b-1 expressions in females compared to males and a down-regulation of miR-137, -181c and -9 expression levels with high dietary fat intake. This raises an intriguing possibility that women consuming high-fat diets may be at higher risk for SPT dysregulation and thus AD. Therefore, our results lend support to epidemiological factors such as age, gender and diet epigenetically regulating miRNAs and contributing to loss-of-function of miR-137, -181c, -9 and 29a/b-1, resulting in reduced suppression of SPT expression, and thereby increasing the ceramide levels and Aβ generation seen in sporadic AD.

Group	Ref #	Age	Sex	Braak Stage	PMI	MMSE score	Front NP count	Front NFT count	ApoE allele
Control	1132	95	F	0	3.50	26	3	0	3/4
Control	1159	86	F	0	3.50	28	0	0	3/3
Control	1165	92	M	0	3.33	28	10	0	3/3
Control	1187	85	F	0	2.50	28	0	0	3/3
Control	5163	96	M	2	7.25	27	0	0	2/3
Control	1206	94	F	2	2.25	27	0	0.4	3/3
Control	1221	81	M	2	2.83	29	5.6	0	3/3
AD	1013	80	M	5	2.50		5.8	1	
AD	1073	83	F	5	4.00	4	8.6	3.4	2/4
AD	1098	81	F	5	2.75	15	6.2	2	3/3
AD	1174	96	M	5	3.50	22	19.2	4	2/3
AD	1194	99	F	5	2.10	16	15.4	3.4	3/4
AD	1201	94	M	5	2.00	22	6	0.2	3/3
AD	1215	91	F	5	3.00	13	15.2	7.2	3/3

Table 1: Patient information. Patient information including reference number (Ref #) age, gender, braak stage, post mortem interval (PMI), MMSE score, neuritic plaque (NP) count, neurofibrillary tangle (NFT) count and ApoE genotype. This information was provided by the University of Kentucky (UK) Alzheimer's disease center tissue bank (ADC).

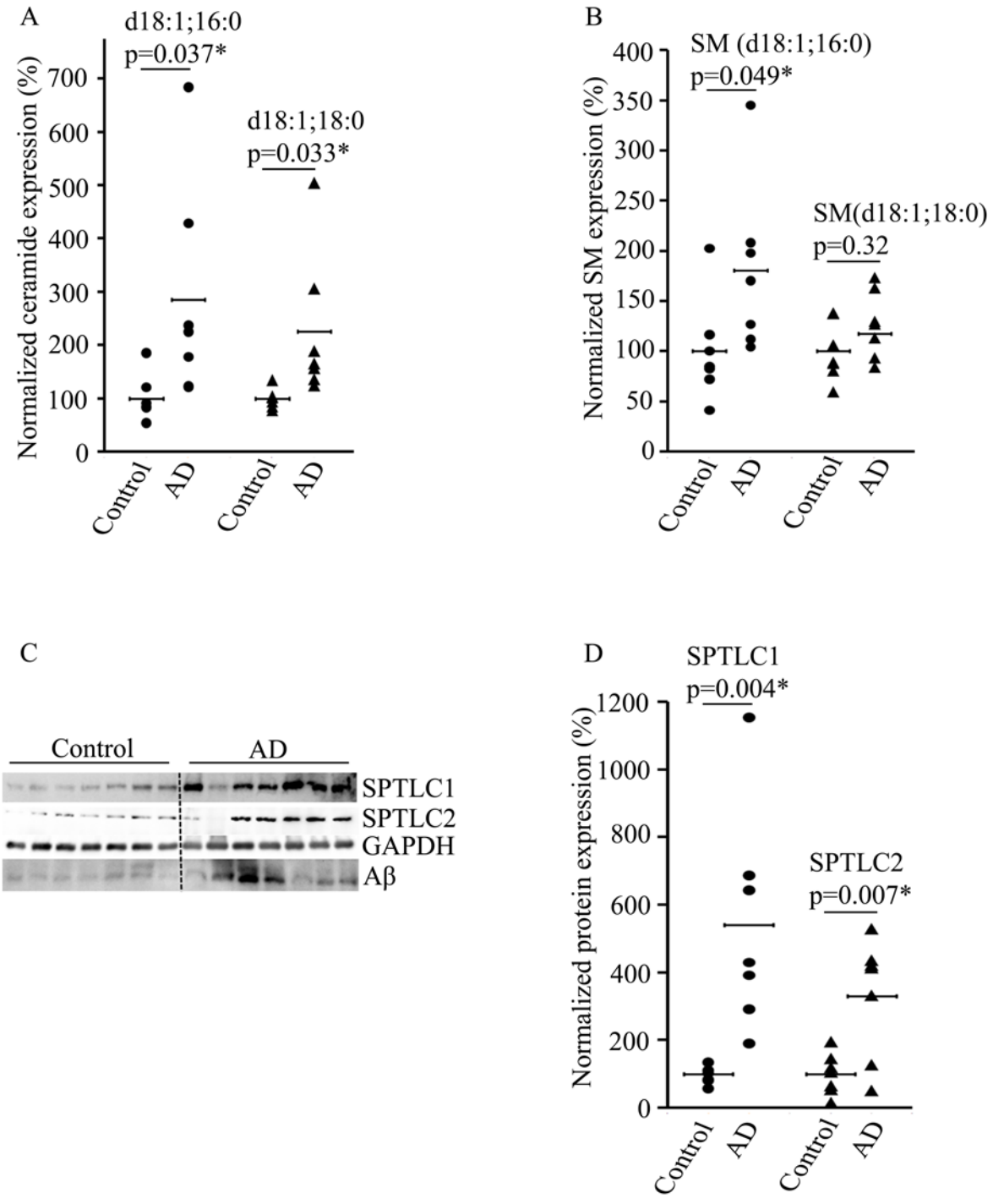

Figure 1: SPTLC1 and SPTLC2 are up-regulated in sporadic AD brain. **(A)** Ceramide levels, d18:1; 16:0 and d18:1; 18:0 were significantly increased in the subgroup of AD patients

Figure 1 (cont'd)

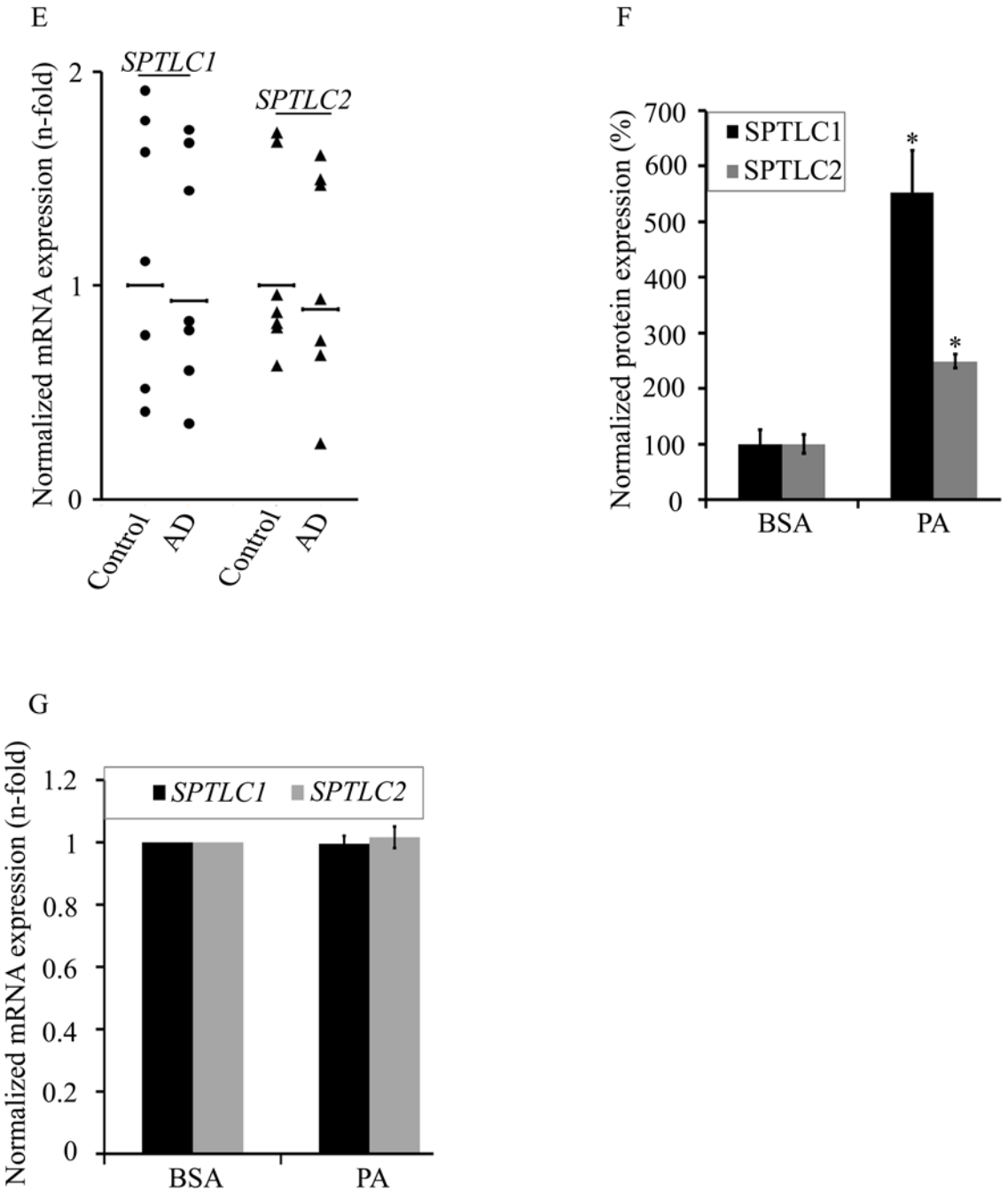

(Figure 1 legend continues) (n=7). **(B)** Sphingomyelin d18:1; 16.0 were significantly increased while d18:1; 18:0 levels were unchanged in the subgroup of AD patients. The frontal brain cortices were analyzed via tandem mass spectrometry and the normalized concentrations are

Figure 1 (cont'd)

(Figure 1 legend continues) shown as a percentage of the average control (n=7). The samples were normalized to internal standard (d18:1, 12:0) concentration and to brain total protein concentration. **(C)** Western blot of SPTLC1 (probed with LCB1 antibody), SPTLC2 and Aβ-3kDa fragment (probed with 4G8 antibody), See Table 1 for neuritic plaque numbers in individual brains. **(D)** SPTLC1 and SPTLC2 protein levels of frontal cortices of control brains (n=7) vs. sporadic AD brains (n=7) were determined by western blotting and the expression levels were quantified by normalizing to GAPDH and is represented as a percentage of the control brain average expression. **(E)** qRT-PCR of *SPTLC1* and *SPTLC2* mRNA from control (n=7) and sporadic AD patients (n=7). Relative expressions shown are normalized to *GAPDH* and control brain average expressions. **(F)** SPTLC1 and SPTLC2 protein quantification of wild-type primary rat astrocytes treated with palmitate for 24 hrs. Error bars represent standard error derived from three independent experiments and normalized to β-Actin and represented as a percentage of the control treatment (BSA) expression (*, $p<0.05$). **(G)** qRT-PCR of *Sptlc1* and *Sptlc2* mRNA from wild-type primary rat astrocytes treated with palmitate and BSA. Relative expressions shown are normalized to *Gapdh* and expressions in BSA control treatment. Error bars represent standard error derived from six or more independent experiments. The statistical significance between control and AD brains, and palmitate and BSA treatments, were determined by 2-tailed student *t* tests.

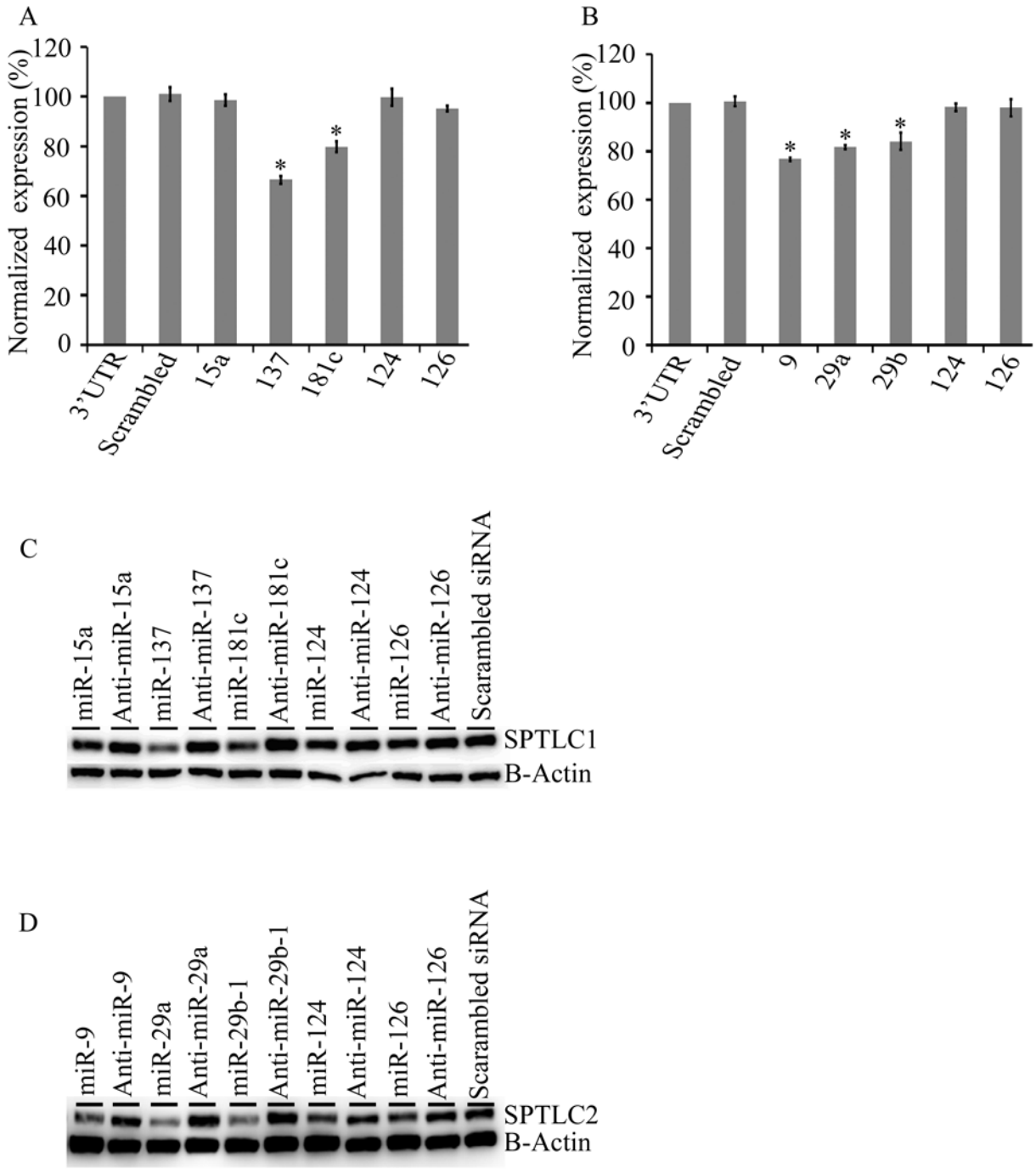

Figure 2: SPTLC1 and SPTLC2 are miRNA targeted genes. **(A)** Human *SPTLC1* 3'UTR luciferase and Renilla luciferase constructs were transfected into wild-type rat primary astrocytes with the indicated miRNA oligonucleotides at a final concentration of 100 nM. Normalized (to Renilla) sensor luciferase activity is shown as a percentage of the *SPTLC1* 3'UTR plasmid. Error

Figure 2 (cont'd)

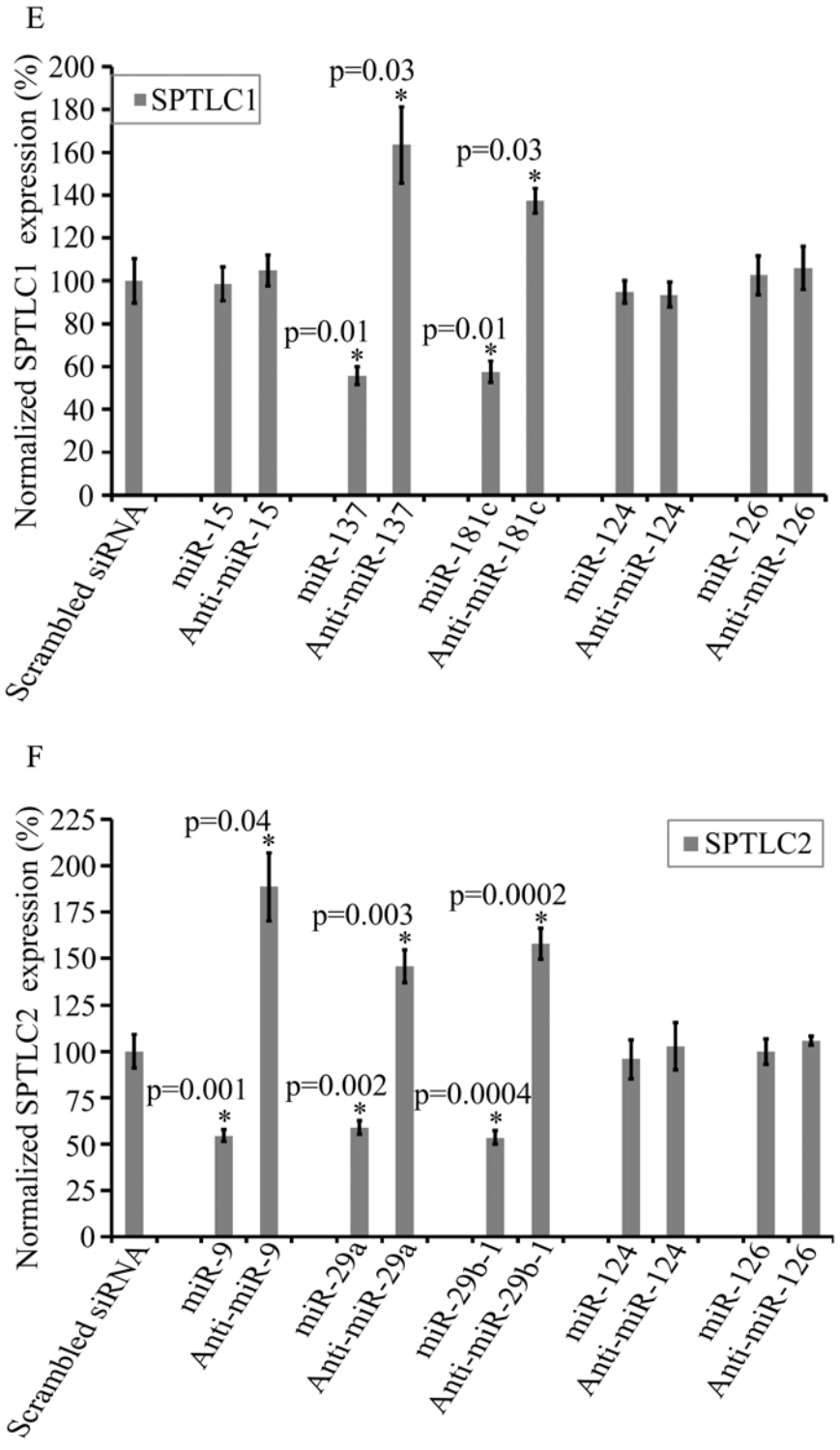

(Figure 2 legend continues) bars represent standard errors derived from three or more experiments (*, $P<0.02$). **(B)** Human *SPTLC2* 3'UTR luciferase and Renilla luciferase constructs

Figure 2 (cont'd)

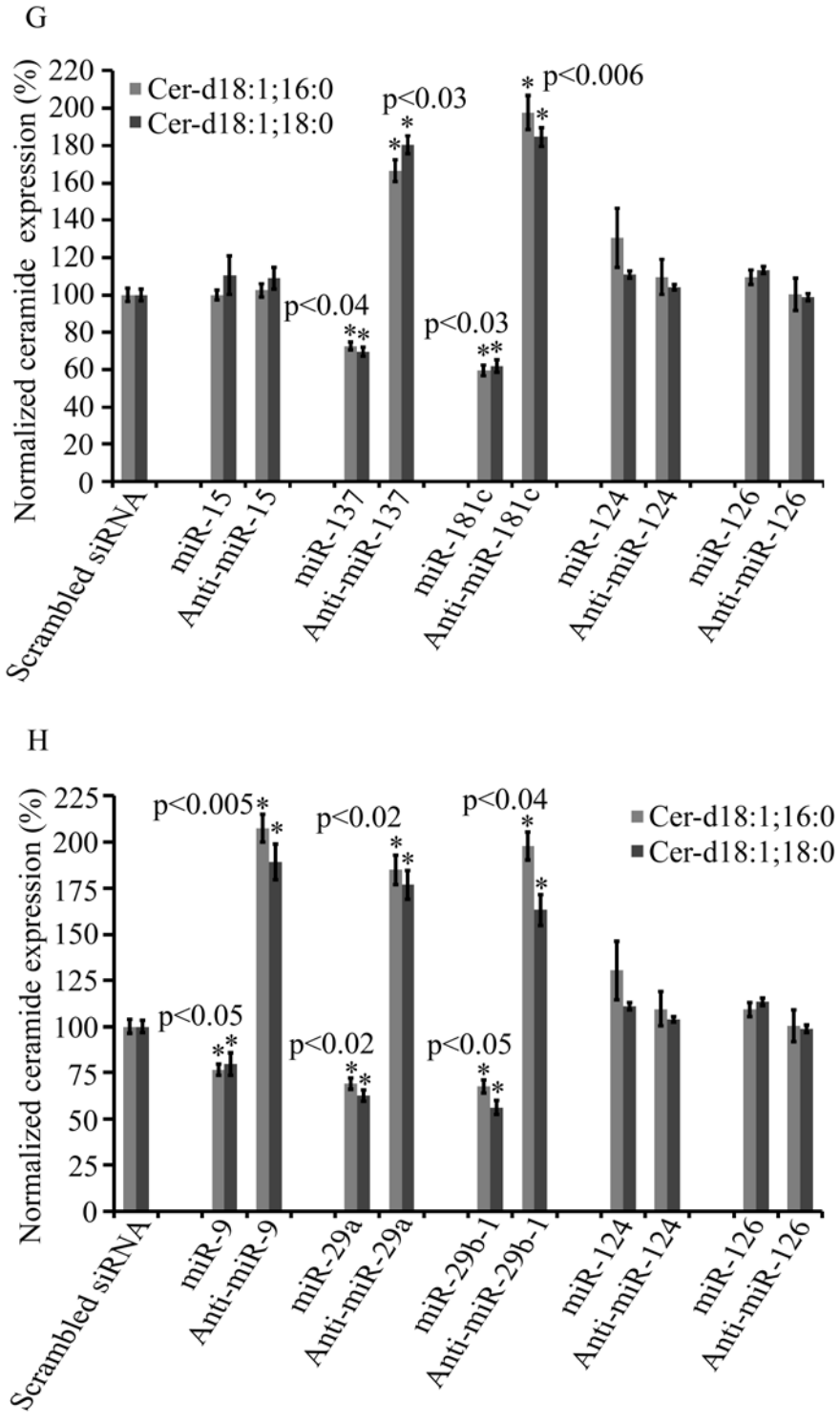

(Figure 2 legend continues) were transfected into wild-type rat primary astrocytes with the

Figure 2 (cont'd)

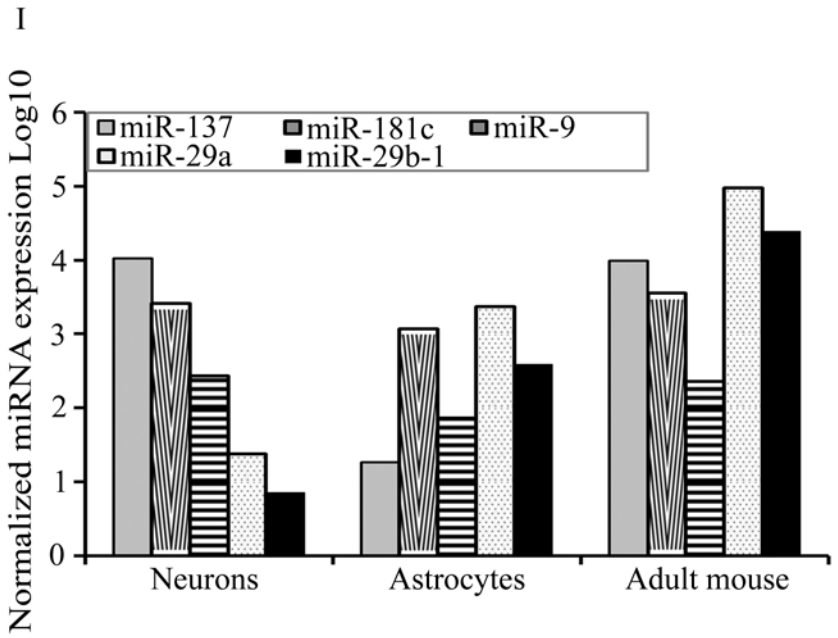

(Figure 2 legend continues) indicated miRNA oligonucleotides at a final concentration of 100 nM. Normalized (to Renilla) sensor luciferase activity is shown as a percentage of the *SPTLC2* 3'UTR plasmid. Error bars represent standard errors derived from four or more experiments (*, $P<0.007$). **(C)** and **(D)** Representative western blot analysis of endogenous SPTLC1 (probed with LCB1) and SPTLC2 in wild-type primary astrocytes treated with 100nM (final concentration) of miRNA (oligonucleotides) or anti-miRs (anti-sense), with scrambled siRNA as controls. **(E)** and **(F)** Quantification of endogenous SPTLC1 and SPTLC2 protein levels by normalizing to β-actin or GAPDH. **(G)** and **(H)** Cellular ceramide levels of primary rat astrocytes transfected with miRs or anti-miRs. Cellular ceramide levels were analyzed via tandem mass spectrometry and the normalized concentrations are shown as a percentage of the scrambled siRNA. The samples were normalized to internal standard (d18:1, 12:0) concentration and to cellular total protein concentration. Error bars represent standard errors derived from three or more experiments conducted with 48-72 hr transient transfections. **(I)** Cellular wild-type rat

Figure 2 (cont'd)

(Figure 2 legend continues) primary astrocytes, neurons, and 6 month old mouse brain cortical endogenous miRNAs expression levels were quantified by qRT-PCR. Relative expressions shown are normalized to RNU6B. Statistical significance between scrambled siRNA and candidate miRs treated primary astrocytes was determined by 2-tailed student *t* tests.

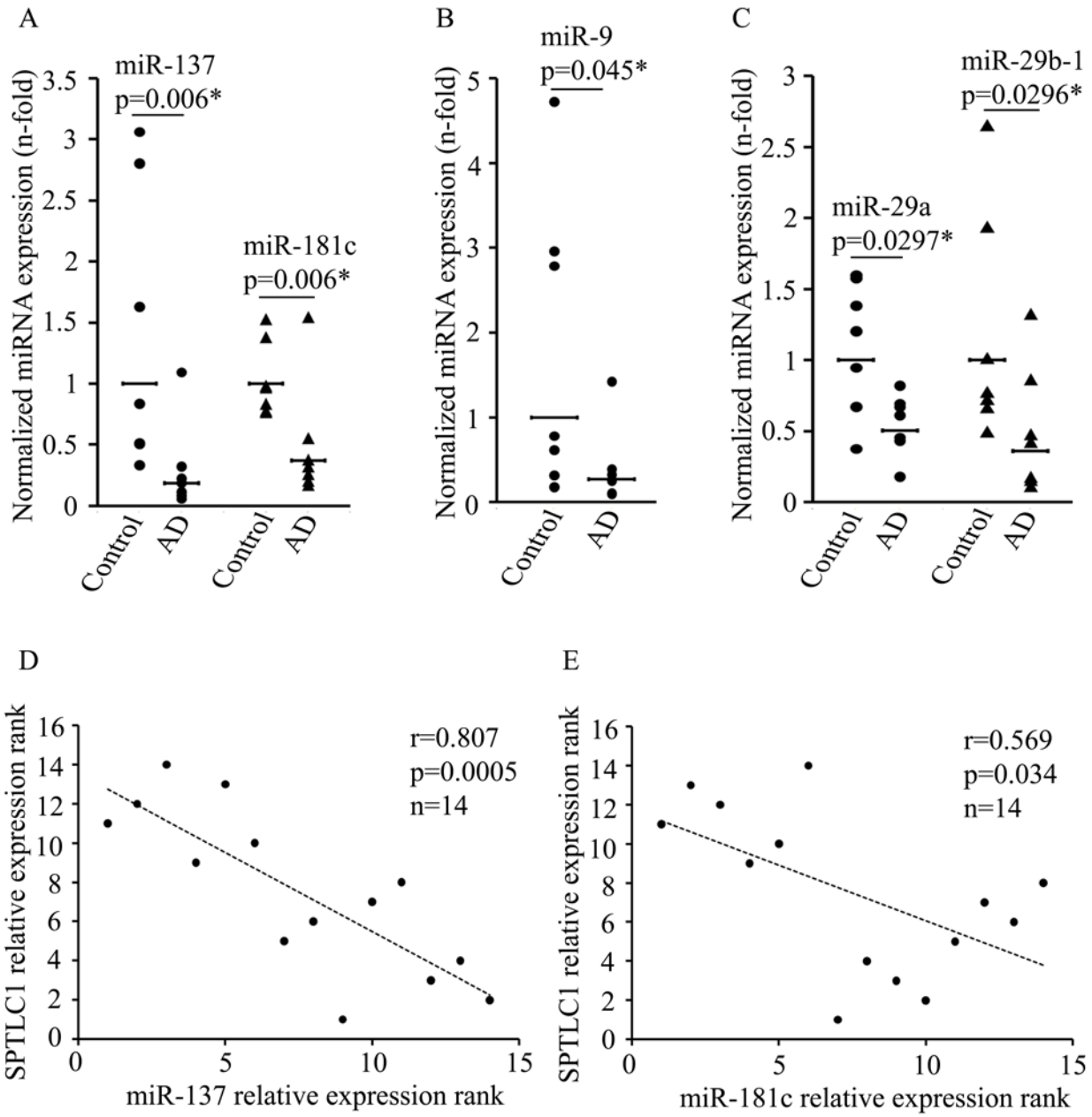

Figure 3: **Misregulation of miR-137,-181c,-9 and -29a/b-1 in AD brain. (A)** miR-137, -181c, **(B)** -9, and **(C)** -29a and -29b-1 levels were quantified by qRT-PCR in controls (n=7) and AD (n=7) frontal brain cortices. Relative expressions shown are normalized to RNU6B and average control brain expressions. The statistical significance between control and AD brains were determined by 2-tailed student *t* tests. **(D-E)** Spearman's correlation test demonstrates significant

Figure 3 (cont'd)

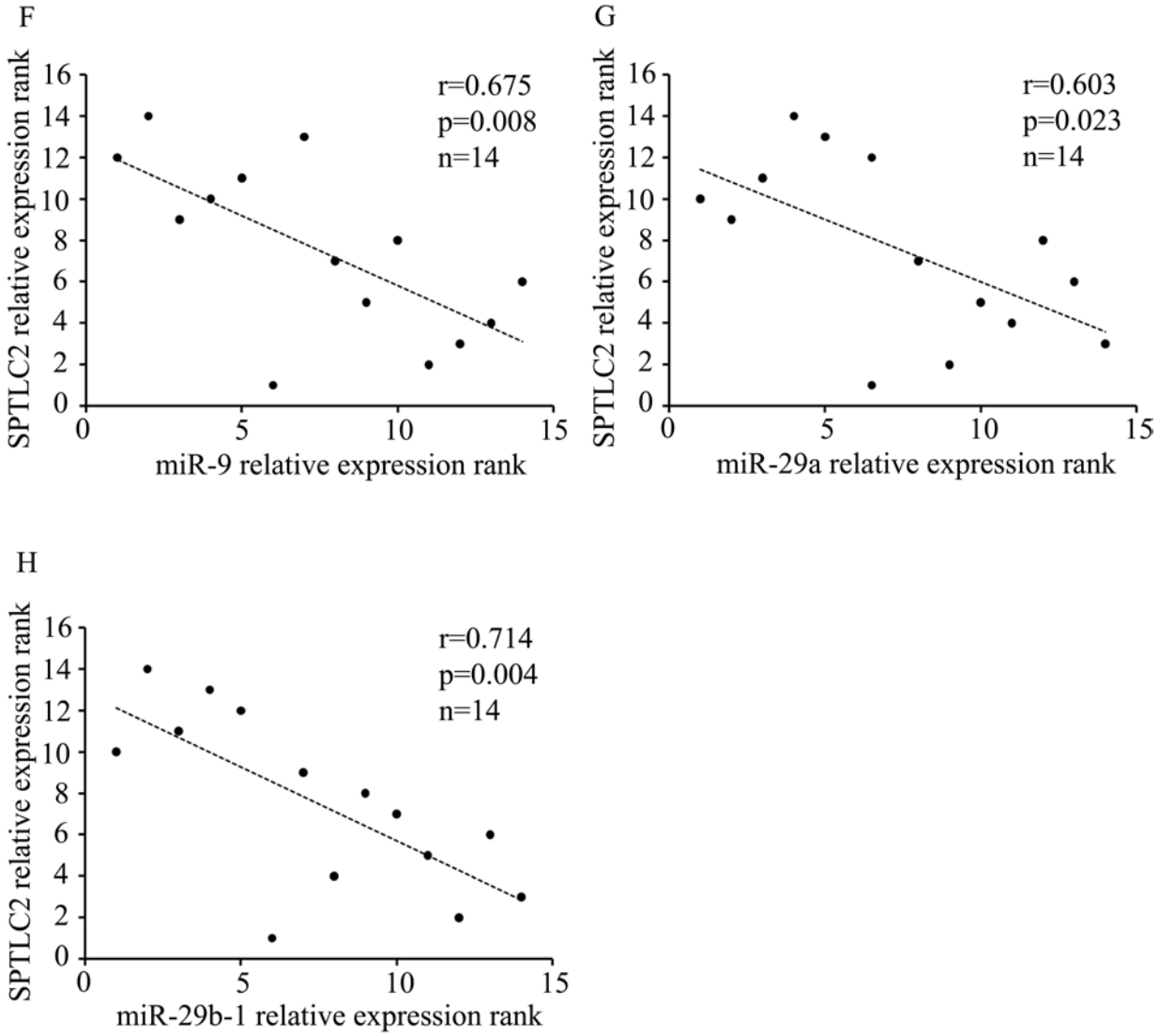

(Figure 3 legend continues) negative correlation between miR-137, -181c and SPTLC1 expression in the entire sample set (control and AD) (n=14). **(F-H)** Spearman's correlation test demonstrates significant negative correlation between miR-9, -29a, -29b-1 and SPTLC2 expression in the entire sample set (control and AD) (n=14). The significance of the correlation was determined by two-tailed T distribution tests.

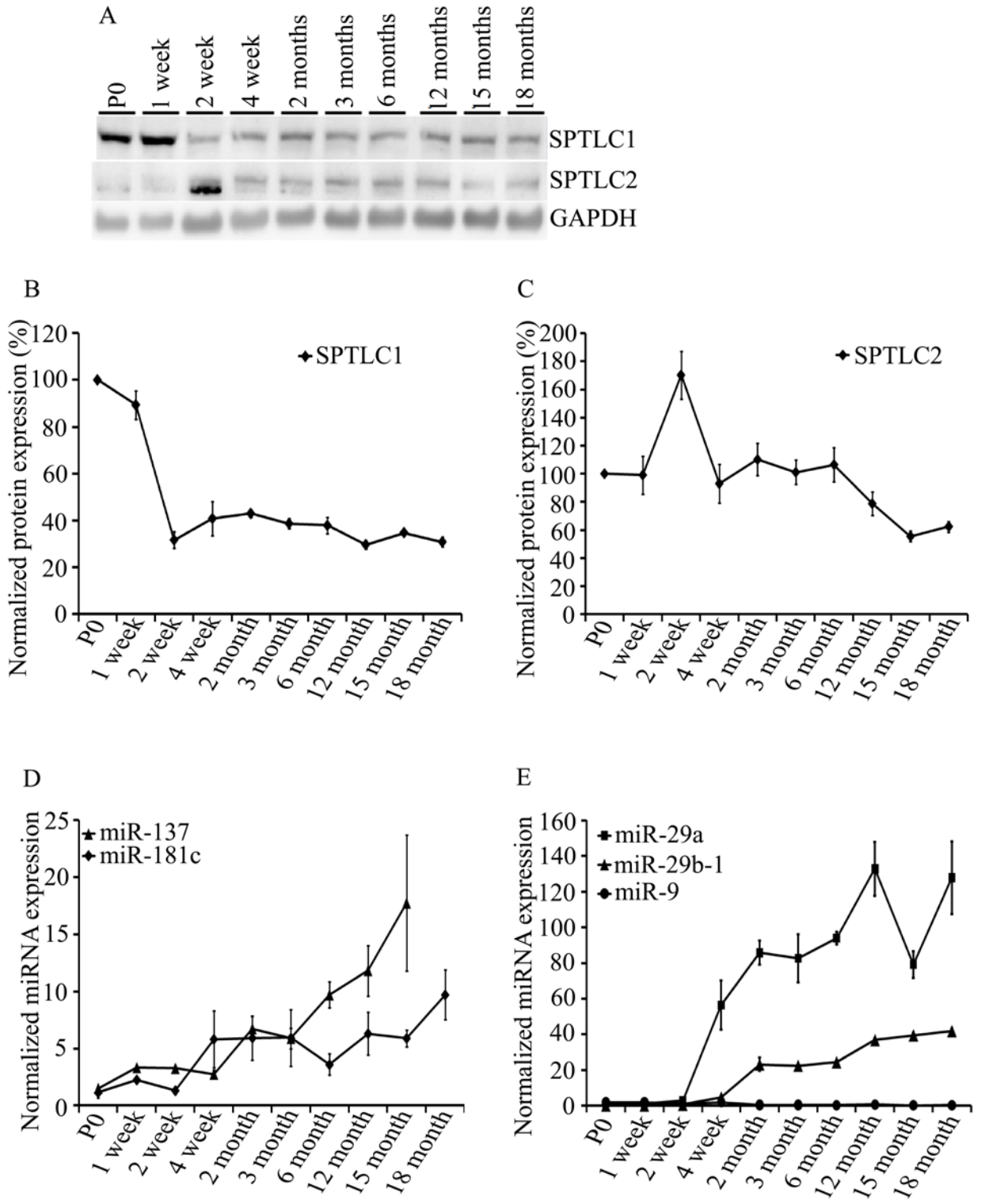

Figure 4: Developmental co-regulation of miR-137,-181c, -29a, 29b-1, SPTLC1 and SPTLC2. (A) Western blot analysis of SPTLC1 and SPTLC2 of postnatal day 0 (P0) to 18

Figure 4 (cont'd)

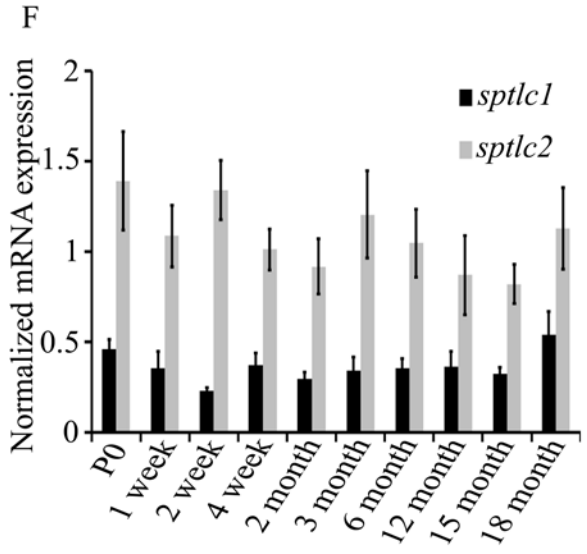

(Figure 4 legend continues) month old mouse brain cortices (n=3 for each age group). *Gapdh* was used as the loading control. **(B)** Quantification of SPTLC1 expression from Western blots normalized to GAPDH and the average expressions represented as a percentage of average P0 expression. **(C)** Quantification of SPTLC2 expression from Western blots normalized to GAPDH (n=3 for each age group) and the average expressions represented as a percentage of average P0 expression. **(D)** Relative expression levels of miR-137, and -181c, **(E)** -9, -29a and -29b-1 were measured by qRT-PCR in mouse brain cortices with RNU6B used as the normalizing control. **(F)** Relative mRNA expression levels of *Sptlc1* and *Sptlc2* were measured by qRT-PCR with *Gapdh* as the normalizing control.

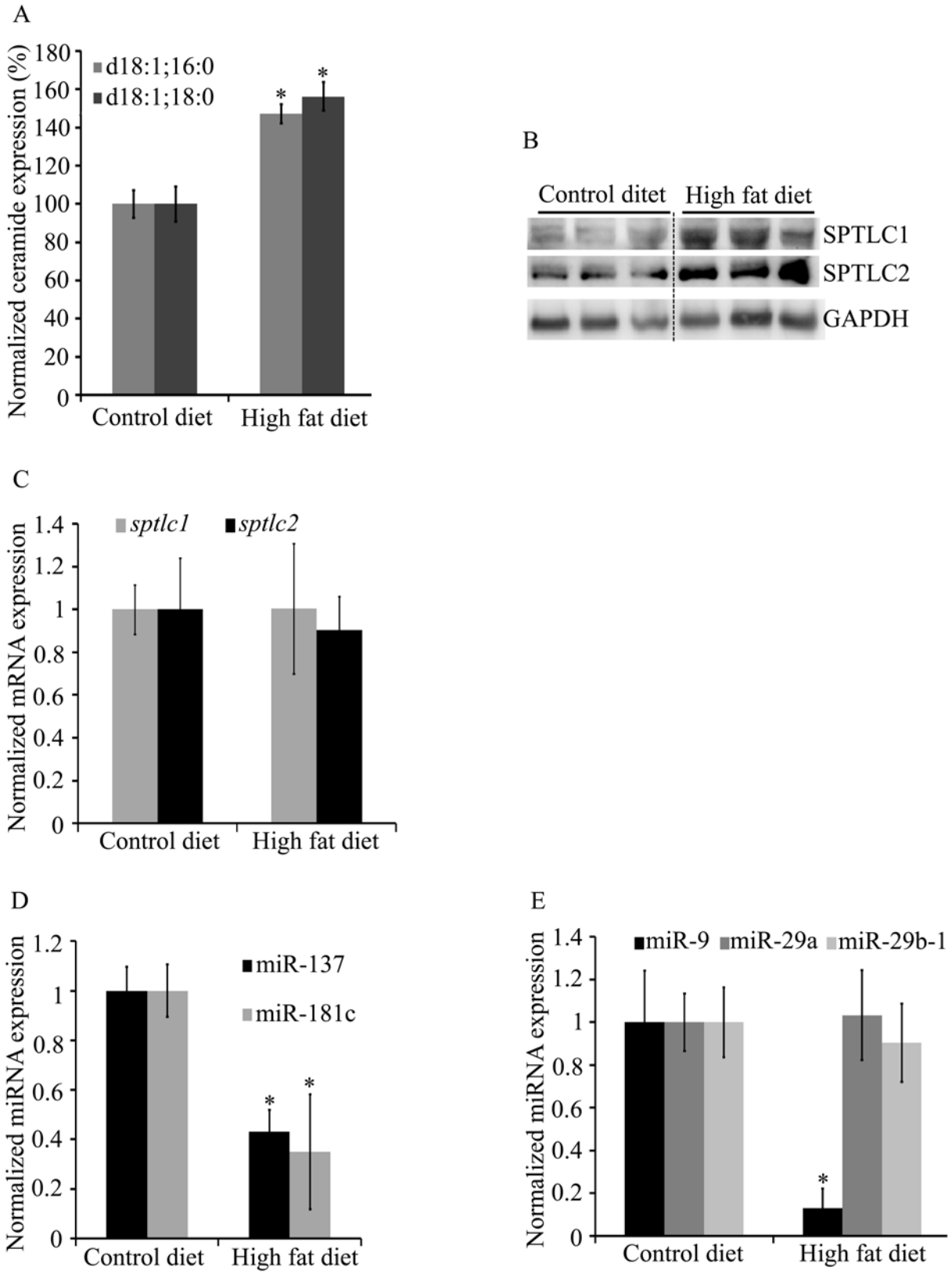

Figure 5: Regulation of miR-137,-181c, -9, SPTLC1 and SPTLC2 with diet. Male wild-type

Figure 5 (cont'd)

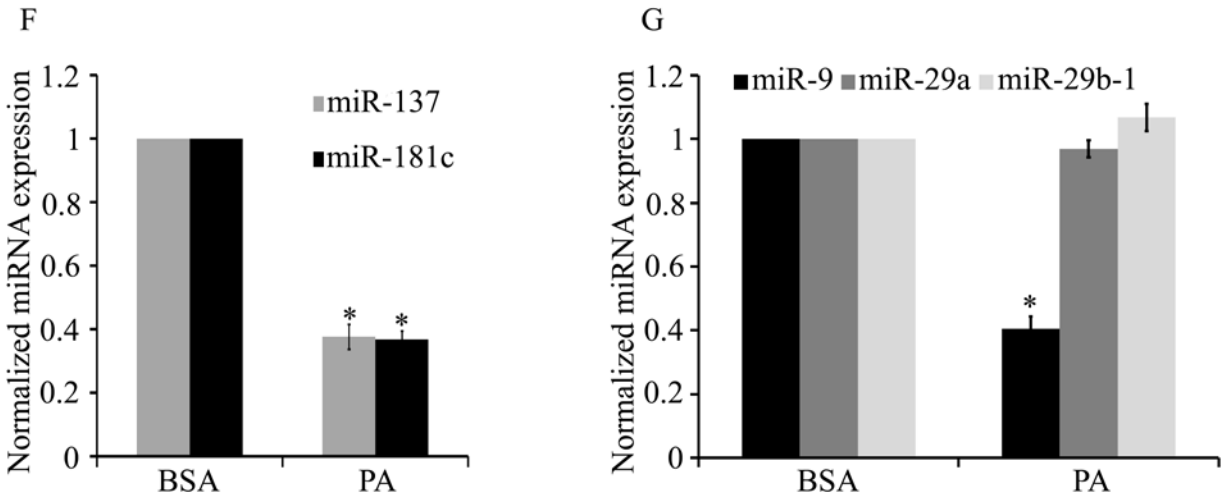

(Figure 5 legend continues) mice were fed a 60%kcal diet for a period of 5 months starting at 4 months of age. **(A)** Ceramide levels, d18:1; 16:0 and d18:1; 18:0 were significantly increased in mice fed a high-fat diet (n=3). The brain cortices were analyzed via tandem mass spectrometry and the normalized concentrations are shown as a percentage of the average control chow diet fed mice (n=3). The samples were normalized to internal standard (d18:1, 12:0) concentration and to brain total protein concentration. **(B)** Western blot analysis of SPTLC1 and SPTLC2 in brain cortices of mice fed a control diet (n=3) or high-fat diet (n=3). GAPDH was used as the loading control. **(C)** *Sptlc1* and *Sptlc2* mRNA expression levels were measured by qRT-PCR. Relative expressions shown are normalized to *Gapdh* and average expression levels in the chow control diet. **(D** and **E)** The expression levels of miR-137, -181c, -9, (*, $P<0.04$) -29a and -29b-1 in high-fat diet fed mice cortices were measured by qRT-PCR. Relative expressions shown are normalized to RNU6B and average chow control diet expressions. **(F** and **G)** The expression levels of miR-137, -181c, -9, (*, $P<6.0E-05$) -29a and -29b-1 in palmitate-treated astrocytes were measured by qRT-PCR. Relative expressions shown are normalized to RNU6B and BSA control

Figure 5 (cont'd)

(Figure 5 legend continues) treatment expressions. Error bars represent standard errors derived from 6 or more experiments. The statistical significance between control chow diet and high-fat diet, and palmitate and BSA treatments, were determined by 2-tailed student *t* tests.

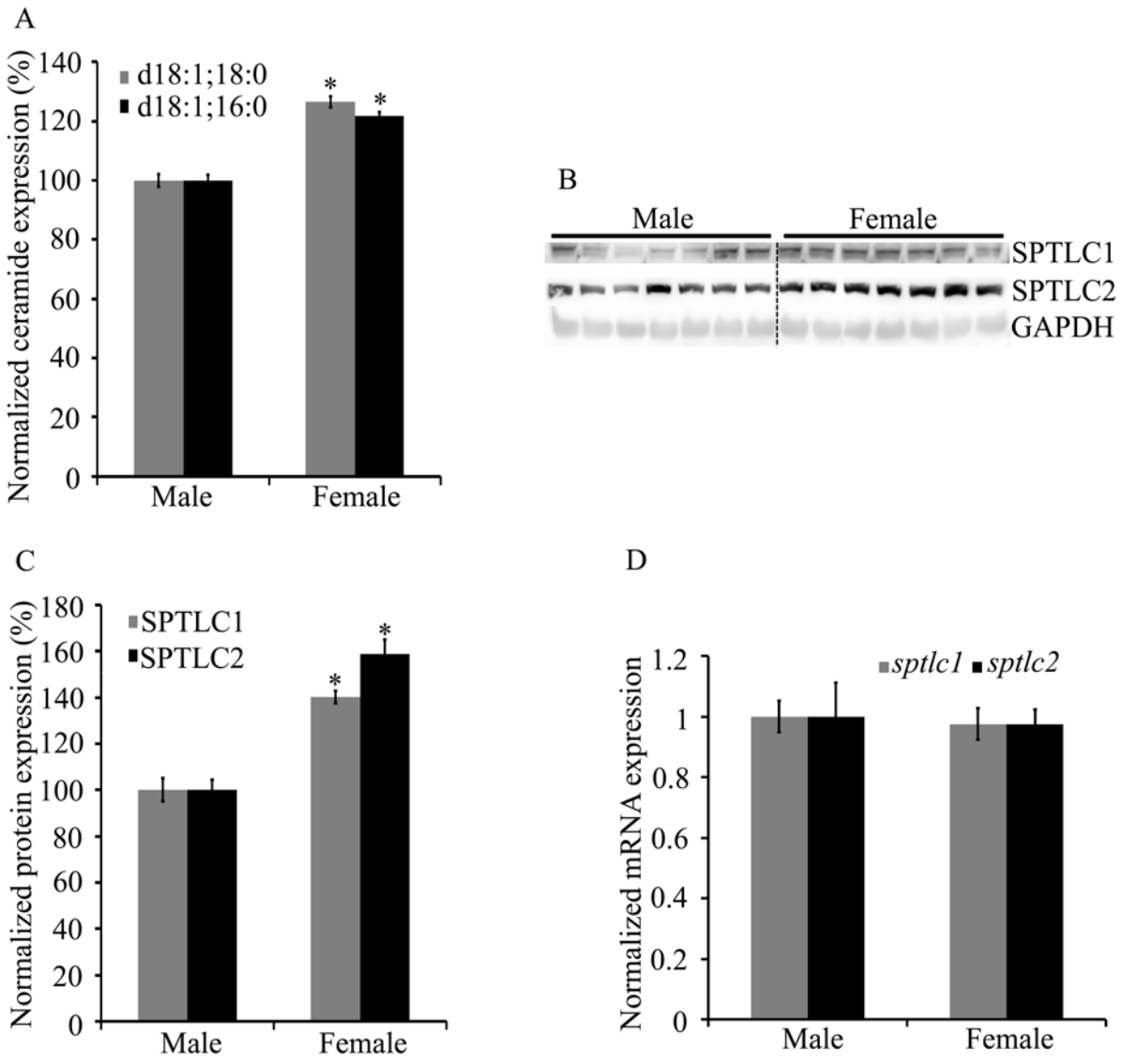

Figure 6: Gender specific differential regulation of miR-137, -181c, -29a, 29b-1, SPTLC1 and SPTLC2. **(A)** Ceramide, d18:1; 18: and d18:1; 16:0 were measured in 9 month old male (n=7) and female (n=7) wild-type mice brain cortices by tandem mass spectrometry and the normalized concentrations are shown as a percentage of the males (n=7). The samples were normalized to internal standard (d18:1, 12:0) concentration and to brain total protein concentration (*, $P<0.005$). **(B** and **C)** SPTLC1 and SPTLC2 protein quantification from Western blots of the brain cortices of females normalized to GAPDH and the average expression

Figure 6 (cont'd)

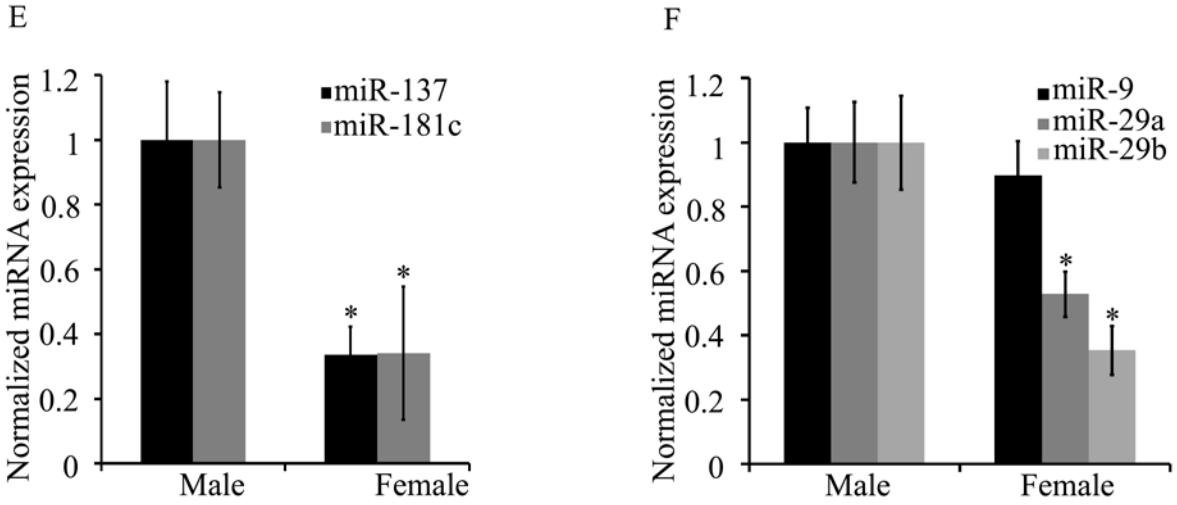

(Figure 6 legend continues) levels represented as a percentage of the average male expression levels (*, $P<0.02$). **(D)** *Sptlc1* and *Sptlc2* mRNA expression levels were measured by qRT-PCR. Relative expressions shown are normalized to *Gapdh* and average male expressions. **(E)** The expression levels of miR-137 and -181c (*, $P<0.04$) and **(F)** miR-29a/b-1 (*, $P<0.04$) and -9 were measured by qRT-PCR. Relative expressions shown are normalized to RNU6B and average male expressions. The statistical significance between male and female expressions was determined by 2-tailed student *t* tests.

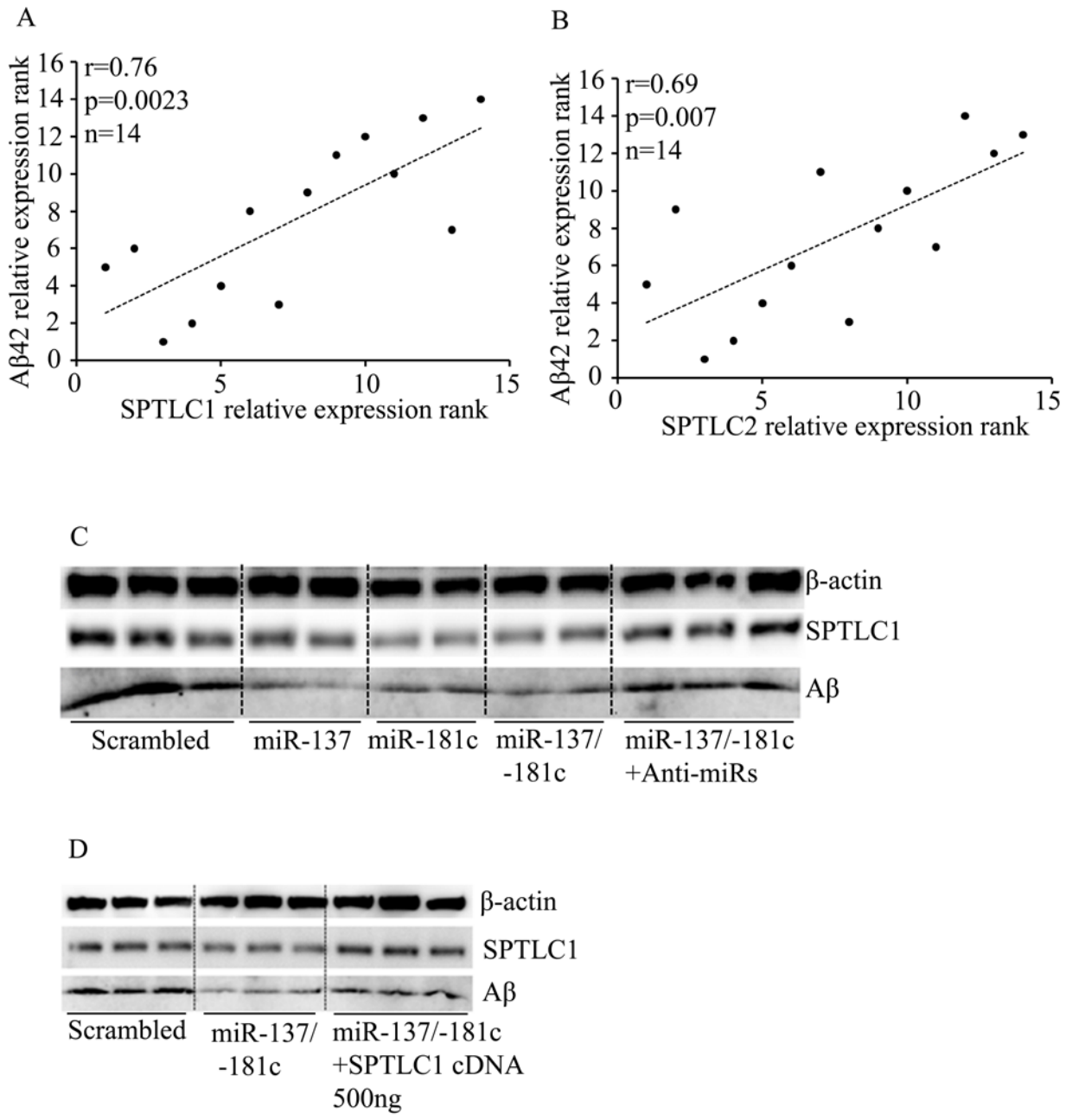

Figure 7: Modulation of SPTLC1 and Aβ by miR-137 and -181c. Spearman's correlation test demonstrates significant positive correlation between **(A)** SPTLC1 protein (western blot) and $A\beta_{42}$ protein (ELISA) expressions, and **(B)** SPTLC2 protein (western blot) and $A\beta_{42}$ protein (ELISA) expressions in the brain cortices of the subgroup of samples (control and AD) (n=14).

Figure 7 (cont'd)

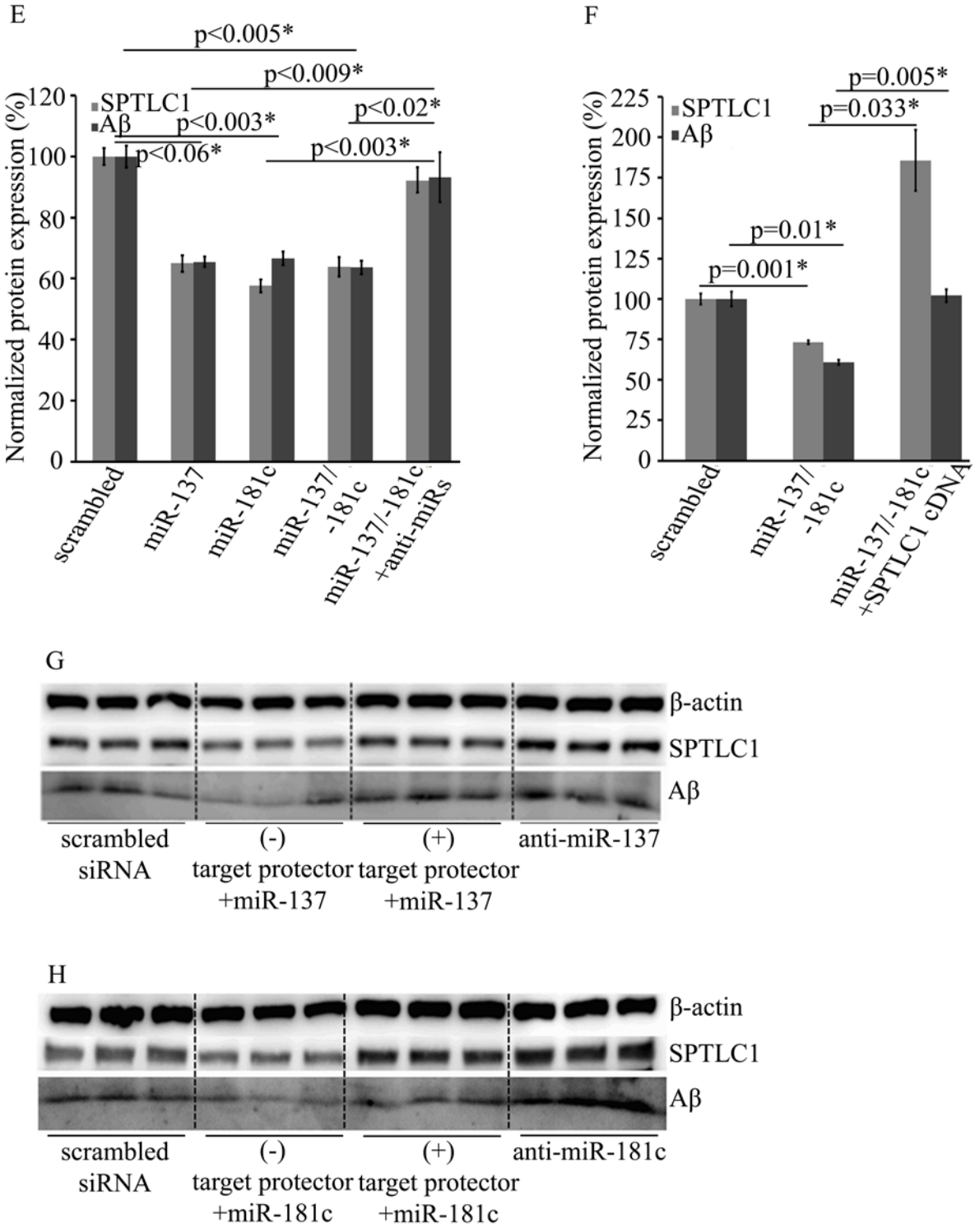

(Figure 7 legend continues) The significance of the correlation was determined by two-tailed T

Figure 7 (cont'd)

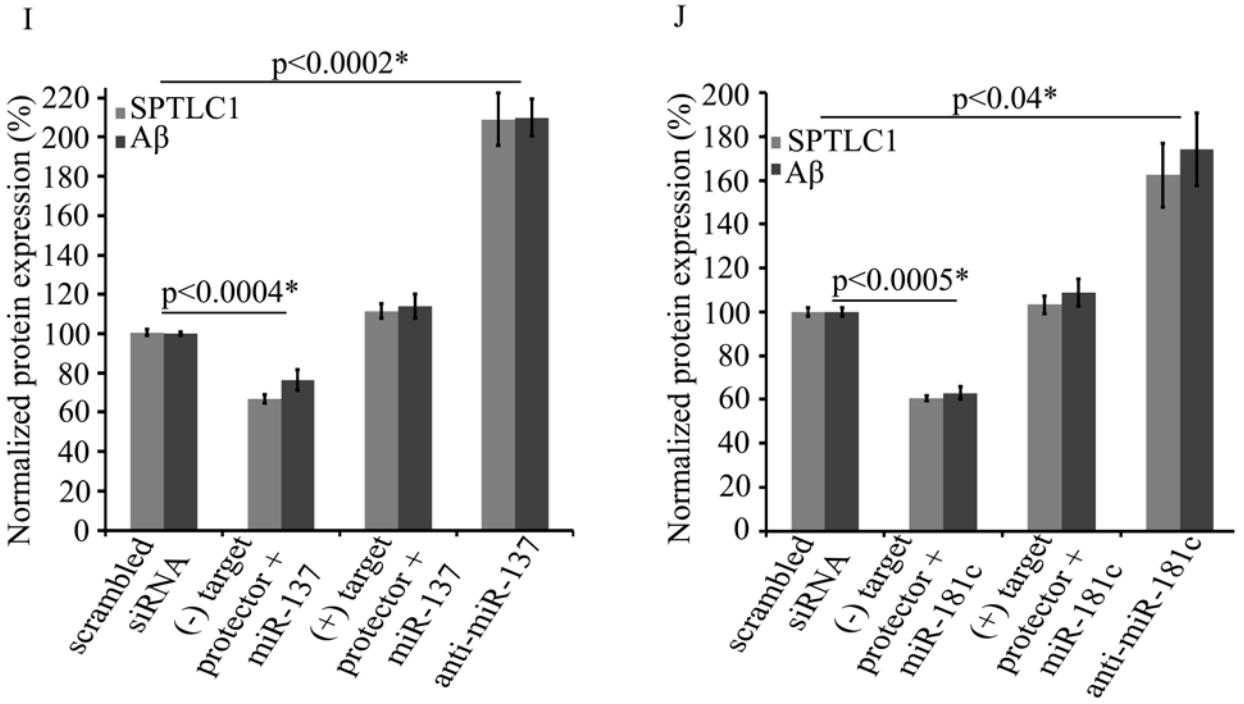

(Figure 7 legend continues) distribution tests. **(C** and **E)** Western blot analysis of SPTLC1 (probed with LCB1 antibody) and cellular Aβ (3kD-probed with Aβ antibody) levels in primary astrocytes expressing APP Swedish mutation following transfection with miRs alone or in combination with anti-miRs. **(D** and **F)** Western blot analysis of SPTLC1 (probed with LCB1 antibody) and cellular Aβ (3kD-probed with Aβ antibody) levels in primary astrocytes expressing APP Swedish mutation following transfection with miRNA alone or in combination with human *SPTLC1* cDNA. **(G** and **I)** miR-137 along with either negative or positive "target protectors" or anti-miR-137, and **(H** and **J)** miR-181c along with either negative or positive "target protectors" or anti-miR-181c were transfected into primary astrocytes expressing APP Swedish mutation. β-actin or GAPDH was used as the loading controls. Error bars represent standard errors derived from three or more experiments conducted with 48 hr transfections (final

Figure 7 (cont'd)

(Figure 7 legend continues) concentration of 100 nM). Statistical significance between scrambled siRNA and candidate miRs treated primary astrocytes were determined by 2-tailed student *t* tests.

CHAPTER 3: BLOOD SERUM MIRNA: NON-INVASIVE BIOMARKERS FOR ALZHEIMER'S DISEASE

Publication: **Geekiyanage, H**., Jicha, G. A., Nelson, P. T., Chan, C., 2012. Blood serum miRNA: Non-invasive biomarkers for Alzheimer's disease. ***Experimental Neurology*** 235(2): 491-6

ABSTRACT

There is an urgent need to identify non-invasive biomarkers for the detection of sporadic Alzheimer's disease. I previously studied miRNAs in AD autopsy brain samples and reported a connection between miR-137, -181c, -9, -29a/b and AD, through the regulation of ceramides. In this study, the potential role of these miRNAs as diagnostic markers for AD was investigated. I identified that these miRNAs were down-regulated in the blood serum of probable AD patients. The levels of these miRNAs were also reduced in the serum of AD risk factor models. Although the ability of these miRNAs to conclusively diagnose for AD is currently unknown, our findings suggest a potential use for circulating miRNAs, along with other markers, as non-invasive and relatively inexpensive biomarkers for the early diagnosis of AD, however, with further research and validation.

Keywords: Alzheimer's disease, microRNA, blood serum

3.1 Introduction

Alzheimer's disease is the most common cause of dementia with a worldwide population of over 24 million, a number expected to double in the next 15 years (Ferri et al., 2005). Early and accurate diagnosis of AD is crucial, enabling early treatments to slow or delay the progression of the disease and provide prognostic information. Current methods of neuro-imaging biomarkers include magnetic resonance imaging (MRI) structural analyses (Barber; Mungas et al., 2002). However, the sensitivity of these imaging techniques does not afford sufficient demarcations in the medical temporal atrophy between AD and non-AD dementia to provide clear and decisive diagnosis (Wahlund et al., 2000; Scheltens et al., 2002). Functional neuro-imaging techniques have been developed for probable diagnosis (Ballard et al., 2011), but again with insufficient accuracy in discriminating between AD and control individuals (Dougall et al., 2004). Even though positron emission tomography (PET) (PiB) imaging has been able to distinguish cases with probable AD from normal and non-AD cases, wide variations in sensitivity and specificity have been reported (Patwardhan et al., 2004). Aβ (Sjogren et al., 2002) and hyperphosphorylated tau (de Souza et al., 2011) levels in the cerebrospinal fluid (CSF) have also been suggested as diagnostic markers for AD and show great promise. However, the ability to identify biomarkers through less invasive procedures, such as in a blood test, would be significant. Attempts to measure Aβ levels in blood, thus far, have led to inconsistent results (Irizarry, 2004; Blennow et al., 2010; Hampel et al., 2010; Ballard et al., 2011; Hansson et al., 2011).

In addition to proteins, blood serum contains circulating miRNAs, endogenous small RNAs of 21–25-nucleotides that post-transcriptionally regulate gene expressions (Lagos-Quintana et al., 2001). MiRNAs have been reported to be transported in blood in liposomes

(Kosaka et al., 2010), high density lipoproteins (Vickers et al., 2011), Argonaute2 (Arroyo et al., 2011; Turchinovich et al., 2011), and other proteins (Wang et al., 2010a), protecting them from being degraded. Recently, circulating miRNA levels have been proposed as potential diagnostic tools for a number of diseases (Gilad et al., 2008; Wang et al., 2010a; Zeng et al., 2011). MiRNAs have been shown to be differentially expressed in AD patients (Lukiw, 2007; Cogswell et al., 2008; Hebert et al., 2008; Wang et al., 2008) and altered in response to Aβ (Schonrock et al., 2010). In the previous study I showed that miR-137, -181c, -9 and -29a/b are involved in AD by modulating ceramide levels (Geekiyanage and Chan, 2011). I showed that ceramides, a sphingolipid, are increased in the brain cortices of a subgroup of sporadic AD patients along with SPT levels, the rate limiting enzyme in the *de novo* synthesis of ceramide. I demonstrated that SPTLC1 and SPTLC2, two subunits of SPT, are post-transcriptionally regulated by miR-137/-181c; and miR-9-29a/b, respectively. I observed significant correlations between SPT, their corresponding miRNAs (miR-137, -181c, -9 and -29a/b), and Aβ in the autopsy AD brain samples, as well as a direct involvement of SPT and miR-137/-181c in Aβ production through transfection studies. Hebert et al. (Hebert et al., 2008) had previously demonstrated the involvement of miR-29a/b in Aβ production. In addition, I showed negative relationships between SPT and their respective miRNAs in AD risk factor models, where miRNA levels were observed to decrease in mice fed a high-fat diet and in female mice, thereby suggesting a potential therapeutic value (Geekiyanage and Chan, 2011). Here, I investigated the expression levels of these miRNAs in the blood sera of a subgroup of mild and severe sporadic AD patients and mouse risk factor models to assess the potential of using these miRNAs as early diagnostic markers.

3.2 Material and Methods

Patient information. AD (n=7), MCI (n=7) and control (n=7) blood serum samples were from the University of Kentucky (UK) Alzheimer's disease center tissue bank (ADC). The samples have been clinically diagnosed by neurologists, neuropsychologists, and other staff members in the ADC clinic. A complete description of the samples including age of the patient, gender, MMSE scores and the clinical diagnoses is provided in Table 2. The standard MMSE test in the UDS battery was used with no correction factors. The discrimination of AD, MCI and control cases were performed using current consensus-based methodologies which are previously well-described in a clinical-pathological consensus conference (Jicha et al., 2011). Based on this study, I placed individuals with MMSE scores of 29 and 30 (n=7) in the "control" group and individuals with MMSE scores of 10-20 (n=6) and 1 subject with MMSE score of 8 in the "probable AD" group. Finally, based on Jicha, et al. 2011, I placed subjects with MMSE scores of 23-28 in the "MCI/probable Early AD" group. The MCI subjects included in this study only contains patients exhibiting amnestic MCI (indicative of prodromal AD) and not indicative of other type of MCI (e.g., vascular changes on MRI, or Parkinsonism). The patient dietary information is not available. Blood samples were obtained from living research subjects with appropriate IRB approval. Blood sera were separated by centrifugation at 3000 rpm for 5 min.

Mice blood serum collection. Wild type C57/BL on a hybrid background, C3H/He (Charles River) x C57BL/6 (Jackson laboratories) were used in the diet and gender specific studies. Blood was collected from mice under anesthesia through puncturing of the aorta into venous collection tubes coated with clot activator and silicone. Blood serum was separated by centrifugation at 1600 g for 15 min following 30 min of clotting at room temperature. All

procedures conducted were approved by the Institutional Animal Care and Use Committee at Michigan State University.

Quantitative RT-PCR (qRT-PCR). Total miRNAs were extracted using miRNeasy Mini Kit (Qiagen) and RNeasy MinElute Cleanup Kit (Qiagen) and total RNA was quantified using ND-1000 nanodrop spectrophotometer. Quality control was performed by assessing the OD ratio of 260/280 nm. In addition the PCR products were run on agarose gels. qRT-PCR was conducted using miScript SYBR Green PCR Kit (Qiagen) and MyiQ real time PCR detection system following reverse transcription using miScript Reverse Transcription Kit (Qiagen) according to manufacturer's instructions. All miRNA primers were purchased from Qiagen and the relative expressions were calculated using the comparative CT method with spiked cel-miR-39 (Kroh et al., 2010), internal miR-22, internal miR-191 and internal miR-126 as the normalizing controls for human sera and internal miR-22 as the normalizing control for mouse sera. Quantitave RT-PCR was conducted in triplicates (technical replicates).

Statistical analysis. Statistical significances were determined using both 2 tailed *t* tests and Mann-Whitney tests for the human sera samples and 2 tailed *t* tests were used on mice sera samples.

3.3 Results

MiRNAs are down-regulated in blood serum of probable AD patients

The expression levels of the miRNAs, that were previously shown to regulate SPT and Aβ, and were down-regulated in the brain cortices of a subgroup of sporadic AD patients

(Geekiyanage and Chan, 2011), were quantified in blood sera of 7 control (MMSE scores 29 and 30), 7 amnestic MCI/ probable early AD (MMSE scores 23-28) and 7 probable sporadic AD (MMSE scores 8-19) subjects (see Table 2 for patient information). Currently there is no generally agreed upon normalizing RNA with respect to blood serum or plasma. The generally used normalizing ribosomal RNA (RNU6B etc.) in miRNA analysis is typically not present in the blood. Therefore, the human blood sera from patients were spiked with C-elegance miRNA-39, cel-miR-39 (Kroh et al., 2010), prior to miRNA extraction. Cel-miR-39 was selected as it demonstrates no sequence homology to any known human, mouse, or rat miRNA. In addition miR-22 and miR-191 are abundantly expressed in the blood serum (Qiagen, 2011) and have not shown to be differentially expressed in the literature with respect to AD and therefore were also used for normalization. Further, I have observed that miR-126 expression levels remained unchanged in the brains of AD patients. Therefore, the expressions of the respective miRNAs in the blood serum were also normalized to miR-126. The expression levels of miR-137, miR-181c, miR-9, miR-29a and miR-29b (Figure 8) were significantly (both $P<0.05$, student's *t* test and Mann-Whitney test) down-regulated in the blood serum of probable AD patients when normalized to spiked cel-miR-39 (Figure 8A), internal miR-22 (Figure 8B), internal miR-191(Figure 8C) or internal mir-126 (Figure 8D). The expression levels of the respective miRNAs (Figure 8) were significantly (both $P<0.05$, student's *t* test and Mann-Whitney test) down-regulated in the blood serum of amnestic MCI/ probable early AD patients when normalized to spiked cel-miR-39 (Figure 8A), internal miR-22 (Figure 8B), internal miR-191(Figure 8C) or internal mir-126 (Figure 8D) with the exception of miR-137, where the down regulation was not statistically significant when normalized to spiked cel-miR-39 and internal miR-191. However, a

statistical significance may be achieved with the exclusion of the case exhibiting an MMSE score of 28, from the amnestic MCI/ probable early AD group.

Decreased miRNA expression levels in the blood serum of high-fat diet fed mice

High dietary fat intake is identified as a potential risk factor for AD (Refolo et al., 2000; Oksman et al., 2006; Julien et al., 2010; Baker et al., 2011; Bayer-Carter et al., 2011). I previously showed that the expression levels of miR-137, miR-181c and miR-9 were down-regulated in the brain cortices of high-fat diet fed mice (Geekiyanage and Chan, 2011). The miRNA expression levels were measured in the blood serum of male wild-type mice fed a 60% kcal high-fat diet for a period of 5 months (starting at 4 months of age). In accordance with the expression levels in the brain, the expression levels of miR-137 (P=0.045, student's t test), miR-181c (P=0.046) and miR-9 (P=0.03) (Figure 9) expression levels were down-regulated in the blood serum of mice fed a high diet (see Appendix B, Figure 28 for correlations). As the expression levels of miR-22 were stable across the human sera samples, miR-22 was used for normalization of miRNA expressions in the sera of mice fed a high-fat diet.

miRNA are differentially expressed in blood serum according to gender

Research suggests that AD pathology may be more prevalent in females than in males (Bachman et al., 1992; Henderson and Buckwalter, 1994; Ripich et al., 1995; Brookmeyer et al., 1998; McPherson et al., 1999; Alberca et al., 2002; Burns and Zaudig, 2002). I previously reported that the miR-137, miR-181c and miR-29a/b-1 expression levels are down-regulated in the cerebral cortices of female wild-type mice compared to males (Geekiyanage and Chan, 2011). Here I demonstrate that the expression levels of miR-137 (P=0.01), miR-181c (P=0.02)

and miR-29b-1 (P=0.046) expression levels are down-regulated (Figure 10) in the blood serum of female mice (9 months of age) vs. male mice. However, the expression levels of miR-29a did not differ between the groups. As the expression levels of miR-22 were stable across the human sera samples, miR-22 was used for normalization of miRNA expressions in female vs. male mice sera.

3.4 Discussion

MiRNA levels were down-regulated in the sera of patients with probable AD (MMSE scores 8-19) and amnestic MCI/probable early AD (MMSE scores 23-28) compared to normal patients (MMSE scores 29 and 30). This suggests a potential role for these miRNAs as early diagnostic markers. Moreover, screening for miRNAs in the sera as biomarkers, that i) directly affect a fundamental feature of AD neuropathology, ii) are diagnostically sensitive enough to detect, iii) can detect AD early in the course of the disease progression, and iv) are non-invasive, simple to perform and inexpensive, make them potentially good diagnostic biomarkers in accordance with the criteria described by the National Institute on Aging (1998).

In the previous study (Geekiyanage and Chan, 2011) I identified that a subgroup of AD patients display increased levels of ceramide along with increased SPTLC1/2 protein levels in neocortices. However, the SPTLC1/2 mRNA levels did not differ from their control counterparts. I observed negative correlations between the expression levels of miR-137/-181c and SPTLC1, and between miR-9/-29a/b and SPTLC2 protein expressions, in these autopsy brain samples. These results in combination with cell culture studies suggested that SPTLC1/2 are post-transcriptionally regulated by their respective miRNAs. Similar negative relationships were identified between SPTLC1/2 and the corresponding miRNAs in AD risk factor models, i.e.

high-fat diet and gender specific. In addition, positive correlations between SPTLC1/2 and Aβ, and negative correlations between the respective miRNAs and Aβ were observed in these brain samples. Cell culture studies with "target protectors" and over-expression assays showed a direct effect of miRNAs on SPT and in turn on Aβ protein expression. These results together suggested that these miRNAs and SPT are involved in AD and represents a potential therapeutic target. In this current study, I suggest a prospective use for the circulating miRNAs as diagnostic markers.

I also observed that the same miRNAs were down-regulated in the blood serum of high-fat diet and gender specific models. Expression of miR-137 is negatively regulated, epigenetically and transcriptionally by MeCP2 and Sox2 (Szulwach et al., 2010). Additionally, Sox2 genetic polymorphisms are associated with diabetic neuropathy in female patients but not in males (Gu et al., 2009), providing a possible explanation for the dysregulation of miR-137 in female mice. Research performed on the treatment for Rett syndrome, a disease caused by mutations in MeCP2, suggests an increase in MeCP2 levels with the consumption of a high-fat diet (Haas et al., 1986; Liebhaber et al., 2003). This may provide a potential explanation for the down-regulated miR-137 levels observed in mice fed a high-fat diet. Further, miR-181c is positively and transcriptionally regulated by Akt1 (Androulidaki et al., 2009). Akt activity has been observed to be decreased in response to high-fat diet (Tremblay et al., 2001), providing a possible explanation for the reduced miR-181c levels observed in mice fed a high-fat diet. Interestingly, Akt1 expression levels have been shown to decrease considerably with age in the myocardial tissue of women (Camper-Kirby et al., 2001) while MeCP2 expression levels increases with age in frontal cortices of males and females (Samaco et al., 2004). The reduction in Akt expression in these elderly women may provide an explanation for the gender specific reduction of miR-181c observed with the mice in this study. However, further analysis is needed

including age matched male samples to conclude the gender specific regulation of miR-181c by Akt. MiR-9 is negatively regulated by RE1-silensing transcription factor (REST) while it is positively regulated by cAMP-response element binding protein (CREB) (Laneve et al., 2010). In contrast, NFκB, c-Myc and hedgehog signaling transcriptionally repress miR-29a/b (Mott et al., 2010). High dietary fat intake has been shown to activate cortical NFκB in rats (Zhang et al., 2005); however I did not observe miR-29a/b-1 to be down-regulated in mice fed a high-fat diet. Differential expression patterns of hepatic miR-29 family have been observed between different mouse strains fed with methyl-deficient diets (Pogribny et al., 2010), suggesting species and strain variations may contribute to the unchanged miR-29a/b expression level observed in this study. In support of the gender difference observed in the miRNA expressions in this study, estrogen is known to protect neurons against inflammation by suppressing the activation of NFκB (Wen et al., 2004). However, this protection may be reduced in post-menopausal elderly women making them more vulnerable to NFκB mediated suppression of miR-29a/b.

It must be noted that the blood serum samples used in this study were only clinically diagnosed and further studies are necessary to assess their ability to discriminate them from other forms of dementia. In addition, independent validation of these miRNAs as biomarkers will also be required. I note that the circulating miR-137, -181c, -9 and 29a/b levels are low in the blood serum. Nevertheless, the qRT-PCR are able to distinguish specifically between normal and AD patients.

The discrimination of the AD patients was performed using a current consensus-based methodology described in (Jicha et al., 2011). Nevertheless, it is acknowledged that comorbid pathologies can contribute to the development of cognitive impairment, and thereby confound the application of the Preclinical Alzheimer's disease Workgroup recommendations (Jicha et al.,

2011). Therefore, I recognize the possibility that some subjects included in this study may contain non-AD pathologies. Consequently, all clinical diagnosis may not necessarily coincide directly with AD neuropathological features, i.e. some amnestic MCI/probable early AD and probable AD subjects included in this study may not develop AD neuropathologies and some normal subjects may develop AD. Finally, as with any biomarker, other diseases with similar risk factors, cerebovascular disease, cardiovascular disease and diabetes (Beeri et al., 2009; Slevin and Krupinski, 2009; Ewers et al., 2010; McClean et al., 2011), may have similar blood miRNA profiles. Although, these diseases play a significant role in AD as major risk factors (Carlsson, 2010; Caselli et al., 2011; Ettorre et al., 2011), and thus would provide insight into the possible risk of developing AD, further studies are needed to determine whether these miRNAs can be used to distinguish AD from these other diseases. Therefore, whether these miRNA profiles could provide conclusive diagnosis is currently unknown, nonetheless, miRNA profiles along with other biomarkers and cognitive tests could potentially provide a more comprehensive and early diagnosis and prognosis of AD.

MMSE	Clinical diagnosis based on Jicha et al. 2011	Group	Age	Gender
30	Normal	Normal	90	Female
30	Normal	Normal	91	Male
29	Normal	Normal	84	Male
29	Normal	Normal	88	Male
30	Normal	Normal	82	Female
29	Normal	Normal	88	Female
30	Normal	Normal	85	Male
25	Early AD	Amnestic MCI/Probable Early AD	94	Female
25	MCI	Amnestic MCI/Probable Early AD	85	Female
28	MCI	Amnestic MCI/Probable Early AD	87	Male
27	MCI	Amnestic MCI/Probable Early AD	86	Female
23	Early AD	Amnestic MCI/Probable Early AD	87	Female
24	Early AD	Amnestic MCI/Probable Early AD	88	Female
25	Early MCI	Amnestic MCI/Probable Early AD	89	Female
17	AD	Probable AD	89	Female
16	AD	Probable AD	84	Female
19	AD	Probable AD	96	Female
17	AD	Probable AD	90	Male
8	AD	Probable AD	86	Female
15	AD	Probable AD	92	Female
13	AD	Probable AD	80	Male

Table 2: Patient information. Patient information includes MMSE scores, clinical diagnosis, age and gender. This information was provided by the University of Kentucky (UK) Alzheimer's disease center tissue bank (ADC). The discrimination of AD and control cases were performed using current consensus-based methodologies which are previously well-described in a clinical-pathological consensus conference (Jicha et al., 2011).

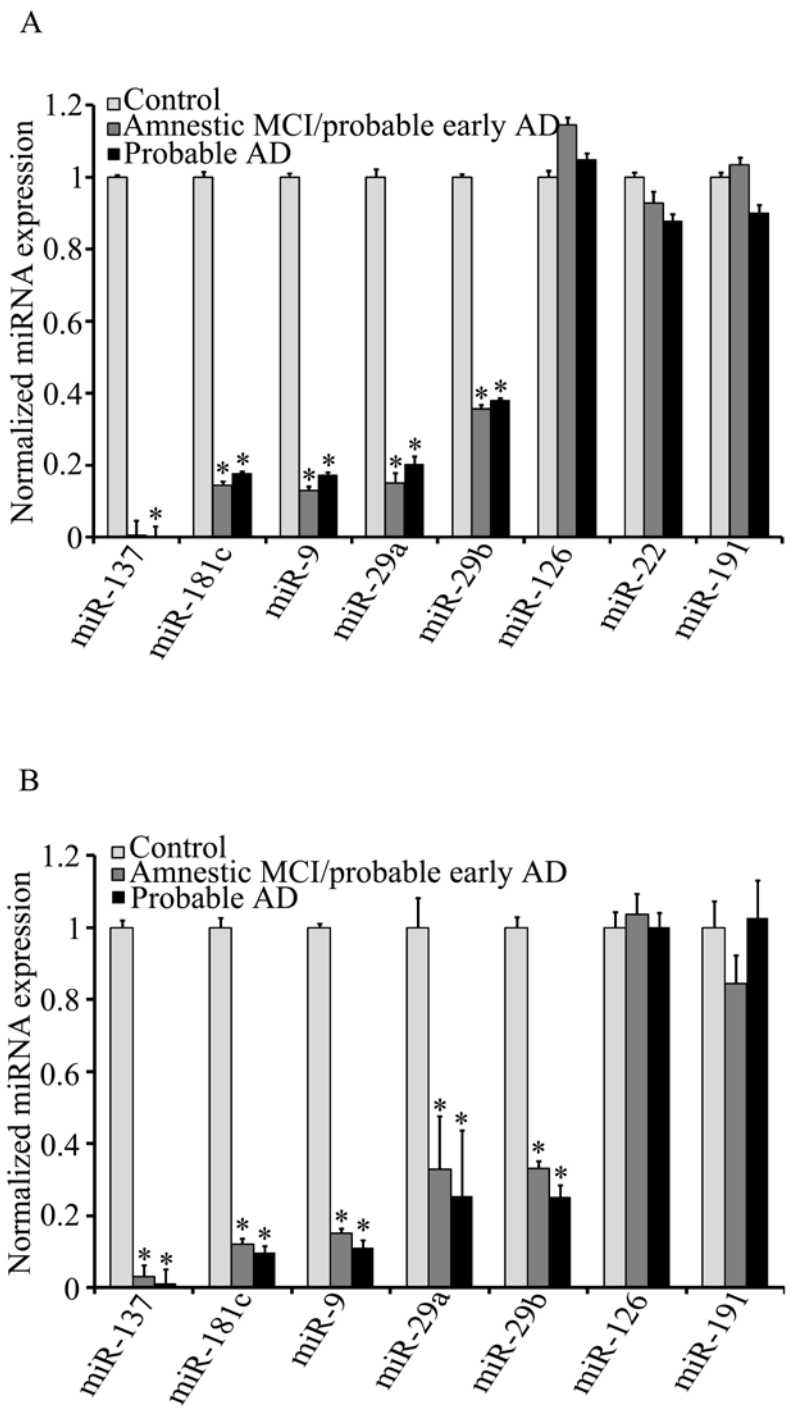

Figure 8: **Down-regulated miRNA expression levels in probable AD patients**. The expression levels of miR-137, -181c, -9, -29a and -29b in blood serum of probable AD (n=7), amnestic MCI/Probable Early AD (n=7) and control (n=7) patients measured by qRT-PCR. Relative expressions shown are normalized to spiked cel-miR-39 **(A)** internal miR-22 **(B)** internal miR-

Figure 8 (cont'd)

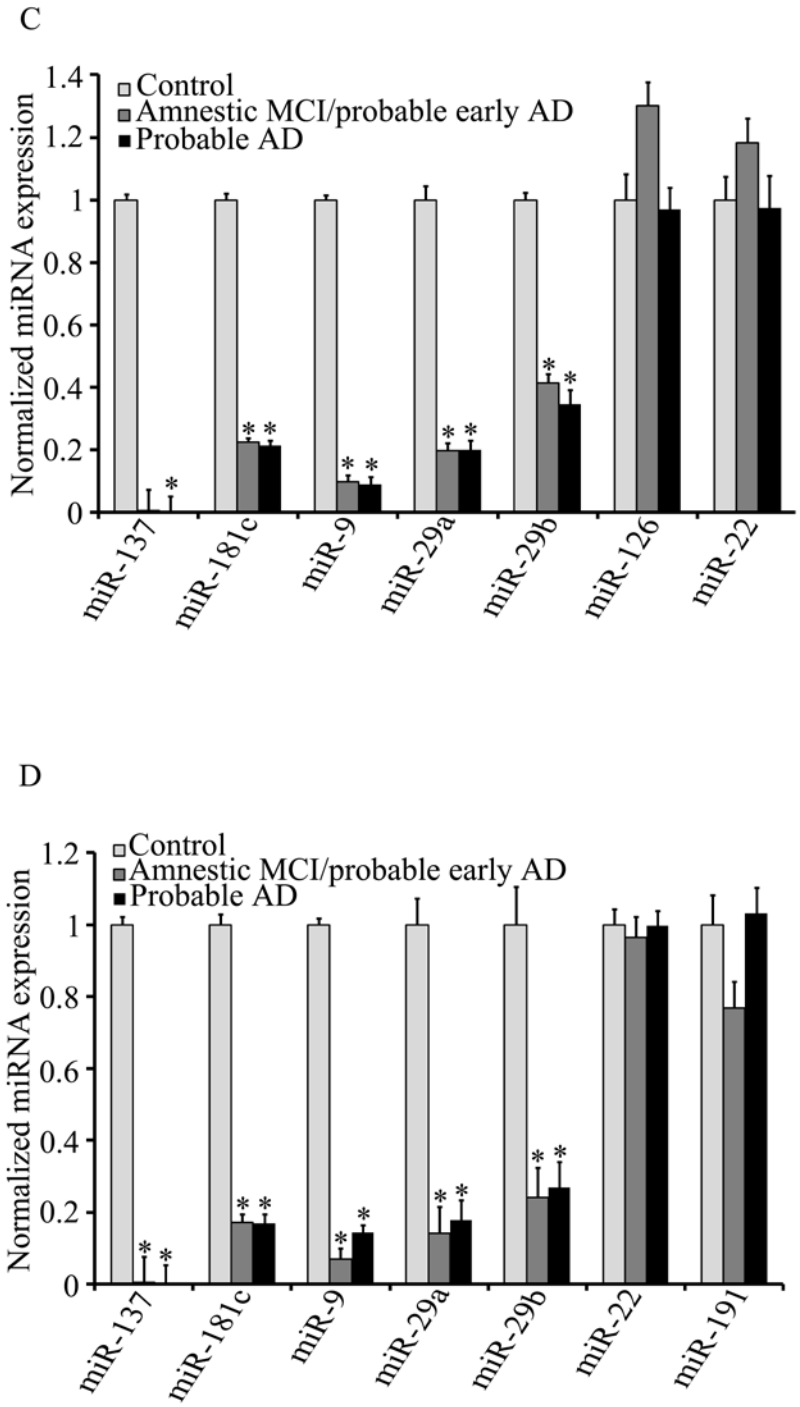

(Figure 8 legend continues) 191 **(C)** and internal miR-126 **(D)** and average control patient

Figure 8 (cont'd)

(Figure 8 legend continues) expressions. The statistical significance between control and AD sera were determined by 2-tailed student *t* tests and Mann-Whitney tests (*, $P<0.05$).

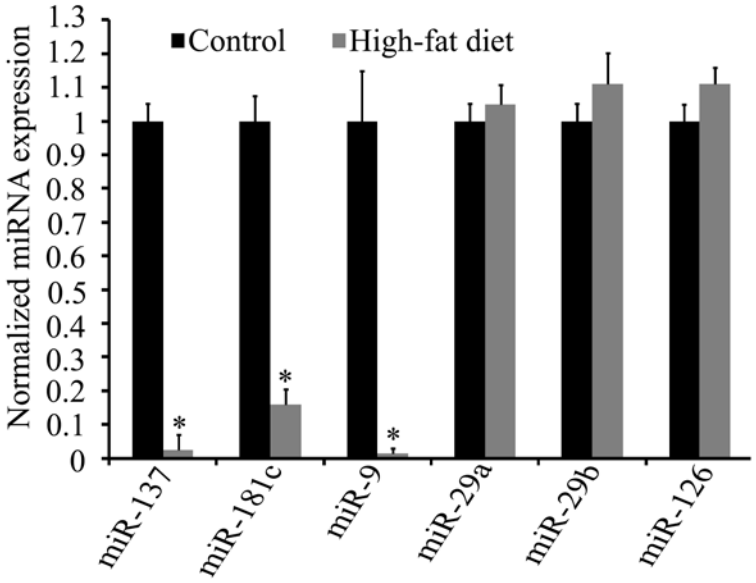

Figure 9: Reduced miRNA expression in high-fat diet fed mice. The expression levels of blood serum miR-137 (*, $P<0.05$), -181c (*, $P<0.05$), -9, (*, $P<0.04$) -29a and -29b in mice fed a high-fat diet were measured by qRT-PCR. The expression of miR-126 is shown as a control. Relative expressions shown are normalized to miR-22 and average chow control diet expressions. The statistical significance between control and AD sera were determined by 2-tailed student *t* tests.

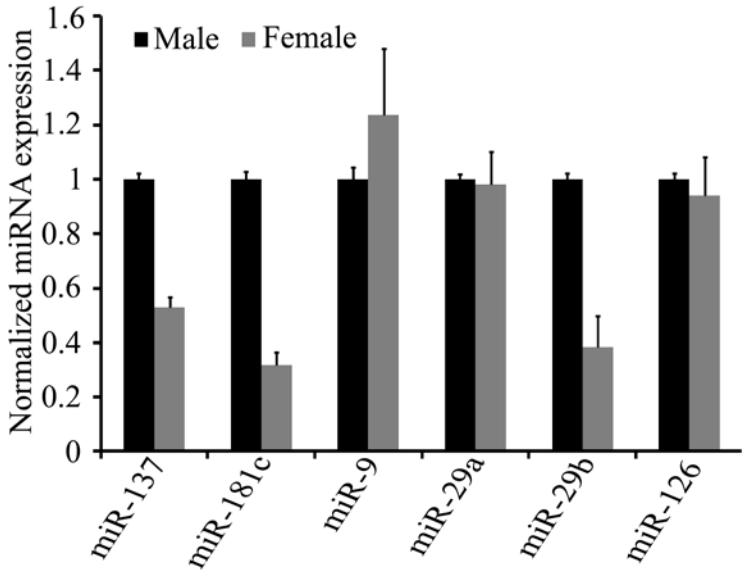

Figure 10: Gender specific down-regulation of miRNA. The expression levels of blood serum miR-137 (*, $P<0.02$), -181c (*, $P<0.02$), -29a, -29b (*, $P<0.05$), and -9 in male and female mice (n=6) were measured by qRT-PCR. The expression of miR-126 is shown as a control. Relative expressions shown are normalized to miR-22 and average male (n=6) expressions. The statistical significance between control and AD sera were determined by 2-tailed student *t* tests.

CHAPTER 4: INHIBITION OF SPT REDUCES AB AND TAU HYPERPHOSPHORYLATION IN A MOUSE MODEL, A POTENTIALLY SAFE THERAPEUTIC STRATEGY FOR ALZHEIMER'S DISEASE

Publication: **Geekiyanage, H**., Upadhye, A., and Chan, C., 2012. Inhibition of SPT reduces Aβ and tau hyperphosphorylation in a mouse model, a potentially safe therapeutic strategy for Alzheimer's disease. (In review)

ABSTRACT

The contribution of autosomal dominant mutations to the etiology of familial Alzheimer's disease is well characterized. However, the molecular mechanisms contributing to sporadic AD are less understood. Increased ceramide levels have been evident in AD patients. I previously reported (Geekiyanage and Chan, 2011) that increased ceramide levels, regulated by increased SPT, directly mediate Aβ levels. Therefore, I inhibited SPT in an AD mouse model (TgCRND8) through subcutaneous administration of L-cylcoserine (LCS). The cortical $A\beta_{42}$ and hyperphosphorylated tau levels were down regulated with the inhibition of SPT/ceramide. Positive correlations were observed between cortical SPT, ceramide and $A\beta_{42}$ levels. With no evident toxic effects observed, inhibition of SPT could be a potentially safe therapeutic strategy to ameliorate the AD pathology. I previously observed that miR-137, -181c, -9 and 29a/b post-transcriptionally regulate SPT levels (Geekiyanage and Chan, 2011), and the corresponding miRNA levels in the blood sera are potential diagnostic biomarkers for AD (Geekiyanage et al., 2012). Here, I observe a negative correlation between cortical $A\beta_{42}$ and sera $A\beta_{42}$, and a

positive correlation between cortical miRNA levels and sera miRNA levels suggesting their potential as non-invasive diagnostic biomarkers.

Keywords: Alzheimer's disease, serine palmitoyltransferase, inhibition, amyloid beta, tau hyperphosphorylation, microRNA

4.1 Introduction

There is consistent evidence suggesting ceramide, a sphingolipid, is increased in Alzheimer's disease patients (Han et al., 2002; Cutler et al., 2004; Satoi et al., 2005; He et al., 2010). Several *in vitro* and *in vivo* studies indicate associations between ceramides and Aβ, and signifying elevated ceramide levels as a possible risk factor for AD (Cutler et al., 2002; Gulbins and Kolesnick, 2003; Puglielli et al., 2003; Kalvodova et al., 2005; Mattson et al., 2005). Membrane ceramides, the major component of lipid rafts, in addition to stabilizing BACE1 (Puglielli et al., 2003; Costantini et al., 2007), facilitates Aβ production by translocating the pathogenic secretases to the primary location of amyloidogenesis (Lee et al., 1998; Vetrivel et al., 2004; Vetrivel et al., 2005; Hur et al., 2008; Haughey et al., 2010), the lipid rafts (Sisodia, 1992; Cordy et al., 2003; Ehehalt et al., 2003; Wada et al., 2003; Won et al., 2008). In a previous study I demonstrated that SPT, the first rate limiting enzyme in the *de novo* ceramide synthesis pathway (Merrill et al., 1985; Hanada et al., 1997; Hannun and Obeid, 2008), regulates ceramide levels through elevated SPTLC1 and SPTLC2 levels in AD (Geekiyanage and Chan, 2011). I found that SPT, post-transcriptionally regulated by miRNAs, directly regulates Aβ levels in AD (Geekiyanage and Chan, 2011).

Activation of SPT raises ceramide levels (Perry et al., 2000) while inhibition of SPT decreases ceramide levels, both *in vitro* and *in vivo* (Hojjati et al., 2005b; Holland et al., 2007; Patil et al., 2007; Strettoi et al., 2010). L-cylcloserine has been established to be a potent inhibitor of SPT (Sundaram and Lev, 1984a, b; Williams et al., 1987). Long-term subcutaneous administration of LCS on alternate days for 2 months exclusively reduced brain cerebroside levels (Sundaram and Lev, 1989), which essentially consist of ceramides. The route of LCS

administration, subcutaneous or intraperitoneal, not only determined the class of glycolipids inhibited, but also influenced the extent of the side effects, with minimal toxic effects observed with prolonged subcutaneous (as oppose to intraperitoneal) administration (Sundaram and Lev, 1985). In contrast, oral administration has demonstrated little reduction in brain cerebroside levels (Sundaram and Lev, 1989).

Given that research demonstrate inhibition of SPT decreases neuronal cell death by Aβ (Cutler et al., 2004) and induces non-amyloidogenic processing of amyloid beta precursor protein (APP) (Sawamura et al., 2004), and our findings that show SPT directly regulates Aβ levels (Geekiyanage and Chan, 2011), here I investigated the inhibition of SPT as a potential therapeutic strategy for AD. Concomitantly, our observations show that high-fat diet increases cortical ceramide and SPT levels (Geekiyanage and Chan, 2011), and other research suggest high dietary fat intake is a potential risk factor for AD (Julien et al., 2010). Therefore, I sought to incorporate the dietary risk component into our study, with emphasis on the inhibition of SPT as a potential therapeutic strategy for AD.

4.2 Material and Methods

Mice. TgCRND8 mice, an early-onset transgenic mouse model, encoding the double mutant form of the amyloid precursor protein 695 (KM670/671NL1V717F) under the control of the PrP gene promoter was used for this study (Chishti et al., 2001). DNA was extracted for genotyping using QIAamp DNA mini kit (Qiagen) following PCR and gel electrophoresis from tail tips from mice ear-tagged for identification. The primers used were APP: 5'-AACAGAAGGACAGACAGCAC-3' and 5'-GTTTCCGTAACTGATCCTTG-3'

12 TgCRND8 mice (7 males and 5 females) were fed a control chow diet and 13 TgCRND8 mice (5 males and 8 females) were fed a 60% kcal high-fat diet (D12492, Research Diets) starting at 4 weeks of age and continuing up to 4 months of age, while 13 other TgCRND8 mice (5 males and 8 females) were administered 10 mg/kg of LCS subcutaneously via surgically implanted osmotic pumps (ALZET, 2004) at 3 months of age, that delivered LCS at a constant rate of 0.25 uL/hour for a period of 28 days, while being fed the 60% kcal high-fat diet stating from 4 weeks to 4 months of age. Mice were selected into the 3 treatment groups based on the availability. A computerized randomized selection method was incorporated due to the high mortality rate observed in the colony. Mice were randomly assigned to the 3 treatment groups at the outset of the experiment (i.e. there was no strategy incorporated to exclusively include or exclude mice to a treatment group). Due the high mortality rate, mice were supplemented to each treatment group as they became available in order to make the sample sizes relatively equivalent. 78 mice were fed a control chow diet or a high-fat diet with only 12 mice fed a control chow diet and 13 mice (1 eliminated due to infection) fed a high-fat diet surviving to term (4 months of age) and 14 mice survived until surgery (3 months of age) (survival rate ~50% (38 out of 78 survived)). 14 mice were administered with LCS and 13 mice survived to term while 1 mouse died of the *Pasteurella pneumotropica* infection in the colony (survival rate of ~90% from the time of surgery (28 days)) (see Appendix C, Figure 29 for random assignment to treatment and survival information). All mice were euthanized (12 controls, 13 high-fat diet and 13 LCS administered) at 4 months of age and their brains were sectioned for histopathology, and the brain cortices and blood sera were extracted for ceramide, protein and RNA analyses.

The colony had a severe *Pasteurella pneumotropica* infection which was lethal in addition to the 40% mortality rate observed in TgCRND8 mice (Chishti et al., 2001). Infected

mice from the control chow diet and high-fat diet categories were treated with Baytril (Bayer) subcutaneously or orally (dissolved in their daily water consumption). However, all animals, but 1 in the high-fat diet category, in the control chow and high-fat diet categories that were treated with Baytril died from the infection. All mice that underwent surgical implantation were administered a single dose of the analgesic meloxicam (1-2 mg/kg) subcutaneously at the time of surgery while Baytril (0.003%) was dissolved in their daily water consumption (250 mL) from 2 days prior to surgery until the time of euthanasia (see Appendix C, Table 3 for information on nutrient and drug treatment on the 3 categories). The 1 animal that survived in the high-fat diet category treated with Baytril was eliminated from this study to maintain homogeneity in the group. This mouse showed increased brain cortical ceramide levels by ~21% (d18:1; 16:0) - ~37% (d18:1; 18:0) compared with the average ceramide levels in the mice fed a control chow diet, possibly suggesting that the reduced ceramide and $A\beta_{42}$ observed in this study is due to inhibition of SPT and not the oral administration of Baytril. It must be noted that a placebo control treatment for LCS (i.e. saline) was not incorporated in this study due to the limited number of animals available with the increased deaths and slow breeding rates. All procedures conducted were approved by the Institutional Animal Care and Use Committee at Michigan State University.

Special staining. Tissue samples previously fixed in 10% neutral buffered formalin were processed and vacuum infiltrated with paraffin on the ThermoFisher Excelsior tissue processor followed by embedding with the Thermo Fisher Histo-Centre III embedding station. Once the blocks were cooled, excess paraffin was removed from the edges and placed on a Reichert Jung 2030 rotary microtome faced to expose the tissue sample. Once the blocks were faced they were

cooled and finely sectioned at 8µM. Sections were dried overnight at room temperature followed by incubation at 56°C to ensure adherence to the slides for 2 – 24 hours. Slides were removed from the incubator and de-paraffinized with 2 changes of xylene for 5 minutes each, 2 changes of absolute ethanol for 2 minutes each, 2 changes of 95% ethanol for 2 minutes each, and under running tap water for 2 minutes followed by a distilled water rinse.

Thioflavin-S staining was conducted according to (Klatt, 1994-2012) with 5 minutes in 1% aqueous Thioflavin-S followed by 5 minutes in 70% ethanol with several distilled water rinses and mounting with aqueous media.

Bielschowsky staining was conducted according to (Sheehan, 1980) with modifications. A preliminary 20% aqueous silver nitrate impregnation at 37°C for 10 minutes is followed by an ammonical silver treatment at 37°C for 8 minutes. 1% ammonium hydroxide stops the fiber development and silver is deposited on the neurofibrils and axons, and reduce to a visible metallic silver (black) by the actions of the formaldehyde reducing agent in a water bath at 70°C for 2-3 minutes followed by 1% ammonium hydroxide and 5% sodium thiosulfate incubations to remove any unreduced silver from the tissue. No counter-stain was employed. Dehydration and clearing was performed using 1 change of 95% ethanol for 2 minutes, 4 changes of 100% ethanol for 2 minutes each, 4 changes of xylene for 2 minutes each, followed by cover-slipping with synthetic mounting media for permanent retention and visualization. All staining were conducted double-blinded manner.

Immunohistochemistry. Formalin fixed specimens were processed, embedded in paraffin and sectioned on a rotary microtome at 4µm. Sections were placed on adhesive slides and dried at room temperature followed by 56 ° C overnight drying. The slides were

subsequently de-paraffinized in xylene and hydrated through descending concentrations of ethanol to distilled water. Slides were placed in Tris buffered saline pH 7.5 for 5 minutes for pH adjustment. Heat induced (in a rice steamer for 30 minutes followed by 10 minutes at room temperature) or enzyme induced epitope retrieval (10 minutes at 37 °C) was conducted followed by subsequent rinses and blocking for endogenous peroxidase using 3% hydrogen peroxide/methanol bath (1:4 ratio) for 30 minutes at room temperature followed by running tap and distilled water rinses. Following pretreatments, standard avidin – biotin complex staining steps were performed at room temperature on the Dako Autostainer by rinsing with Tris buffered saline + Tween 20 between staining steps. Slides were blocked for non-specific protein with normal goat serum (Vector Labs) for 30 minutes. Endogenous biotin was blocked by incubation in avidin D (Vector Labs) and d-biotin (Sigma) for 15 minutes. Rabbit polyclonal antibodies were diluted in normal antibody diluent (NAD) (Scytek – Logan) and incubated for 1 hour at room temperature. Biotinylated goat anti-Rabbit and IgG H+L (Vector Labs) were diluted to 11 µg/ml and incubated for 30 minutes followed by a 30 minute incubation with R.T.U. VectaStain Elite ABC Reagent (Vector Labs). The reaction was developed with Nova Red (Vector Labs) for 15 minutes followed by counterstaining in Gill 2 hematoxylin (Richard-Allan Scientific Co) for 10 seconds and differentiated in 1% aqueous glacial acetic acid and rinsed under running tap water. Slides were then dehydrated through ascending grades of ethanol; cleared through several changes of xylene and cover-slipped using Flotex permanent mounting media. The sections were pretreated with 0.03% Pronase E in TBS at 37°C for 10 minutes for β-amyloid (1:400 dilution) (Cell Signalling Technology) and NF200 (1:100 dilution) (Sigma), and Scytek citrate Plus at pH 6.0 in a steamer (30 minute), and on the bench top (10 minute) for SPTLC2 (1:100 dilution)

(Abcam), with no pretreatment for SPTLC1 (1:100 dilution) (Proteintech group). All staining were conducted double-blind.

Quantification of plaques. For Thioflavin-S (fluorescence) and Aβ (transmitted light) antibody, whole-brain sections were imaged with an Olympus FluoView FV1000 Confocal Laser Scanning Microscope (Olympus America, Inc, Center Vally, PA) configured with the 4x UPlanFLN (NA 0.13). Identical imaging parameters were used for all sections. Individual images across the brain section were collected using the Multi Area Time Lapse Controller within the Olympus FluoView Advanced Software (version 3.1). The individual images were then stitched together to generate a single image of the entire brain slice using the Multi Area Time Lapse Viewer within the Olympus FluoView Advanced Software. The default threshold adjusting parameter with adjusted brightness in the NIH-imageJ particle analyses was used to determine plaque area and integrated densities with the same thresholding parameters for all the sections while the plaque numbers were counted manually. Imaging quantification and counting were conducted in a double-blinded manner.

Bright-field image generation with camera. The Olympus DP72 camera and DP2-BSW software (version 2.2) were used to generate images under bright-field. The area imaged was the right or left cortex area above the hippocampus, configured with either 10x UPlanSApo (NA 0.40), 20x UPlanSApo (NA 0.50) or 40x UPlanSApo (NA 1.00) oil immersion objective.

Protein extraction and western blot analysis. Mouse brain cortices, homogenized in 5M guanidine HCl/ 50mM Tris HCl, were lysed followed by protein extraction and western blot

analyses using NuPAGE® Novex 12% Bis-Tris Gels, as described previously (Geekiyanage and Chan, 2011). Protein quantifications were conducted by normalizing to β-Actin. Western blots were quantified using Quantity One (BioRad) version 4.5.

Enzyme-linked immunosorbent assay (ELISA). Proteins were extracted with 5M guanidine HCl/ 50mM Tris HCl from mouse cortices and blood sera. ELISA was performed for human-$A\beta_{42}$ using KHB3441 (Invitrogen) according to the manufacturer's instruction. The cortical $A\beta_{42}$ levels were calculated by normalizing to the total protein levels measured by Bradford's assay. The experiment was conducted in duplicates (technical replicates).

Quantitative RT-PCR (qRT-PCR). Total miRNAs were extracted from brain cortices and blood sera using miRNeasy Mini Kit (Qiagen) and RNeasy MinElute Cleanup Kit (Qiagen), total RNA was quantified using ND-1000 nanodrop spectrophotometer as described previously (Geekiyanage and Chan, 2011; Geekiyanage et al., 2012). RNU6B was used as the normalizing control for cortical samples (Geekiyanage and Chan, 2011) while miR-22, which was found to be abundant and stable in blood sera of AD patients, was used as the normalizing control for sera samples as described previously (Geekiyanage et al., 2012). The experiment was conducted in triplicates (technical replicates).

Ceramide quantification. Lipids were extracted from homogenized mouse brain cortices and blood sera according to Bligh and Dyer (Bligh and Dyer, 1959) following tandem mass spectrometry (MS/MS) using Quattro Premier XE (Waters), Acquity ultra performance liquid chromatography (Waters) (LC-MS/MS) and Mass Lynx 4.1 software. External ceramide

standards and C12:0 internal standards were purchased from Avanti, Polar Lipid Inc. The experiment was conducted in duplicates (technical replicates).

Lactate Dehydrogenase (LDH) Enzyme Assay. LDH assay kit specific for measuring sera LDH levels, IDTox™ LDH color endpoint assay kit was purchased from ID Labs Biotechnology Inc. The assay was conducted according manufacturer's instructions.

Antibodies. The antibodies used were, LCB1 (BD Transduction Laboratories™), SPTLC1 (proteintech group), SPTLC2 (Abcam), β-Actin (Sigma), β-Amyloid (cell signaling), Phospho-PHF-tau pSer202/Thr205 Monoclonal Antibody (AT8) (Thermo scientific).

Statistical analysis. Statistical significances were determined by Mann-Whitney U tests and Spearman's correlation (2 tailed-T distribution test).

4.3 Results

In order to investigate the inhibition of SPT as a therapeutic strategy for AD, I used an early onset transgenic model, TgCRND8, encoding a double mutant form of APP 695 (KM670/671NL1V717F) under the control of the PrP gene promoter (Chishti et al., 2001). TgCRND8 mice were fed a control chow diet (n=12) or a 60% kcal high-fat diet (n=13, referred to as "fed a high-fat diet") starting from 4 weeks to 4 months of age. Another group of mice (n=13, referred to as "administered with LCS") were administered 10 mg/kg of a SPT inhibitor, LCS, via subcutaneous surgical implantation of an osmotic pump at 3 months of age, that delivered LCS at a constant rate of 0.25 uL/hour for a period of 28 days, while being fed the 60%

kcal high-fat diet (stating from 4 weeks to 4 months of age). The mice were euthanized at 4 months of age and their brains were sectioned for histopathology while their brain cortices and blood sera were extracted for ceramide, protein and RNA analyses.

Inhibition of SPT/ceramide decreases cortical Aβ levels

Mice administered with LCS showed decreased ceramide levels, d18:1;16:0 ($P < 0.001$, Mann-Whitney U test) and d18:1;18:0 ($P < 0.01$) (Figure 11A), in comparison with mice fed a control chow or a high-fat diet. In addition, mice administered with LCS showed decreased $A\beta_{42}$ levels (Figure 11B) in comparison with mice fed a control chow ($P < 0.001$) or a high-fat diet ($P < 0.01$). Furthermore, statistically significant positive correlations were observed between $A\beta_{42}$ and ceramide d18:1;16:0 (r= 0.656, p= 7.79E-06, Spearman's correlation) (Figure 11C), d18:1;18:0 (r= 0.56, p= 2.43E-04) (Figure 11D) levels in all treatment groups. Mice fed a high-fat diet did not demonstrate a statistically significant change in ceramide and $A\beta_{42}$ levels as compared to their control chow diet counterparts.

The brain sections were stained with thioflavin-S (Figure 12A and B) and antibody (Fig. 12C) for Aβ plaques. The plaque areas and integrated densities were determined using NIH-imageJ for thioflavin-S stained sections, while the plaque numbers were manually counted in both thioflavin-S (Figure 12A) and antibody (Figure 12C) stained sections. The staining, imaging, NIH-imageJ data generation and counting of the plaques were all conducted in a double-blinded manner. Statistically significant differences in the plaque numbers (Figure 12D and 2E), total plaque area (Figure 12F), average area per plaque (Figure 12G) and integrated density (Figure 12H) levels were not observed in the control chow diet (Figure 12I-L), high-fat

diet (Figure 12M-P) and LCS administered (Figure 12Q-T) groups. TgCRND8 is an aggressive Aβ plaque model thus making them relatively insensitive to modulators of plaque levels (Pedrini et al., 2009). This provides a possible explanation for the nominal effect on the Aβ plaque levels observed in this research. In addition, the relatively small sample size in each category may also have hindered possibilities of any observable significant changes due to insufficient statistical power.

High-fat diet increases blood sera ceramide and $A\beta_{42}$ levels

Mice fed a high-fat diet showed increased blood sera ceramide levels (Figure 13A), d18:1;16:0 ($P < 0.01$) and d18:1;18:0 ($P < 0.01$), and $A\beta_{42}$ levels ($P <= 0.01$) (Figure 13B), and mice administered with LCS also showed statistically significant increase in ceramide levels, d18:1;16:0 ($P < 0.05$), with the exception of d18:1;18:0 where the difference was not statistically significant, (Figure 13A); and $A\beta_{42}$ levels ($P < 0.05$) (Figure 13B) compared with their control chow diet counterparts. Mice administered with LCS did not show statistically significant differences in their sera ceramide and $A\beta_{42}$ levels, as compared to mice fed a high-fat diet. However, a statistically significant negative correlation (r= -0.34, p= 0.034) (Figure 13C) was observed between cortical $A\beta_{42}$ and sera $A\beta_{42}$ levels. Additionally, a stronger negative correlation (r= -0.63, p= 6.63E-05) (Figure 13D), was observed between cortical $A\beta_{42}$ and sera $A\beta_{42}$ levels with the elimination of 4 subjects (Figure 13C, circled) as “outliers".

SPT expression levels are decreased with LCS administration

Decreased SPTLC1 (Figure 14A, 14B) protein expression levels were observed in the brain cortices of mice administered LCS in comparison with their high-fat diet fed (Figure 14G-J) counterparts ($P < 0.05$). Decreased levels of SPTLC2 (Figure 14A, 14B) were observed in mice administered LCS (Figure 14W-Z) in comparison with their high-fat ($P < 0.01$) (Figure 14S-V) and control chow ($P < 0.001$) (Figure 14O-R) diets fed counterparts. SPT consists of SPTLC1 and SPTLC2 at a 1:1 ratio (Hanada et al., 2000) and SPTLC1/SPTLC2 complex can be modulated through the regulation of *SPTLC2*, even without parallel regulation of *SPTLC1* (Gable et al., 2000; Yasuda et al., 2003), thus reflecting the similar reductions observed in ceramide (Figure 11A) and SPTLC2 (Figure 14B) levels in the brain cortices of mice administered with LCS. Nevertheless, I observed statistically significant positive correlations between SPTLC1 and ceramide d18:1;16:0 (r= 0.44, p= 0.006) (data not shown), and d18:1;18:0 (r= 0.43, p= 0.007) (data not shown), however, with no statistically significant correlation with $A\beta_{42}$ (r= 0.12, p= 0.47) (data not shown), levels in all treatment groups. Concomitantly, I observed statistically significant positive correlations between SPTLC2 and ceramide d18:1;16:0 (r= 0.57, p= 1.91E-04) (Figure 15A), and d18:1;18:0 (r= 0.56, p= 2.75E-04) (Figure 15C) levels in all treatment groups. Additionally, a statistically significant positive correlation was observed between SPTLC2 and $A\beta_{42}$ (r= 0.43, p= 7.33E-03) (Figure 15E) levels in all treatment groups. Moreover, stronger positive correlations were observed between SPTLC2 and ceramide d18:1;16:0 (r= 0.76, p= 9.80E-06) (Figure 15B), d18:1;18:0 (r= 0.73, p= 3.86E-05) (Figure 15D), and $A\beta_{42}$ (r= 0.71, p= 5.99E-05) (Figure 15F) levels in control chow diet and LCS administered groups, indicative of high variability in biomarker expression levels with high-fat

diet possibly due to individual aberrations in food consumption and metabolic rates. Similarly, stronger positive correlations were observed between SPTLC1 and ceramide d18:1;16:0 (r= 0.53, p= 0.007) (data not shown), and d18:1;18:0 (r= 0.60, p= 0.001) (data not shown) levels in control chow diet and LCS administered groups. Furthermore, I observed that SPTLC1 protein is expressed in the core and the surroundings of the senile plaques in both mouse (Figure 14i) and human (Figure 14ii) brains, while SPTLC2 is present in the core of the senile plaques in the mouse (Figure 14iii) and human (Figure 14iv) brains alike.

Ceramide expression has been observed in neurons (Becker et al., 2008) and astrocytes (Wang et al., 2012). In addition ceramide synthase 5 (CerS5), a palmitoyl-Co-A specific ceramide synthase, is ubiquitously expressed in most cell types within the gray and white matters of the brain (Becker et al., 2008). This suggests the ubiquitous expression of palmitoyl-Co-A in these brain regions. Similarly, I observed that SPTLC1 (Figure 14C-F) and SPTLC2 (Figure 14O-R) are expressed in gray and white matters of the brain. In addition, ceramide has been observed to co-localize with Aβ plaques (Wang et al., 2012). Concomitantly, I observed that SPT (Figure 14i-iv) is co-localized with Aβ plaques, further strengthening the involvement of SPT in ceramide and Aβ production.

Hyperphosphorylated tau expressions are reduced with LCS administration

A decrease in mouse cortical hyperphosphorylated tau protein expression levels was observed with the administration of LCS (Figure 16A and 16B) in comparison with their high-fat ($P < 0.05$) and control chow ($P < 0.01$) diet counterparts. Bielschowsky's silver staining revealed filamentous silver-positive inclusions in control chow (Figure 16C-E), high-fat (Figure 16F-H) diets and LCS administered (Figure 16I-K) mice brains, indicative of the presence of senile

plaques and dystrophic neurites. In addition, anti-neurofilament antibody (NF200) staining showed the neuritic aggregations surrounding the senile plaques in control chow (Figure 16L-O), high-fat (Figure 14P-S) diets and LCS administrated (Figure 16T-W) mice brains.

Changes in cortical miRNA correlate with sera miRNA levels

The expression levels of miR-137 ($P < 0.05$) (Figure 17A), miR-9 ($P < 0.01$) (Figure 17 C), miR-29a ($P < 0.01$) (Figure 17D) and miR-29b ($P < 0.05$) (Figure 17E) were down-regulated in the brain cortices of animals fed a high-fat diet in comparison with their control chow diet counterparts. Similarly, the expression levels of miR-9 ($P < 0.01$) (Figure 17C), miR-29a ($P < 0.01$) (Figure 17D) and miR-29b ($P < 0.05$) (Figure 17E) were down-regulated in the blood sera of animals fed a high-fat diet in comparison with their control chow diet counterparts. Significant differences in the expressions of cortical miR-181c (Figure 17B), and sera miR-137 (Figure 17A) and miR-181c (Figure 17B) levels were not observed.

Statistically significant positive correlations were observed between cortical and sera miR-137 ($r= 0.87$, $p= 3.00E-08$) (Figure 17F), miR-181c ($r= 0656$, $p= 4.60E-04$) (Figure 17G), miR-9 ($r= 0.78$, $p= 5.56E-06$) (Figure 17H), miR-29a ($r= 0.72$, $p= 6.09E-05$) (Figure 17I), and miR-29b ($r= 0.78$, $p= 3.69E-05$) (Figure 17J), in mice fed a control chow and a high-fat diet.

Inhibition of SPT does not cause observable toxic-effects

The total body weight (Figure 18A) of the animals fed a high-fat diet ($P < 0.001$) and animals administered with LCS ($P < 0.001$) were elevated at the time of euthanasia in comparison with their chow control diet counterparts, with no differences in their total brain weights (Figure 18B), thus decreasing the encephalization quotient (EQ) levels (Figure 18C) in

mice fed a high-fat diet ($P < 0.001$) and administered LCS ($P < 0.001$). No differences were observed in body and brain weights of mice administered LCS in comparison to mice fed a high-fat diet. In addition, a statistically significant increase ($P < 0.05$) in body weight was observed from the time of surgery to euthanasia in LCS administered mice (Figure 18D), suggesting the absence of toxic effects that may exhibit alterations in growth, hormonal changes, changes in neurotransmitters that affect food consumption, or nonspecific systemic toxicity (Bailey et al., 2004).

The LDH levels remained unchanged in the blood sera between the 3 treatment groups (Figure 18E) suggesting that LCS administration imposes no toxicity effects on the animals. Further, all but 1 animal administered with LCS, via the surgically implanted osmotic pump, survived to term (28 days). The mouse that did not survive to term was found dead, with vaginal discharge, a classical symptom of the aggressive *Pasteurella pneumotropica* infection in the colony, 6 days shy of the scheduled euthanasia date. In addition, no visual side effects were observed in the mice administered LCS with the exception of 1 mouse demonstrating convulsion on the 2nd day of administration which subsided the next day. The LDH data and physical observations indicate that a daily, 10 mg/kg dose of LCS for a period of 28 days is potentially "safe", with no observed toxic side-effects related to LCS or target in this limited exposure paradigm.

According to FDA drug development and review definitions, effort needs to be taken to use few animals as possible and ensure their humane and proper care. In general, 2 or more species which include rodent and non-rodent models are tested as a drug may affect differently depending on the species. Animal testing is conducted to measure the quantity of the drug absorbed into the blood, how it is broken down chemically in the body, the toxicity of its

metabolites and how fast the drug and its metabolites are secreted from the body. Cycloserine crosses the blood-brain-barrier and has been reported to have a drug half-life of 8-10 hours in humans with 50% of parenteral dose is excreted unchanged in urine in the first 12 hours and a total of 65% is recoverable in the active form over a period of 72 hours. 70%-90% of cylcoserine is rapidly absorbed when it is administered orally and peak plasma concentrations have been achieved in 3-4 hours after a single dose of 20-35 μg/mL in children who have received 20 mg/kg with only small quantities observed after 12 hours (PubChem compound-CID 449215). Cycloserine is currently approved for the treatment of *Mycobacterium avium* complex (MAC) and tuberculosis. In this context, pharmacodynamically cycloserine is used as a broad-spectrum antibiotic (bactericidal or bacteriostatic) and it functions by blocking the formation of peptidoglycans via competitive inhibition of alanine recemase to destroy the bacteria. The oral LD_{50} is 5290 mg/kg in mice. Symptoms of cycloserine overdose include drowsiness, confusion, headache, dizziness, irritability, numbness and tingling, difficulty speaking, paralysis, abnormal behavior, seizures and unconsciousness. Cycloserine is currently available under the brand name Seromycin (250 mg) in the forms of capsules and pulvules (DrugBank, 2012). In addition, blood cytokine/chemokine levels and the drug affect on other tissues (histopathology data) may also provide useful toxicology information.

4.4 Discussion

Previously, I found increased SPT levels in AD directly regulate ceramide and Aβ levels (Geekiyanage and Chan, 2011). In this study, I observed that an AD mouse model administered with a SPT inhibitor, express reduced levels of cortical ceramide and $A\beta_{42}$ oligomer levels not

only in comparison with their high-fat diet counterparts, but also in comparison with mice fed a control chow diet, suggesting that SPT/ceramide could be a potential therapeutic target for AD. Furthermore, post-hoc statistical power analysis conducted on the 13 animals (sample size) administered with 10 mg/kg of the SPT inhibitor demonstrates that the reduction of $A\beta_{42}$ levels (~30% reduction) observed has a power of 97% to yield a significant effect with an effect size (Cohen's *d*) of 2.4 (see Appendix C, Figure 30).

I previously observed that SPT positively correlates with Aβ in human autopsy brain cortices and directly regulates Aβ levels (Geekiyanage and Chan, 2011). In this study I observed that the SPT inhibitor reduced cortical SPT protein levels which in turn decreased ceramide and Aβ levels in the brains of an AD mouse model. In addition, I observed that SPT levels show a significant positive correlation with ceramide and Aβ levels in all groups. Interestingly, I found that SPT encircles and resides in the core of the senile plaques in TgCRND8 mice and humans, further supporting the direct involvement of SPT in Aβ generation. Inhibition of SPT enables the assessment of target engagement, facilitating the early proof of concept and thus increasing the efficiency of early clinical development. Reduced SPT/ceramide levels observed with LCS administration provide information on physical and biological interaction with the molecular target of the drug making them potentially good target engagement biomarkers. The decrease in SPT/ceramide levels along with the decrease in Aβ levels observed with LCS administration shows the combination of target engagement and disease-related biomarkers, validating the proof of concept. This combination of target engagement and disease-related biomarkers is useful in drug development (Wagner, 2008).

The dimeric SPT enzyme contains an essential pyridoxal-5'-phosphate (PLP) cofactor bound to each of the subunits (Lowther et al., 2010). Cycloserine inhibits many PLP-dependent

enzymes (alanine racemace (Fenn et al., 2003; Wu et al., 2008), ArnB aminotransferase (Noland et al., 2002), dialkylglycine decarboxylase (Malashkevich et al., 1999)) by disabling the essential PLP cofactor. Research suggest that LCS is an irreversible inhibitor of SPT. LCS inhibit the PLP-dependent SPT by transamination to form a free pyridoxamine-5'-phosphate (PMP) and β-aminoxyacetaldehyde that remains bound at the active site. LCS binds to the SPT active site and forms a PLP-LCS external aldimine complex. It has been proposed that this occurs via ring opening of the LCS ring followed by decarboxylation. Kinetic studies shows that the half life of the SPT:LCS complex is approximately 15 minutes (Lowther et al., 2010). Bruce W. Craigs group have observed a reduction in SPT protein levels with the treatment of LCS (Choi, 2006). Similarly, in this study I observed a reduction of SPT levels with LCS administration suggesting a possible degradation of the PLP deficient SPT complex.

In my previous study, I observed that high-fat diet increased cortical ceramide levels in wild-type mice (n=3). However, the TgCRND8 mice fed a high-fat diet (n=13) failed to demonstrate a statistically significant increase of ceramide levels in comparison with mice fed a control chow diet. Nevertheless, 9 out of 13 mice demonstrated a statistically significant ($P >$ 0.01) (data not shown) elevation of ceramide levels in high-fat diet fed mice in comparison with mice fed a control chow diet. The TgCRND8 mice fed a high-fat diet (n=13) failed to show a statistically significant difference in $A\beta_{42}$ levels in comparison to mice fed a control chow diet. In support of this, APP/PS1 mice showed no change in cumulative $A\beta_{40}$ and $A\beta_{42}$ levels with a typical western diet (essentially a high-fat diet) (Oksman et al., 2006). In contrast, increased levels of cumulative $A\beta_{40}$ and $A\beta_{42}$ have been observed in TgCRND8 (Pedrini et al., 2009) and 3xTg (Julien et al., 2010) mice fed a high-fat diet. In our study, 5 out of 13 mice fed a high-fat

diet showed statistically significant increase in $A\beta_{42}$ levels ($P > 0.05$) (data not shown) when compared with the control chow diet counterparts. In agreement with other research conducted with TgCRND8 (Pedrini et al., 2009) and APP/PS1 (Oksman et al., 2006) mice, I did not observe differences in Aβ plaque burden with the high-fat diet (n=13). As stated previously (Pedrini et al., 2009), TgCRND8 mice are relatively insensitive to modulators of amyloidosis due to its aggressive amyloid pathology, thus providing a possible explanation for the nominal effects. Nevertheless, a statistically significant positive correlation was observed between cortical ceramide and $A\beta_{42}$ levels in mice fed a control chow diet, high-fat diet and mice administered with the SPT inhibitor, further supporting the involvement of ceramide in Aβ production.

In addition to the reduction in Aβ levels, I observed reductions in hyperphosphorylated tau levels with the inhibition of SPT. Ceramides contribute to Aβ pathology by facilitating the mislocation of BACE1 and γ-secretase to lipid rafts. Under non-pathological conditions the inactive BACE1 and γ-secretase reside outside of lipid rafts while under pathological settings the ceramides facilitate the trafficking of the secretases to lipid rafts where they become active to produce Aβ (Ebina et al., 2009). In addition to stabilizing BACE1, the membrane lipid raft topography affects the efficiency of γ-secretase activity (Fassbender et al., 2001; Wahrle et al., 2002; Zha et al., 2004). This coupled with the fact that over-expression of BACE1 fails to restore suppressed Aβ levels (Hebert et al., 2008), and over-expression of SPT restores Aβ levels (Geekiyanage and Chan, 2011), suggest a potential role of SPT/ceramide in the regulation of γ-secretase activity. Along the same lines, treatments with modulators of γ-secretase reduced Aβ burden, attenuated memory deficits (Schilling et al., 2008; Imbimbo et al., 2009), and reduced hyperphosphorylated tau levels (Lanzillotta et al.) in AD mouse models. Our results suggest that

LCS, a SPT inhibitor, could indirectly function as a possible γ-secretase inhibitor to reduce Aβ production.

Several studies demonstrate increased plasma ceramide levels in rodents fed a high-fat diet (Ichi et al., 2007; Shah et al., 2008). Similarly, I observed an increase in blood sera ceramide levels in mice fed a high-fat diet. Increased ceramide levels have been reported in muscle, adipose tissue and livers of obese rodents and humans (Turinsky et al., 1990; Unger and Orci, 2001; Adams et al., 2004; Samad et al., 2006; Zendzian-Piotrowska et al., 2006). In this study, mice fed an obesity inducing high-fat diet show increased weight at the time of euthanasia, regardless of administration of the inhibitor, due to their continuous consumption. Therefore, the increased ceramide levels observed in the blood sera is possibly due to contributions from muscle, adipose and liver tissues.

Plasma $A\beta_{42}$ levels have been observed to increase before the onset of AD, followed by a decline with disease progression (Schupf et al., 2008; Henry et al., 2012). In addition, other reports have associated low levels of plasma $A\beta_{42}$ with increased dementia (van Oijen et al., 2006; Graff-Radford et al., 2007). Although it is unclear whether abnormal $A\beta_{42}$ metabolism in the brain is precisely emulated by the plasma/sera $A\beta_{42}$ levels (Henry et al., 2012), I nevertheless observed a statistically significant negative correlation between cortical and blood sera $A\beta_{42}$ levels, providing possible connotations for the search of blood Aβ biomarkers.

Previously I observed that miR-137, miR-181c, miR-9 and miR-29a/b are down-regulated in brain cortices of AD patients, and wild-type mice fed a high-fat diet (Geekiyanage and Chan, 2011). In another study I observed that the respective miRNAs were down-regulated in blood sera of AD patients and in wild-type mice fed a high-fat diet suggesting a possible role for these miRNAs as non-invasive diagnostic biomarkers (Geekiyanage et al., 2012). In this

current study I show a positive correlation between the corresponding cortical and sera miRNA, further indicating that sera miRNAs may reflect upon the brain miRNA expression patterns. It is noteworthy that the miRNAs that demonstrate the highest degrees of statistically significant correlations, miR-137 and miR-9, are brain enriched miRNAs. This further strengthens the use of these miRNAs, miR-137 and miR-9, as potential sera biomarkers, i.e. directly reflecting on the brain fraction with minimal interference from other organs. Our prior results show that SPTLC1/2 are post-transcriptionally regulated by miR-137/-181c and miR-9,-29a/b respectively. In our previous study I observed decreased cortical miR-137,-181c,-9 expressions along with increased SPTLC1/2 levels in a small number (n=3) of wild-type mice, fed a high-fat diet for 5 months starting at 4 months of age (Geekiyanage and Chan, 2011). Here I observed a reduction in the cortical miR-137 with no change in miR-181c levels in the AD mouse model fed a high-fat diet for 3 months, providing possible explanations for the predominantly unchanged SPTLC1 levels. Research demonstrates that unless attached to SPTLC1, SPTLC2 is unstable (Gable et al., 2000; Yasuda et al., 2003). Thus due to the 1:1 ratio between SPTLC1 and SPTLC2, unattached SPTLC2 could be degraded providing a possible explanation for the unchanged SPTLC2 levels even with reduced miR-9 and -29a/b levels. It must be noted that the strain differences, age and duration of diet consumption, and the sample size in the previous study could have contributed to the divergences in ceramide, SPT and miRNA levels observed in the 2 studies. Nevertheless both studies found strong correlations between ceramide, SPT and miRNA levels.

Finally, administration of LCS did not show toxic effects as determined by sera LDH levels, brain and body weight. Administering large doses (100 mg/kg) of LCS has shown immediate reduction of brain SPT with significant weight loss (Sundaram and Lev, 1984b) whereas extended administration of lower doses (25 mg/kg) imposed nominal side effects, with

no changes in weight. In addition, chronic LCS administration was found not to affect brain histology, morphology, myelination or memory retention in healthy mice (Sundaram and Lev, 1989). These observations together suggest SPT inhibition could be essentially a "safe" therapeutic target and LCS a possible "drug candidate". In contrast inhibition of ceramide synthase, another enzyme in the ceramide synthesis pathway, by Fumonisin B1 leads to growth inhibition and cytotoxicity (Schmelz et al., 1998). Further, consumption of Fumonisin B1 causes veterinary diseases and contributes to esophageal cancer in humans (Chu and Li, 1994; Yoshizawa et al., 1994). Other inhibitors of SPT, such as ISP-1 are difficult to solubilize and inflict gastrointestinal toxicity when incorporated into the diet (Hojjati et al., 2005b). Additionally, in agreement with previous studies conducted in dogs (Kluepfel et al., 1972) I observed (unpublished observation) that ISP-1 is lethal to mice when administered subcutaneously. Therefore, this study suggests that inhibition of SPT and thus ceramide, through a less-invasive route, can potentially ameliorate the Aβ burden and tau hyperphosphorylation observed in AD with nominal toxicity.

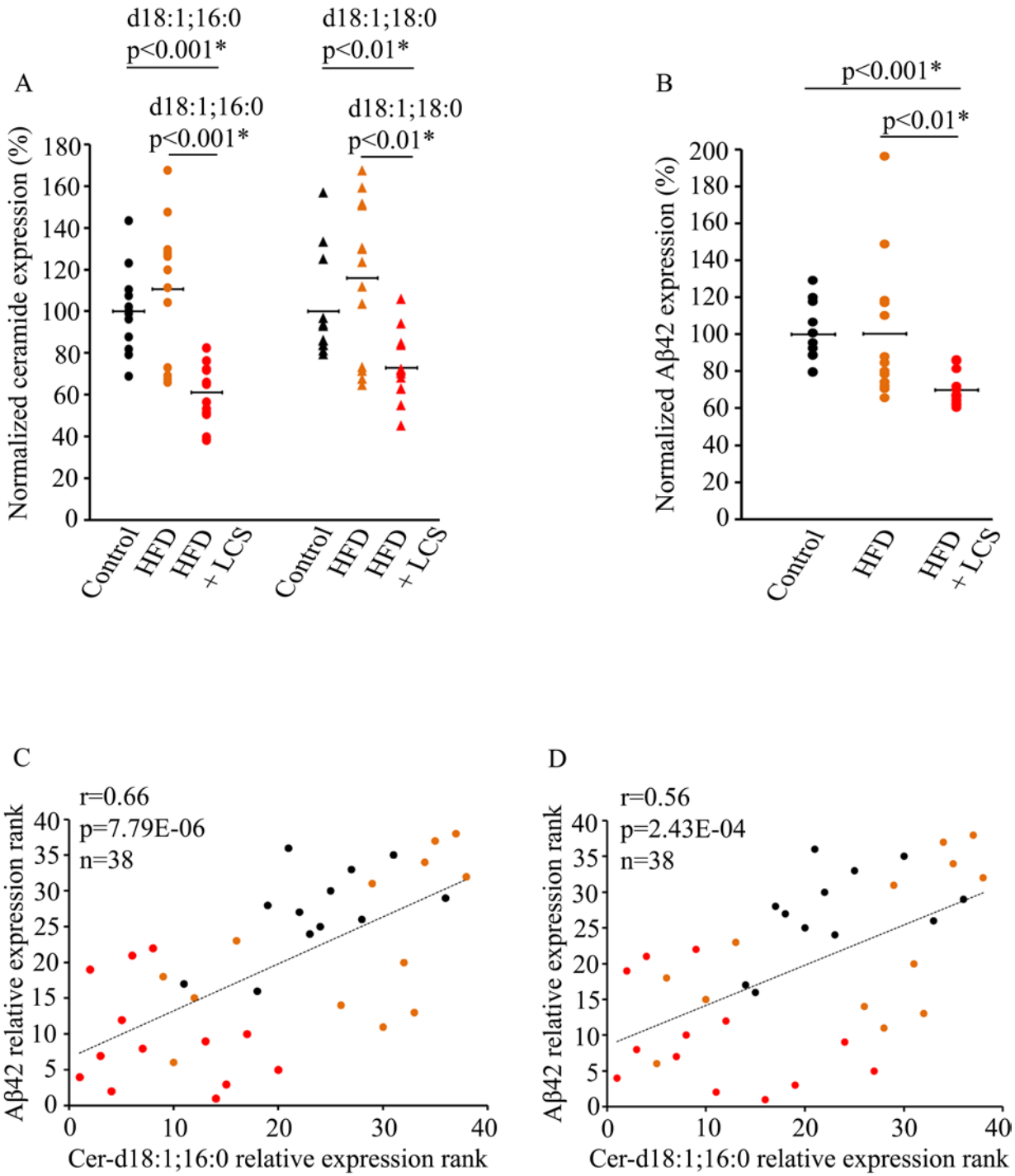

Figure 11: $A\beta_{42}$ is down-regulated with LCS administration. (A) Ceramide levels, d18:1; 16:0 and d18:1; 18:0, were significantly decreased in LCS administered mice (n=13). The brain

Figure 11 (cont'd)

(Figure 11 legend continues) cortices were analyzed via tandem mass spectrometry and the normalized concentrations are shown as a percentage of the average control (n=12). The samples were normalized to internal standard (d18:1, 12:0) concentration and to brain total protein concentrations. **(B)** $A\beta_{42}$ levels were significantly decreased in LCS administered mice (n=13) compared with the control chow and high-fat diet fed mice. The brain cortices were analyzed with ELISA and the normalized concentrations are shown as a percentage of the average control (n=12). The samples were normalized to brain total protein concentrations. The statistical significances were determined by Mann-Whitney U tests. Spearman's correlation tests demonstrate significant positive correlations between cortical ceramides, **(C)** d18:1; 16:0, **(D)** d18:1; 18:0, and $A\beta_{42}$ levels in the entire sample set (control chow, high-fat, diets and LCS administration) (n=38). The statistical significance of the correlation was determined by two-tailed T distribution tests. For interpretation of the references to color in this and all other figures, the reader is referred to the electronic version of this dissertation.

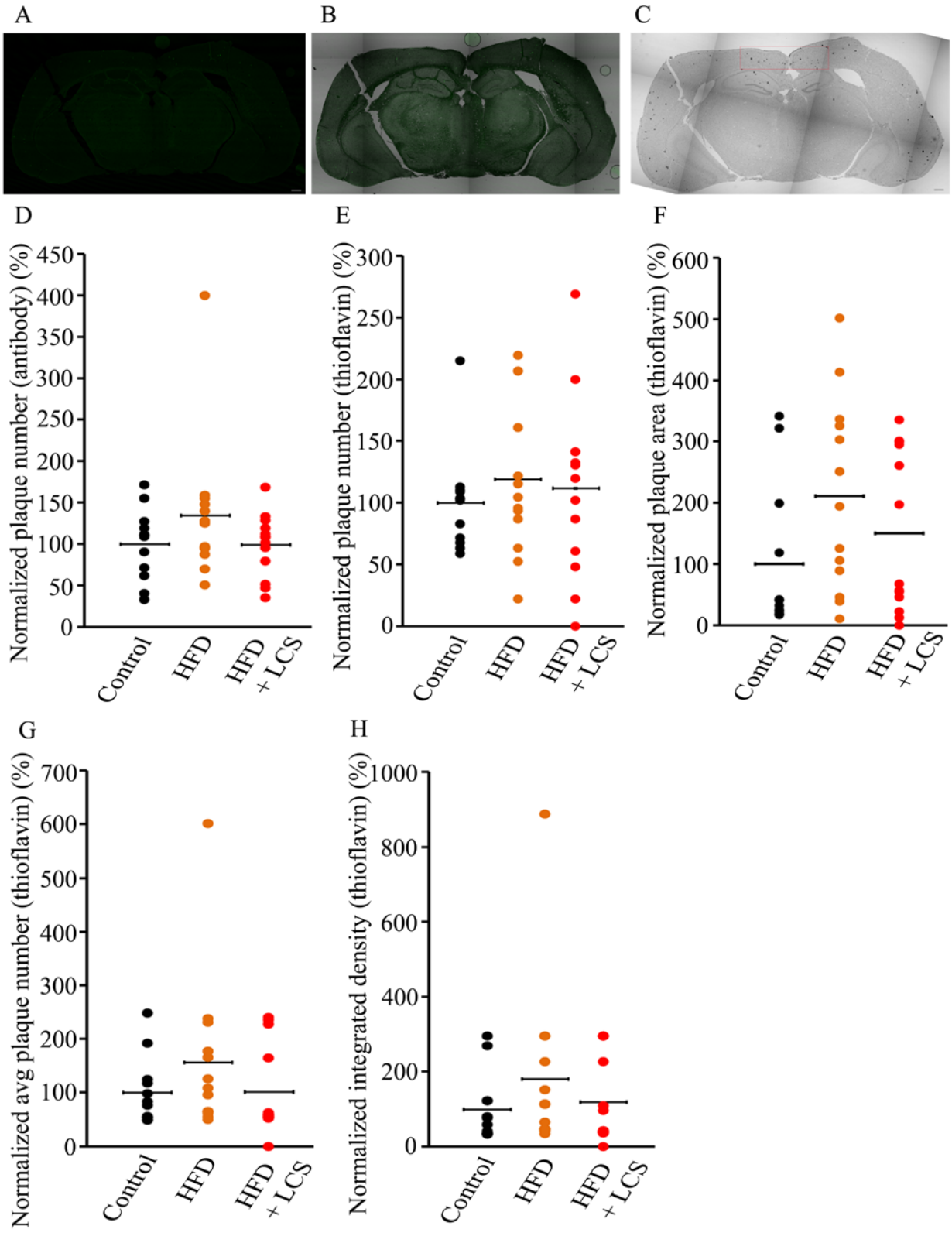

Figure 12: Aβ plaque levels in chow control, high-fat diets and LCS administered mice. The

Figure 12 (cont'd)

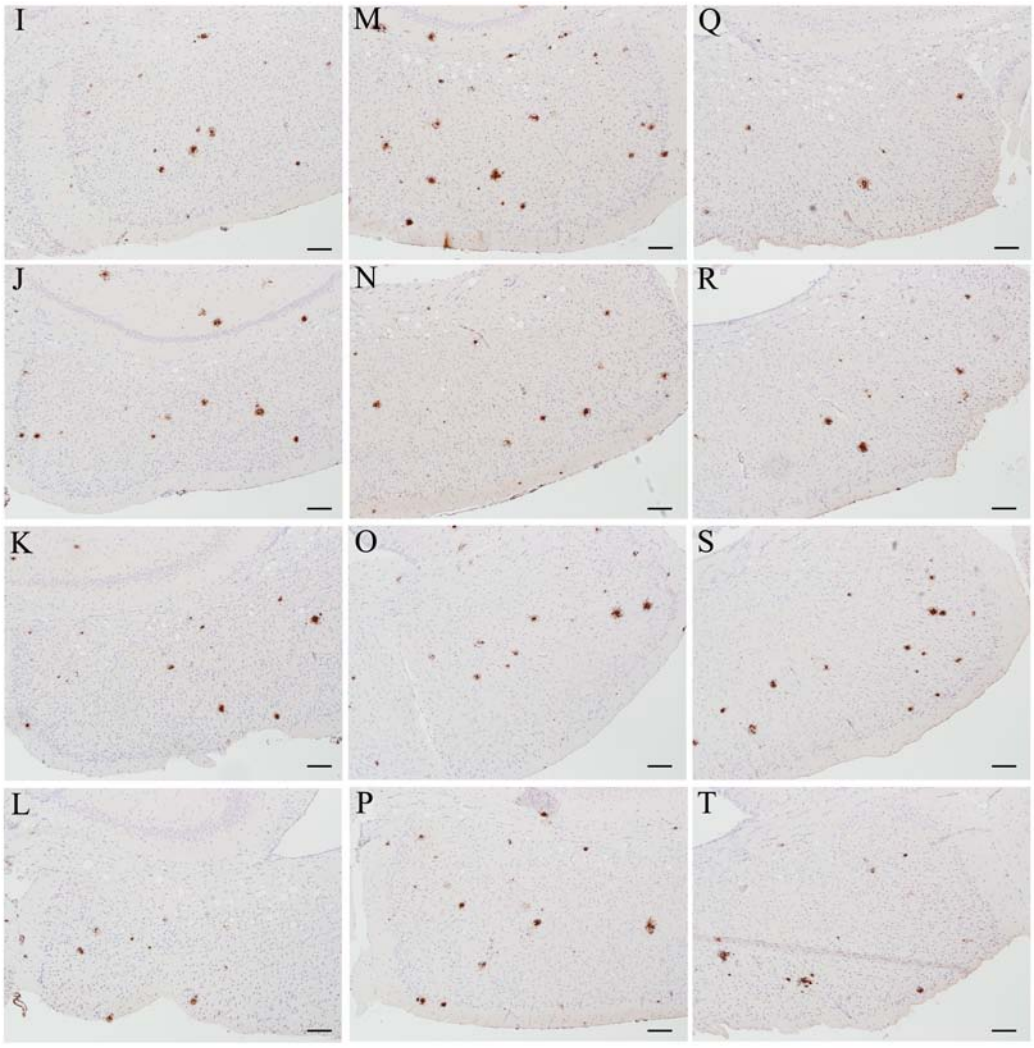

(Figure 12 legend continues) brain sections were stained with **(A)** thioflavin-S and imaged with the fluorescence laser (4X). **(B)** Overlay of a thioflavin-S section with its bright-field image. **(C)** The brain sections were stained with Aβ antibody and imaged with the transmitted laser (4X). All images were stitched together to generate a single image of the entire brain slice. The plaque numbers were manually counted for **(D)** antibody and **(E)** thioflavin-S stained entire sections and the normalized values are shown as a percentage of the average control (n=12). NIH-imageJ particle analysis was used to calculate the **(F)** amyloid plaque area, **(G)** average plaque area and

Figure 12 (cont'd)

(Figure 12 legend continues) **(H)** integrated density per brain section for thioflavin-S stained entire sections and the *(Figure 12 continues)* normalized values are shown as a percentage of the average control (n=12). The antibody stained sections were captured with the camera on bright-field at 10X at the location denoted in red in Fig. 2C for **(I-L)** control chow, **(M-P)** high-fat and **(Q-T)** LCS administration. The statistical analyses were conducted with Mann-Whitney U tests.

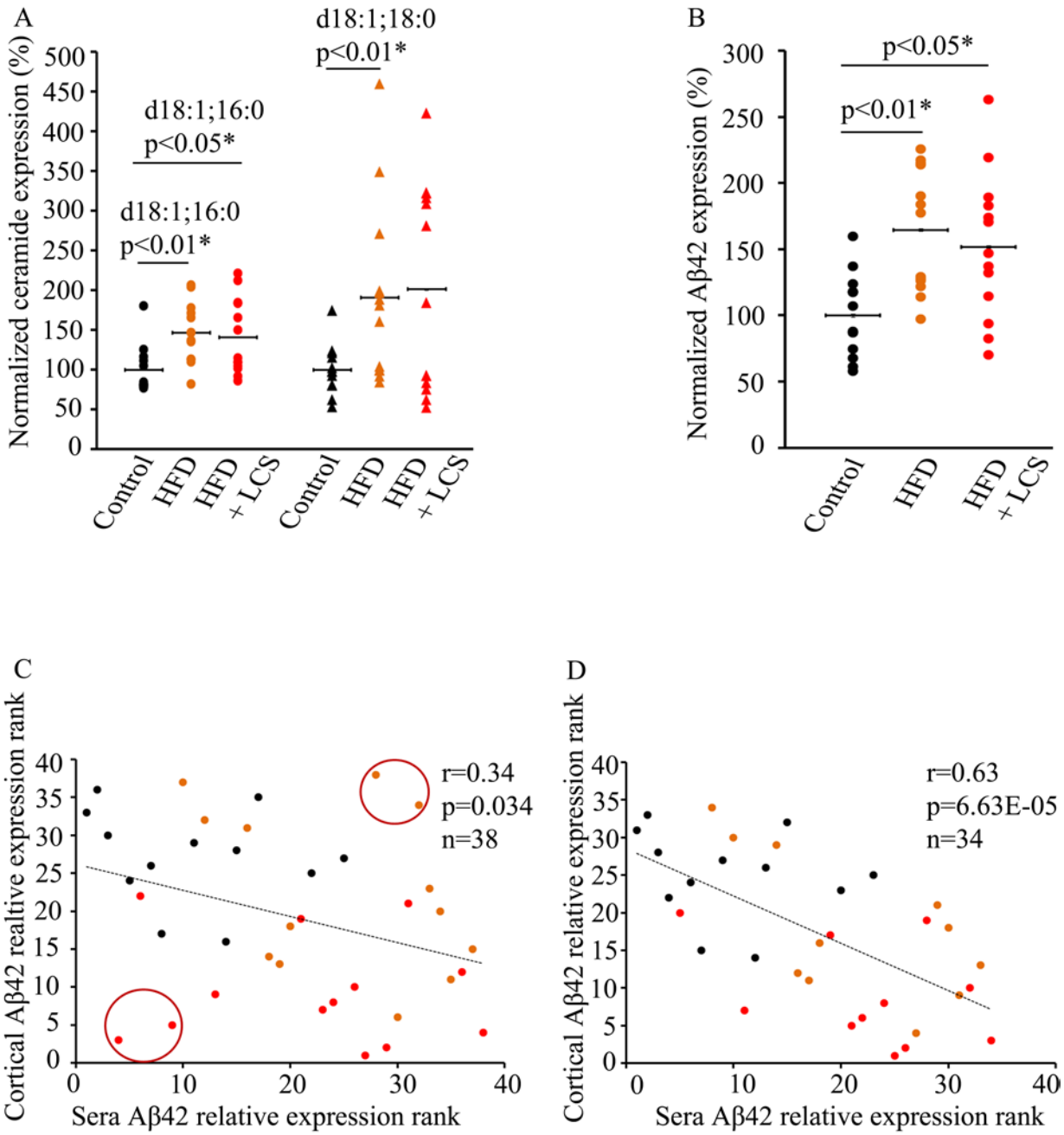

Figure 13: Sera Aβ correlates with cortical Aβ levels. **(A)** Sera ceramide levels, d18:1; 16:0 and d18:1; 18:0, were statistically increased in high-fat (n=13) and, LCS administered mice (n=13) with the exception of d18:1; 18:0. The blood sera were analyzed via tandem mass spectrometry and the normalized concentrations are shown as a percentage of the average control

Figure 13 (cont'd)

(Figure 13 legend continues) (n=12). The samples were normalized to internal standard (d18:1, 12:0) concentration. **(B)** $A\beta_{42}$ levels were significantly increased in high-fat (n=13) and LCS administered mice (n=13). The blood sera were analyzed with ELISA and the normalized concentrations are shown as a percentage of the average control (n=12). The statistical significances were determined by Mann-Whitney U tests. Spearman's correlation tests demonstrate a negative correlation between sera $A\beta_{42}$ and cortical $A\beta_{42}$ levels in the **(C)** entire sample set (n=38) and a statistically stronger significant negative correlation with the **(D)** elimination of 4 subjects as outliers (n=34). The statistical significance of the correlation was determined by two-tailed T distribution tests.

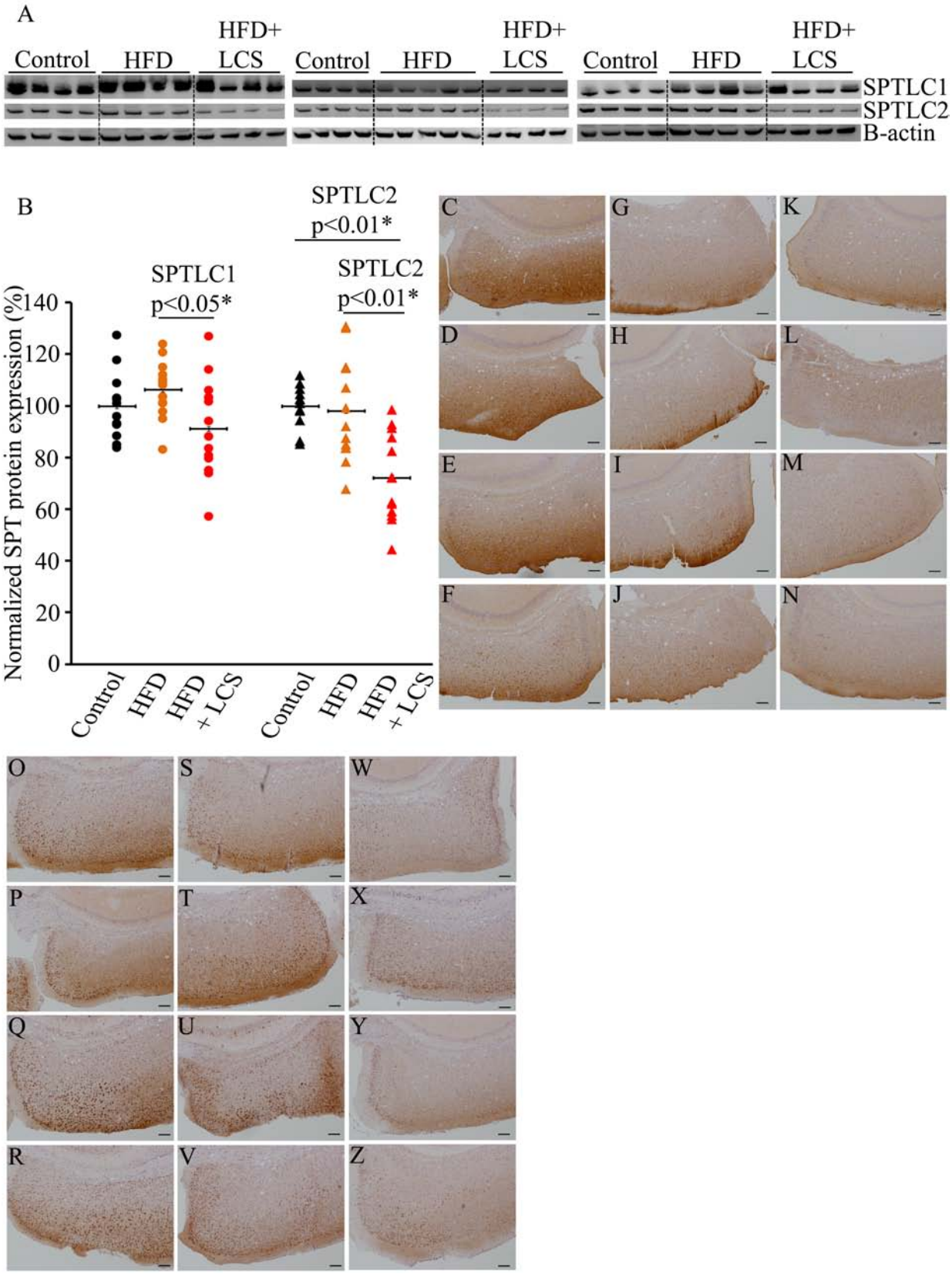

Figure 14: SPT is decreased with the inhibitor. (A) Representative and **(B)** quantification of

Figure 14 (cont'd)

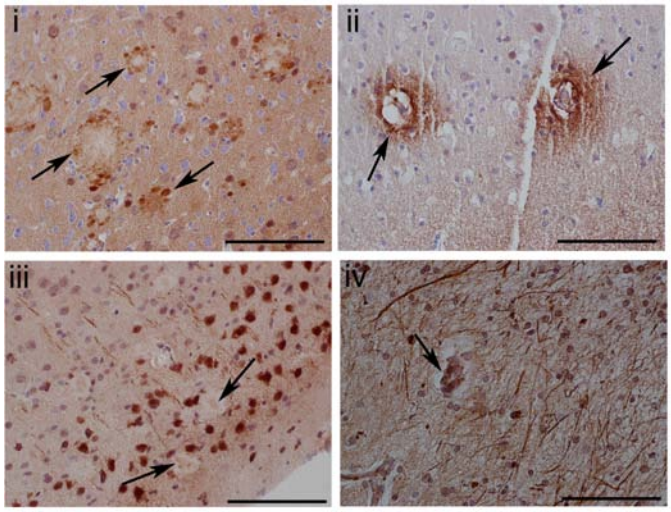

(Figure 14 legend continues) western blots for SPTLC1 (probed with LCB1) and SPTLC2 proteins in control chow (n=12), high-fat (n=13) and LCS administered (n=13) mice. The expression levels were quantified by normalizing to β-actin and represented as a percentage of the control chow mice average expression. The statistical significances were determined by Mann-Whitney U tests. The brain sections were stained with SPTLC1 antibody and were captured with the camera on bright-field at 10X at the location denoted in red in Fig. 2C for **(C-F)** control chow, **(G-J)** high-fat and **(K-N)** LCS administration. The brain sections were stained with SPTLC2 antibody and were captured with the camera on bright-field at 10X at the location denominated in red in Fig. 2C for **(O-R)** control chow, **(S-V)** high-fat and **(W-Z)** LCS administration. Representation of SPTLC1 protein (40X-oil) surrounding the senile plaques and present in the core of the plaques (arrow) in **(i)** mice (13 month old) and **(ii)** humans. Representation of SPTLC2 (40X-oil) protein being present in the core of senile plaques (arrow) in **(iii)** mice (13 month old) and **(iv)** a humans.

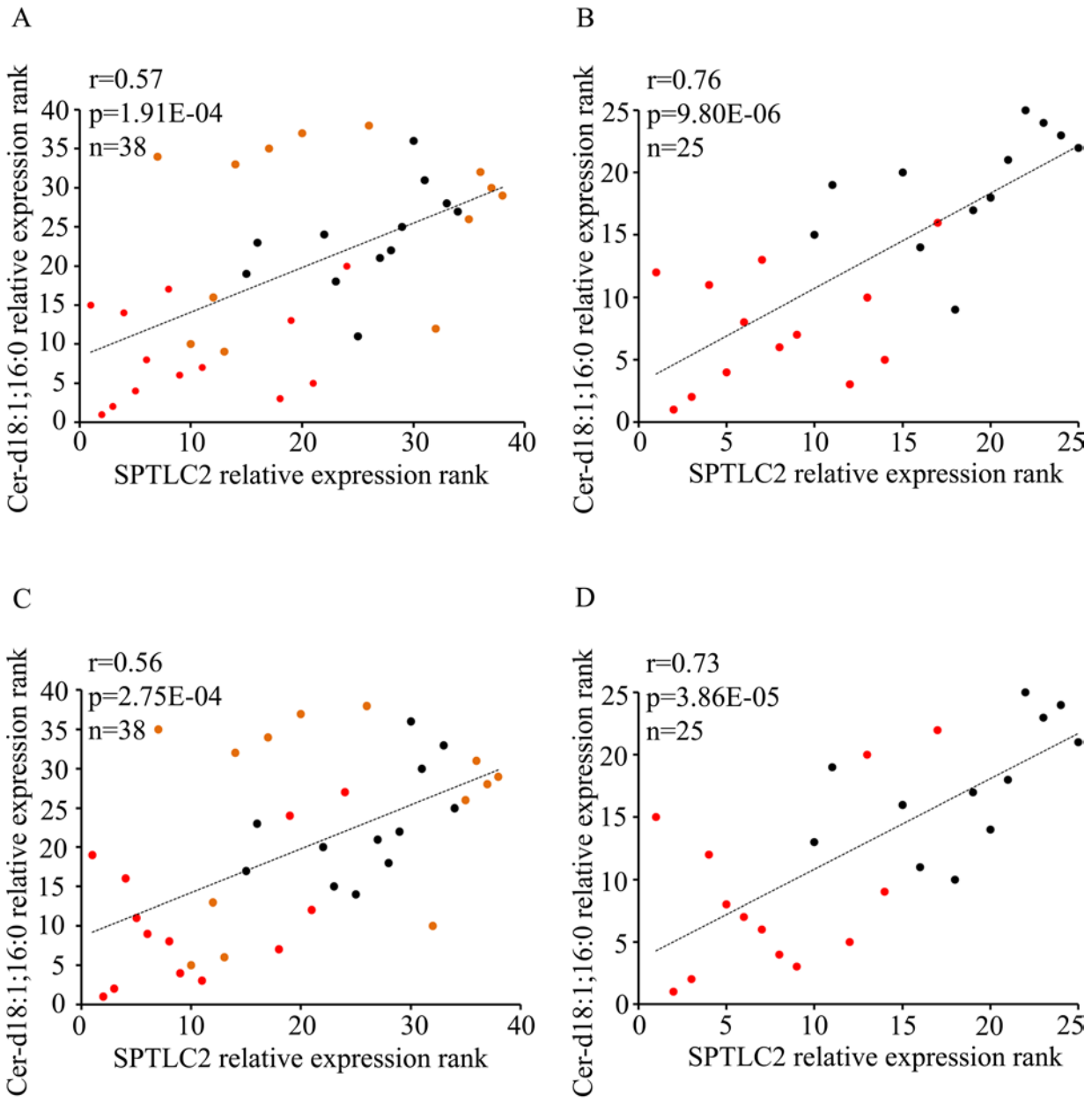

Figure 15: SPT expression correlates with ceramide and Aβ levels. Spearman's correlation tests demonstrate significant positive correlation between cortical SPTLC2 protein levels and **(A)** cortical d18:1; 16:0, **(C)** d18:1; 18:0, and **(E)** $A\beta_{42}$ levels in the entire sample set (control chow, high-fat, diets and LCS administration) (n=38). Stronger positive correlations are observed between cortical SPTLC2 protein levels and **(B)** cortical d18:1; 16:0, **(D)** d18:1; 18:0, and **(F)**

Figure 15 (cont'd)

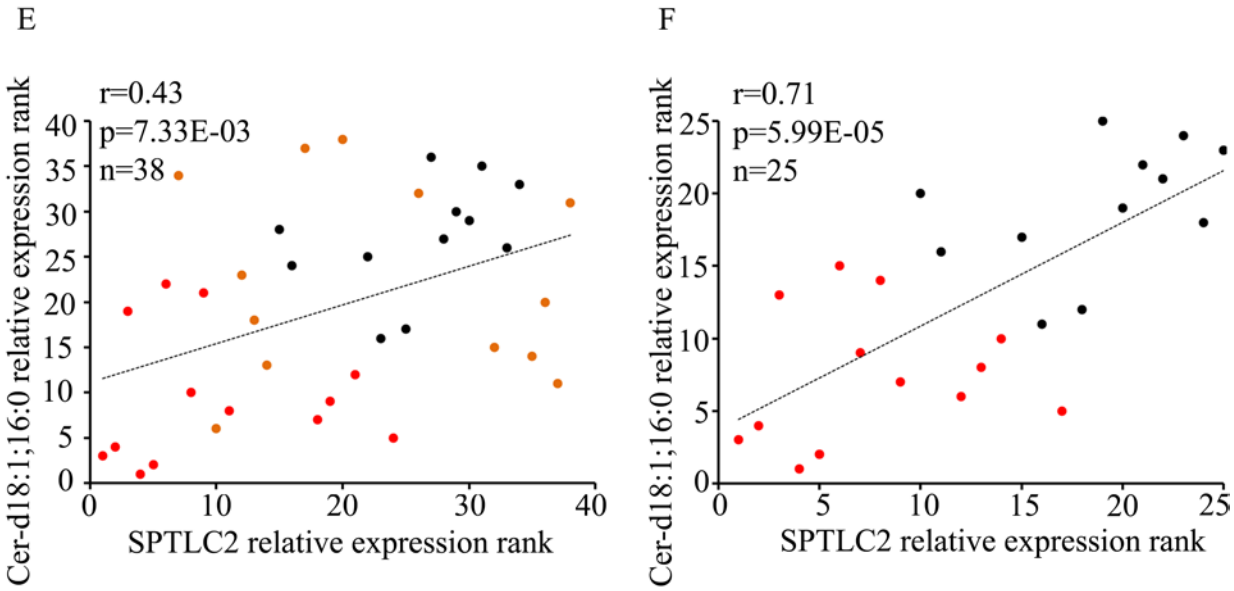

(Figure 15 legend continues) $A\beta_{42}$ levels in control chow diet and LCS administered mice (n=35). The statistical significance of the correlation was determined by two-tailed T distribution tests.

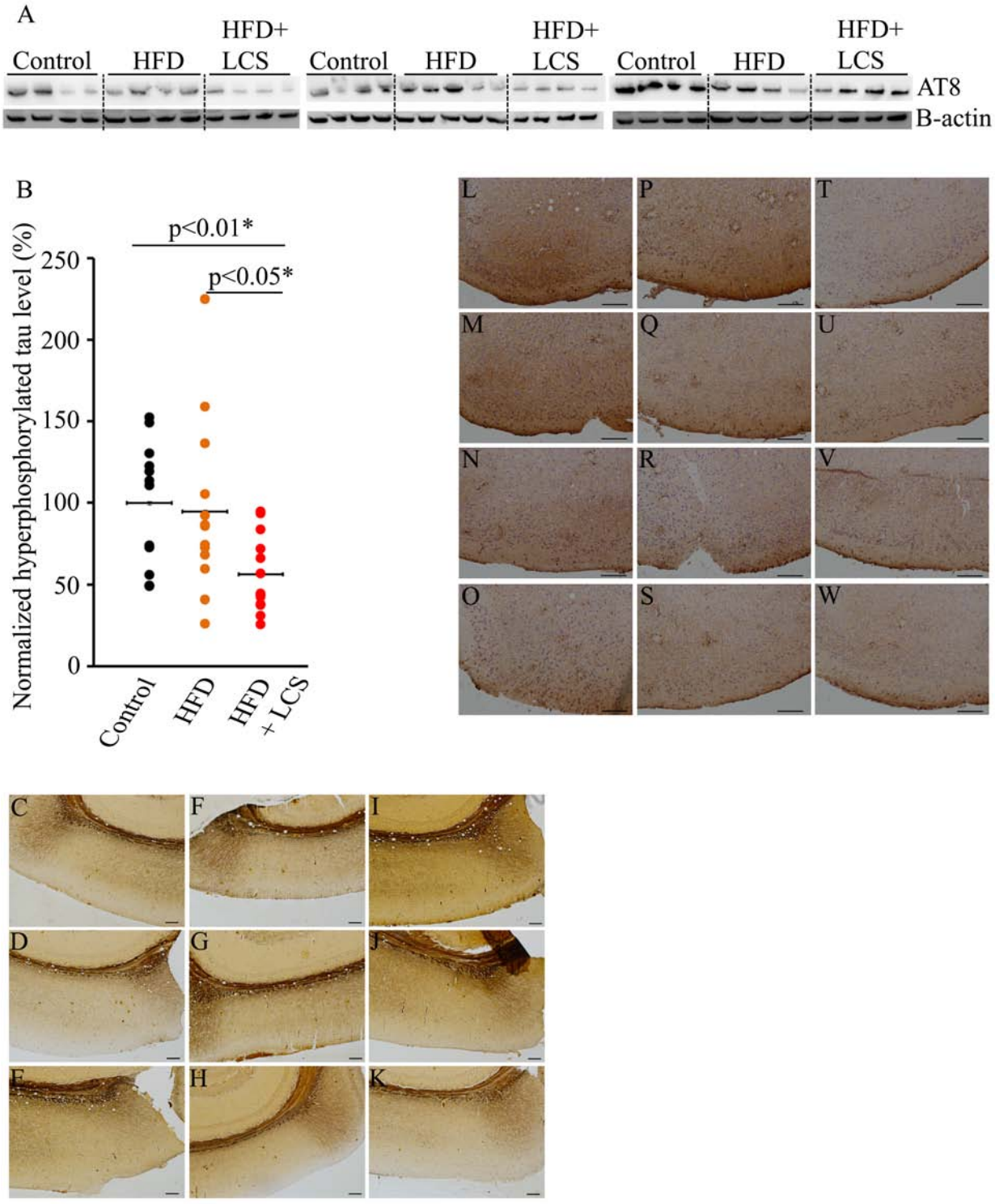

Figure 16: Tau hyperphosphorylation is down-regulated with LCS administration. (A) Quantification and **(B)** representation of western blot for tau hyperphosphorylation (probed with

Figure 16 (cont'd)

(Figure 16 legend continues) AT8) in control chow (n=12), high-fat (n=13) and LCS administered (n=13) mice. The expression levels were quantified by normalizing to β-actin and represented as a percentage of the control chow mice average expression. The statistical significances were determined by Mann-Whitney U tests. The brain sections were stained for Beilschowsky's silver staining and captured with the camera on bright-field at 10X at the location denoted in red in Fig. 2C for **(C-E)** control chow, **(F-H)** high-fat and **(I-K)** LCS administration. The brain sections were stained with NF200 antibody and were captured with the camera on bright-field at 20X at the location denominated in red in Fig. 2C for **(L-O)** control chow, **(P-S)** high-fat and **(T-W)** LCS administration.

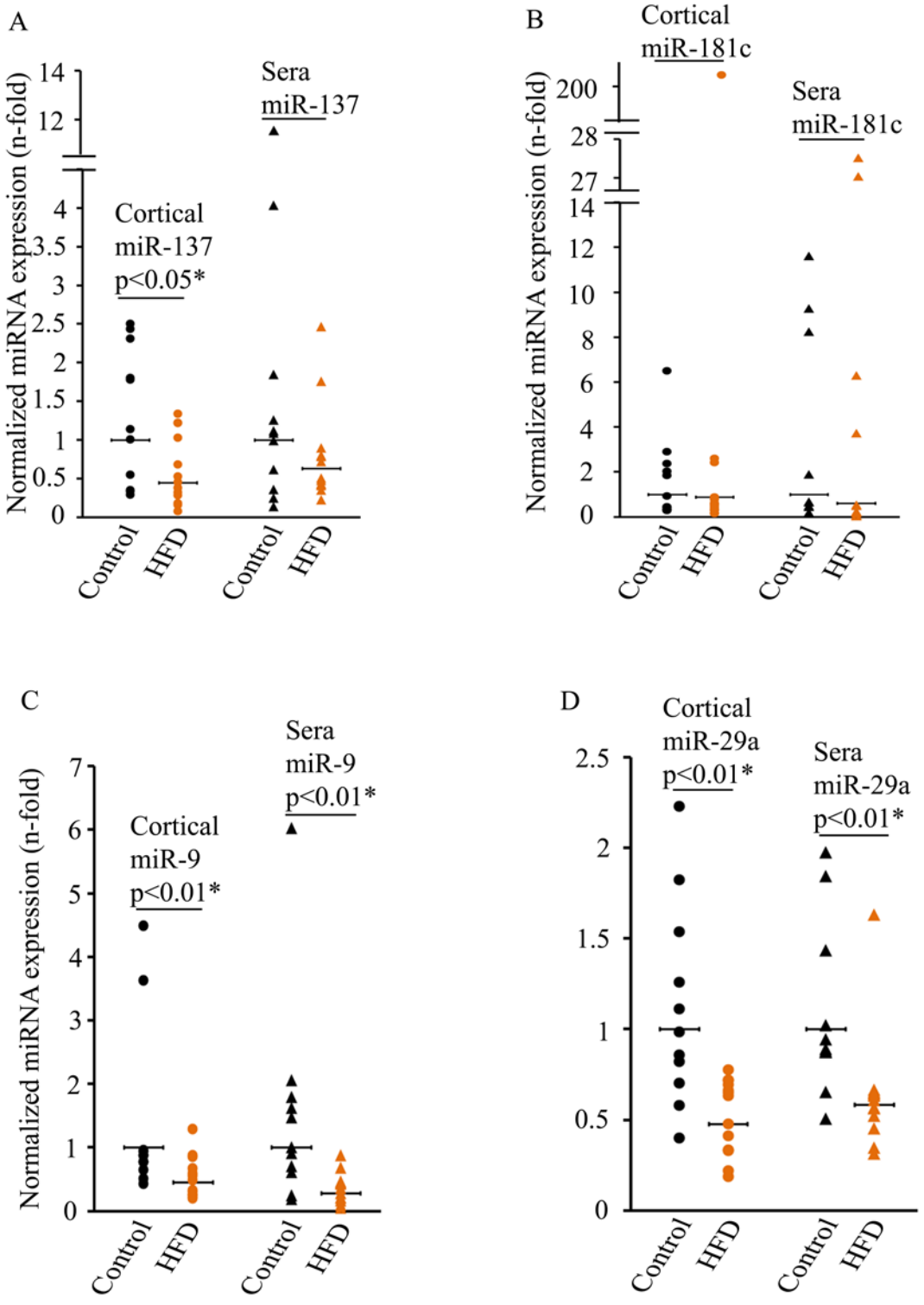

Figure 17: Misregulation of cortical miR-137,-181c,-9 and -29a/b correlate with sera miRNA levels. (A) miR-137, **(B)** -181c, (C) -9, **(D)** -29a and **(E)** -29b levels were quantified by

Figure 17 (cont'd)

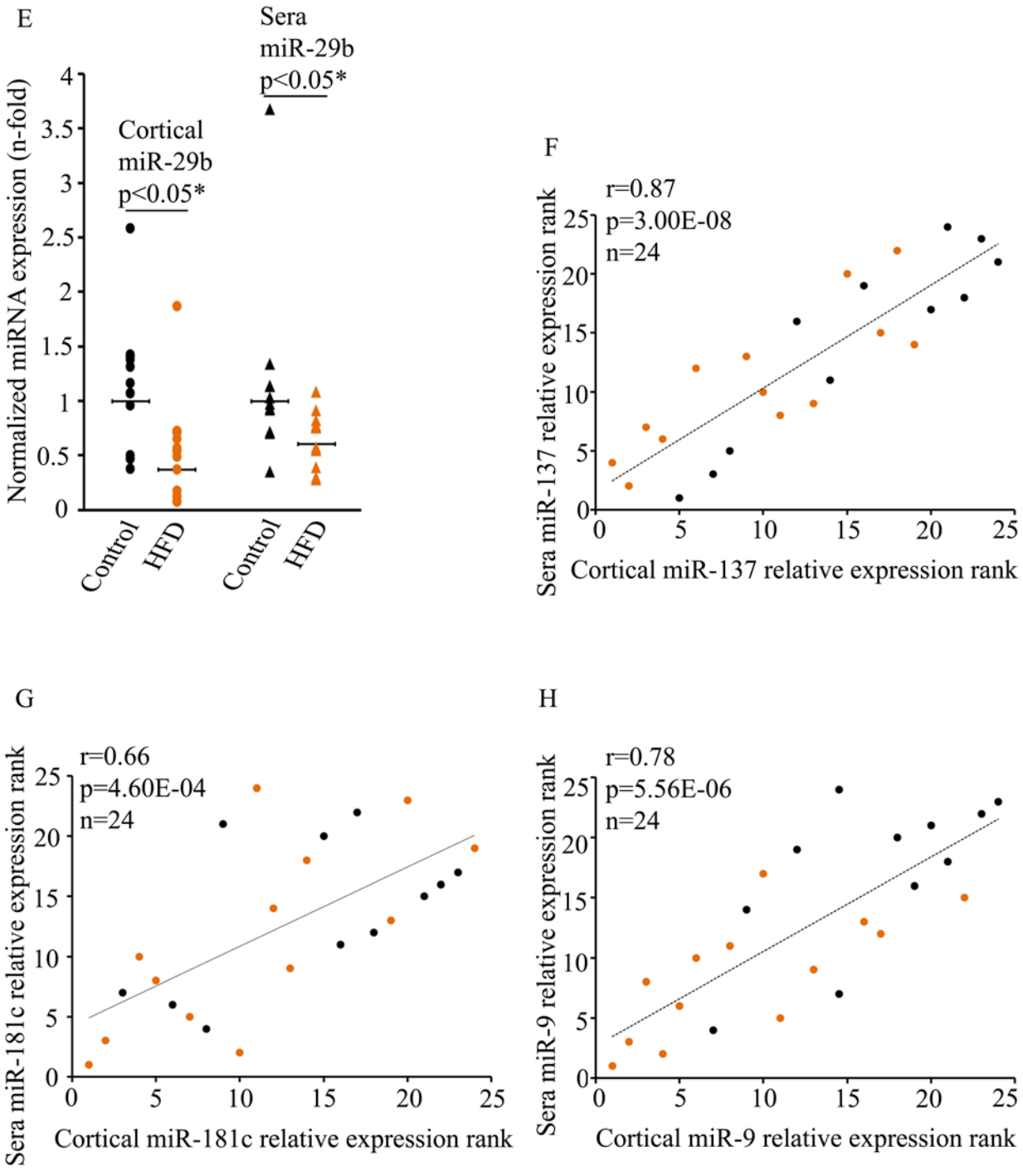

(*Figure 17 legend continues)* qRT-PCR in the cortices and blood sera of control chow (n=11) and high-fat (n=13) diets. Relative expressions shown are normalized to RNU6B for cortical

Figure 17 (cont'd)

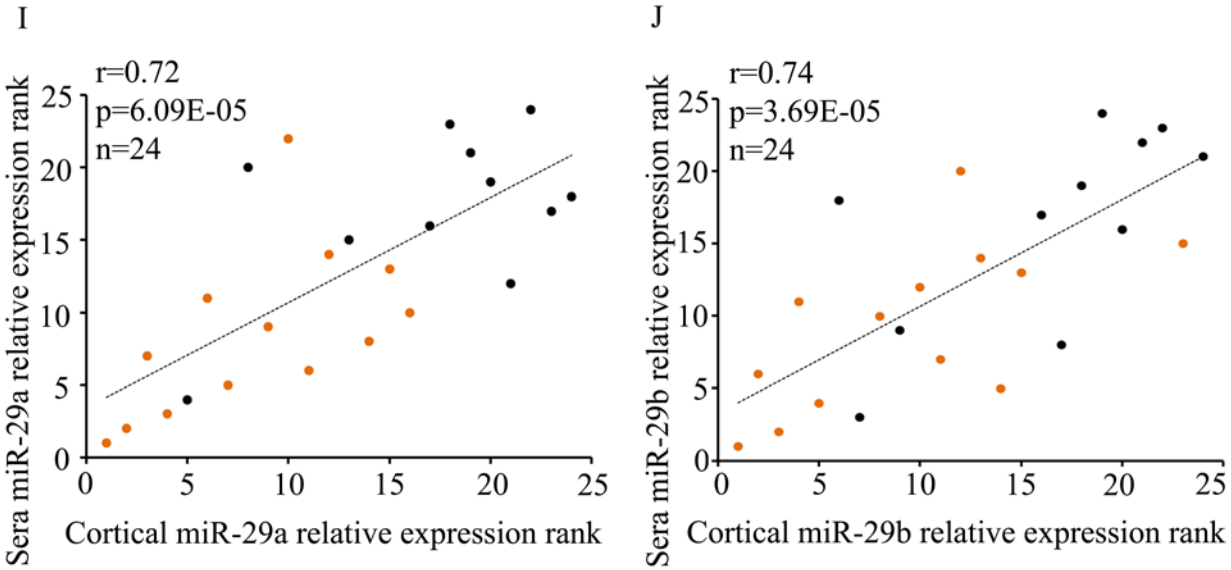

(Figure 17 legend continues) expressions and miR-22 average for sera expressions, and average control chow diet expressions. The statistical significances between control and high-fat diets were determined by Mann-Whitney U tests. Spearman's correlation test demonstrated significant positive correlations between cortical and sera **(F)** miR-137, **(G)** -181c, **(H)** -9, **(I)** -29a and **(J)** -29b in control chow (n=11) and high-fat diet (n=13) fed mice. Note that sufficient serum was not available from 1 control chow diet subject. Therefore, 11 out of 12 control chow diet samples were used for analysis. The significance of the correlation was determined by two-tailed T distribution tests.

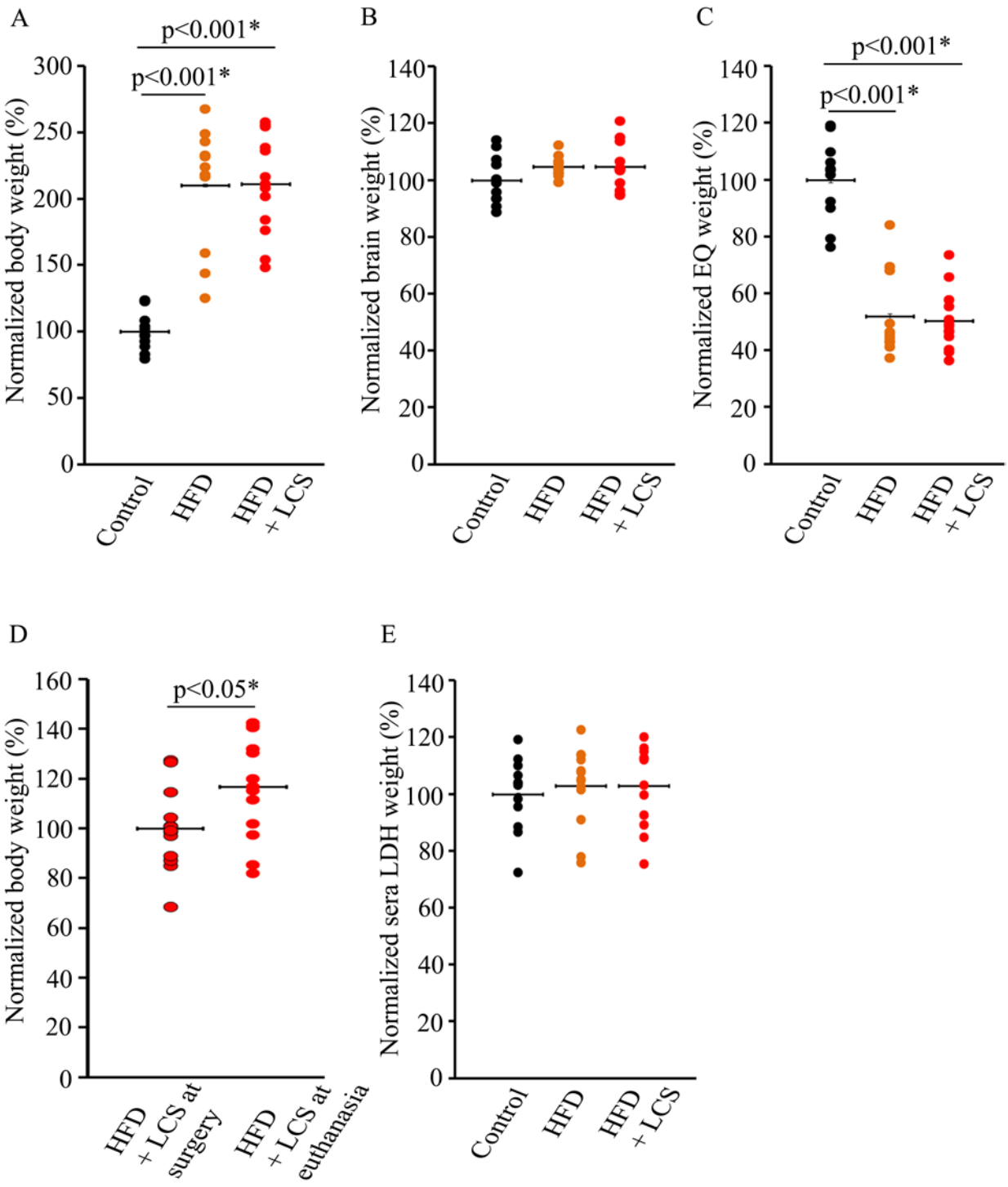

Figure 18: Inhibition of SPT shows no evidence of toxicity. (A) Total body weight, **(B)** total brain weight, and **(C)** EQ at the time of euthanasia, in control chow (n=12), high-fat (n=13) diets and LCS administered (n=13) mice. **(D)** Statistically significant increase in total body weights

Figure 18 (cont'd)

(Figure 18 legend continues) in high-fat fed mice administered with LCS from the time of surgery to euthanasia. **(E)** Blood sera LDH levels at the time of euthanasia in control chow (n=12), high-fat diet (n=13) and LCS administered (n=12) mice. Note that 1 LCS administered subject is unavailable for analysis. Therefore, 12 out of 13 LCS administered samples were used for analysis. The normalized values are shown as a percentage of the average control chow diet samples (n=12). The statistical significances were determined by Mann-Whitney U tests.

CHAPTER 5: CONCLUDING REMARKS AND FUTURE DIRECTIONS

This research suggests that differential expression of ceramide/SPT and miRNAs in AD are potential therapeutic targets for AD. While increased SPTLC1 and SPTLC2 are post-transcriptionally regulated by miR-137, -181c and miR-9, -29a/b respectively, SPTLC1 directly modulates Aβ levels in AD. Differential expressions of SPTLC1/2 and the respective miRNAs were observed in risk factor models of AD indicating that a combination of miRNAs may contribute to regulate SPT and Aβ levels depending on the developmental stage, diet and gender (Geekiyanage and Chan, 2011).

miRNA modulating therapy have been initiated in many disease models and clinical trials (Santaris Pharma, Clinical trials.gov) (Lanford et al., 2010) with the use of chemically modified miRNA, 2'-O-methyl-group-modified oligonucleotides and locked nucleic acid (Elmen et al., 2008b; Elmen et al., 2008a) or lipid-based mimics (Wang et al., 2010b; Wiggins et al., 2010). However, over-expressions of miRNAs need to be conducted intricately with multiple *in vitro* screenings to minimize off-target effects. Thus, it is important to understand the expression patterns of the miRNA of interest and the targeted mRNA/protein. Therefore, on the basis of this research (Chapter 2), understanding the expression patterns of SPTLC1/2 and the respective miRNAs may provide additional information necessary to progress in to therapeutic strategies. This may be achieved through immunohistochemistry and *in situ* hybridizations using E11.5 whole embryos.

This study (Chapter 2) shows that SPTLC1 directly regulates Aβ levels through the post-transcriptional regulation of miR-137 and -181c (Geekiyanage and Chan, 2011). A different study (Hebert et al., 2008) has shown that BACE1 is post-transcriptionally regulated by miR-

29a/b with a causal relationship between miR-29a/b, BACE1 and Aβ levels, where the inhibition of miR-29a/b suppressed Aβ levels. However, the over-expression of BACE1 failed to restore repressed Aβ levels. This study (Chapter 2) demonstrated that miR-29a/b post-transcriptionally regulates the expression of SPTLC2. Additionally I observed a statistically significant positive correlation between SPTLC2 and Aβ levels and a statistically negative correlation between miR-29a/b and Aβ. These observations together suggest a direct role of SPTLC2 in modulating Aβ levels under the regulation of miR-29/b. This hypothesis can be tested by comparing the effects of individual and simultaneous over-expression of *SPTLC2*, *BACE1* and miR-29a/b on Aβ levels in cell culture. In a preliminary study, I observed that transfection of miR-29a/b suppressed Aβ levels in primary astrocytes derived from TgCRND8 mice (Figure 19). As observed by Hebert et al (Hebert et al., 2008), over-expression of BACE1 failed to restore the suppress Aβ levels. However, over-expression of SPTLC2 restored the suppressed Aβ levels suggesting a direct role for SPTLC2 in Aβ modulation through the post-transcriptional regulation of miR-29a/b. Further, the direct role of miR-29a/b and thus SPTLC2 on Aβ production can be assessed through the use of "target protectors" designed against the target sites on *SPTLC2* for miR-29a/b.

In addition to differential expressions of miRNA, increasing research suggest that genetic variations in the 3'UTRs that either inhibit the existing miRNA binding sites or generate illicit sites may play a significant role in disease pathogenesis (Borel and Antonarakis, 2008; Mishra et al., 2008; Sethupathy and Collins, 2008). In neuroscience, a single nucleotide polymorphism (SNP) in the 3'UTR of the fibroblast growth factor 20 (*FGF20*), through the loss of miR-433 presents risk for the development of Parkinson's disease (de Mena et al., 2010). Increase risk for TDP43-positive frontotemporal dementia has been observed with increased binding of miR-656 to the 3'UTR of progranulin (Rademakers et al., 2008). In AD, polymorphisms in miRNA target

sites (PolymiRTS) have been identified in the 3'UTR of *APP* and *BACE1* suggesting that these PolymiRTS may inflict a risk for AD pathogenesis (Delay et al., 2011). Therefore, additional research in the 3'UTRs of *SPTLC1/2* may further elucidate their role in AD.

On a side note, estrogen therapy has been reported to improve cognitive function in post-menopausal women with AD (Fillit et al., 1986; Ohkura et al., 1994; Asthana et al., 1999). However, randomized double blinded control trials derived from these studies report that the improvements in verbal episodic memory and MMSE scores improve at 2 months of estrogen therapy the effects do not manifest at 3 months of treatment and beyond (Wang et al., 2000). Studies suggests that even though estrogen therapy prescribed to older women (>60 years) may have a neutral or a negative effect (Wolf et al., 1999; Binder et al., 2001; Grady et al., 2002; Almeida et al., 2006; Resnick et al., 2006), estrogen therapy prescribed at an identified "critical period", the time of menopause (<49 yeas), could reduce the risk of AD later in life (Maki and Sundermann, 2009; Craig and Murphy, 2010). Currently there are 2 large ongoing randomized controlled trials that have been designed to analyze differences in verbal memory performance in women post-natural-menopause up to 5 years with randomization to either receive placebo or estrogen therapy with or without progesterone (http://clinicaltrials.gov/ct2/show/NCT00114517). Whether estrogen therapy has an effect on ceramide levels remains open for investigation.

Research described in this dissertation not only suggests that the respective miRNAs may be potential therapeutic targets (Chapter 2) but also suggests their role as poteintial diagnostic biomarkers (Chapter 3) (Geekiyanage et al., 2012). I observed that miR-137, -181c, -9 and -29a/b are down-regulated in the blood sera of probable AD and amnestic MCI patients. In addition, the AD mouse model used (TgCRND8) showed statistically significant positive correlations between the cortical and sera miRNA levels, suggesting that the sera miRNA levels

may mirror the brain miRNA expression patterns (Chapter 4). Moreover, the brain enriched/ specific miRNAs, miR-137 and miR-9, showed the strongest correlations, suggesting a minimal influence by other tissues on the sera miRNA levels and thus further strengthening the role of miRNAs, particularly miR-137 and miR-9, as diagnostic biomarkers. Nevertheless, further research is necessary to identify whether these miRNAs can distinguish AD from other forms of dementia and other miRNA modifying diseases, indeed with larger cohorts.

Research in chapter 2 suggested that increased ceramide levels, mediated by increased SPT, increases Aβ levels in AD patients suggesting SPT/ceramide are potential therapeutic targets for AD (Geekiyanage and Chan, 2011). The potential therapeutic application of SPT inhibition was explored in an aggressive mouse model of AD (Chapter 4) (in review). Inhibition of SPT and thus ceramide decreased the Aβ burden and tau hyperphosphorylation with nominal toxic effects at the preclinical stage. Thus, suggesting that inhibition of SPT, through LCS, is essentially a "safe" potential therapeutic strategy to ameliorate the pathological delinquents of AD, at least for the limited exposure paradigm tested. Given the mechanism by which ceramide contributes to AD, through providing a location in lipid rafts for amyloidogenesis and facilitating the trafficking of the pathological secretases to the lipid rafts; inhibition of ceramide via the inhibition of SPT although minimizes Aβ production may not clear the existing plaques. Therefore, inhibition of SPT early in the course of the disease may have increased beneficial therapeutic values.

The use of mouse models in preclinical trials have raised concerns, with some disease modifying treatments that show promise in preclinical mouse studies becoming unsuccessful in clinical trials (Mangialasche et al., 2010). The use of familial AD mouse models to depict sporadic AD, due to their pathophysiological differences, although raises concerns for treatments

focusing on mutations, may possibly be effective for treatments that focus on reducing Aβ levels. AD mice are better models of the early preclinical stages than the later dementia stages (Zahs and Ashe, 2010) suggesting that treatments that are successful in mouse models may have increased benefits in clinical trials if they were administered pre-symtomatically. Although the focal point of the research in chapter 4 was inhibition of SPT and not the inhibitor LCS, this study nonetheless suggests that subcutaneous administration of LCS is essentially a "safe" potential "drug candidate". However, the differences in drug metabolism, pharmacokinetics and the route of administration need to be compared for the effective use of LCS across species. Nevertheless, oral administration of cycloserine is used clinically under the brand name Seromycin (The Chao Center, IN) for the treatment of pulmonary and extrapulmonary tuberculosis and urinary tract infections validating its clinical safety.

It is important to note that placebo effects and functional effectiveness of SPT inhibition were not evaluated in this study (Chapter 4). Therefore, the effect on cognitive impairments including behavioral and electrophysiology studies need to be conducted with LCS administration, along with placebo administration in order to further support the use of SPT inhibition as a therapeutic strategy for AD. Additional validation in other mouse models with increased sample numbers may also provide further information for future possible clinical trials derived from this study (Chapter 4).

Collectively, this research suggests that miR-137, -181c, -9 and -29a/b are potential therapeutic targets and diagnostic biomarkers for AD, and targeting SPT as a therapeutic target is essentially a "safe" potential strategy to modulate the principle hallmarks of AD, Aβ and tau hyperphosphorylation (see schematics, Figure 20).

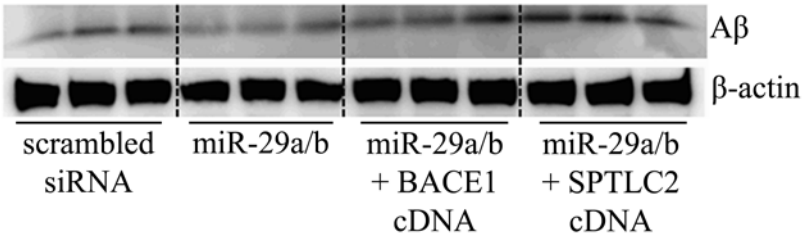

Figure 19: Regulation of Aβ by SPTLC2. Western blot analysis of cellular Aβ (3 kDa-probed with Aβ antibody) levels in primary astrocytes expressing Swedish and Indiana mutations, following transfection with miR-29a/b alone or in combination with human SPTLC2 cDNA or human BACE1 cDNA.

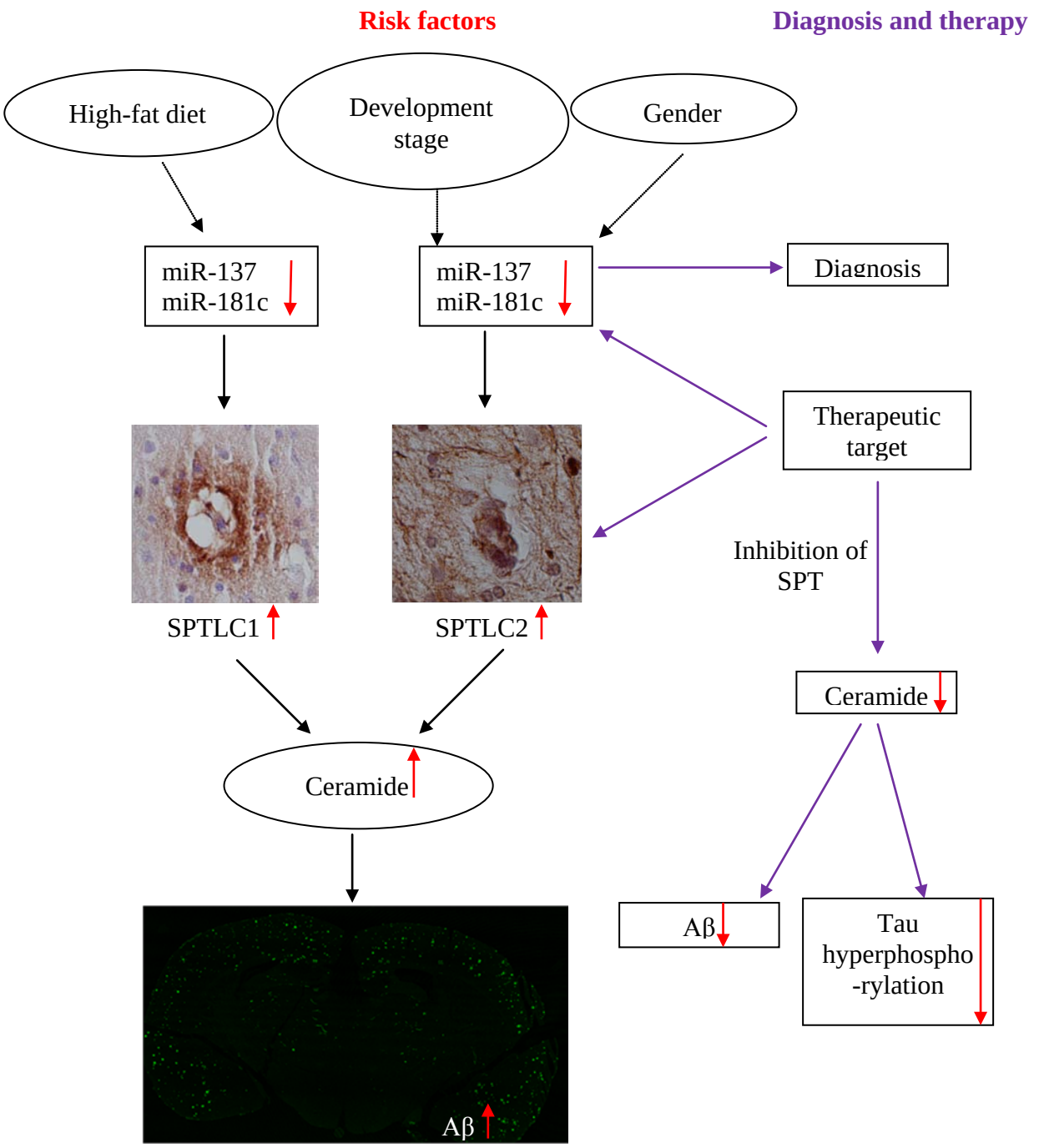

Figure 20: Schematics summarizing the cascade of events described in the dissertation. High-fat diet, age, gender could impose increase risk on the pathogenesis of AD by reducing miR-137, -181c, and miR-9, 29a/b which in turn reduces ceramide levels by post- *(Figure 20*

Figure 20 (cont'd)

legend continues) transcriptionally regulating SPTLC1 and SPTLC2 levels respectively. This suggests that the corresponding miRNAs and SPT are potential therapeutic targets for the treatment of AD. Inhibition of SPT reduces AD pathology, further suggesting its therapeutic use. Reduced miRNA levels in the blood sera could be used as potential non-invasive diagnostic marker for AD.

APPENDICES

APPENDIX A

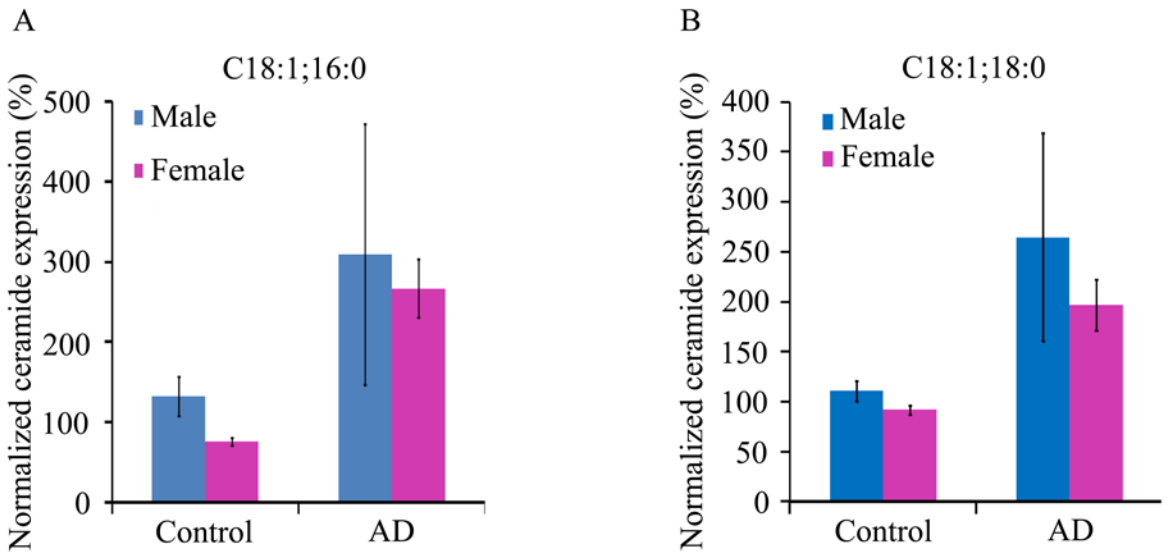

Figure 21: Ceramide levels according to gender. (A) d18:1; 16:0 and **(B)** d18:1; 18:0 in male (n=3) and females (n=4) of control and AD autopsy subgroups. The frontal brain cortices were analyzed via tandem mass spectrometry and the normalized concentrations are shown as a percentage of the average control (n=7). The samples were normalized to internal standard (d18:1, 12:0) concentration and to brain total protein concentration.

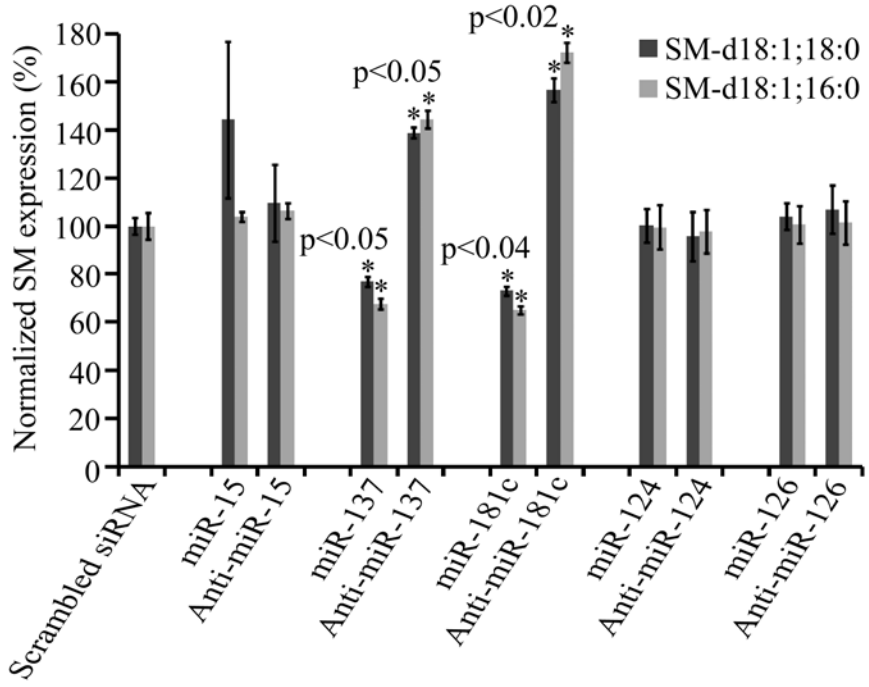

Figure 22: Differential sphingomyelin expression in response to miR-137 and -181c transfections. Cellular sphingomyelin levels of primary rat astrocytes transfected with miRs or anti-miRs (100 nM). Cellular Spingomyelin levels were analyzed via tandem mass spectrometry and the normalized concentrations are shown as a percentage of the scrambled siRNA. The samples were normalized to internal standard (d18:1, 12:0) concentration and to cellular total protein concentration. Error bars represent standard errors derived from three or more experiments conducted with 48-72 hr transfections.

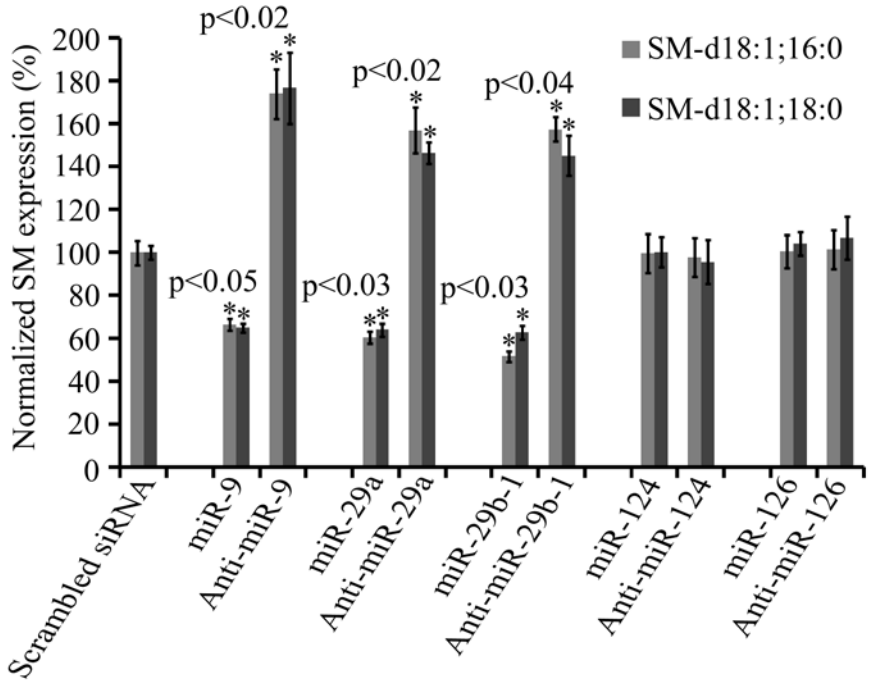

Figure 23: Differential sphingomyelin expression in response to miR-9 and -29a/b transfections. Cellular sphingomyelin levels of primary rat astrocytes transfected with miRs or anti-miRs (100 nM). Cellular Spingomyelin levels were analyzed via tandem mass spectrometry and the normalized concentrations are shown as a percentage of the scrambled siRNA. The samples were normalized to internal standard (d18:1, 12:0) concentration and to cellular total protein concentration. Error bars represent standard errors derived from three or more experiments conducted with 48-72 hr transfections.

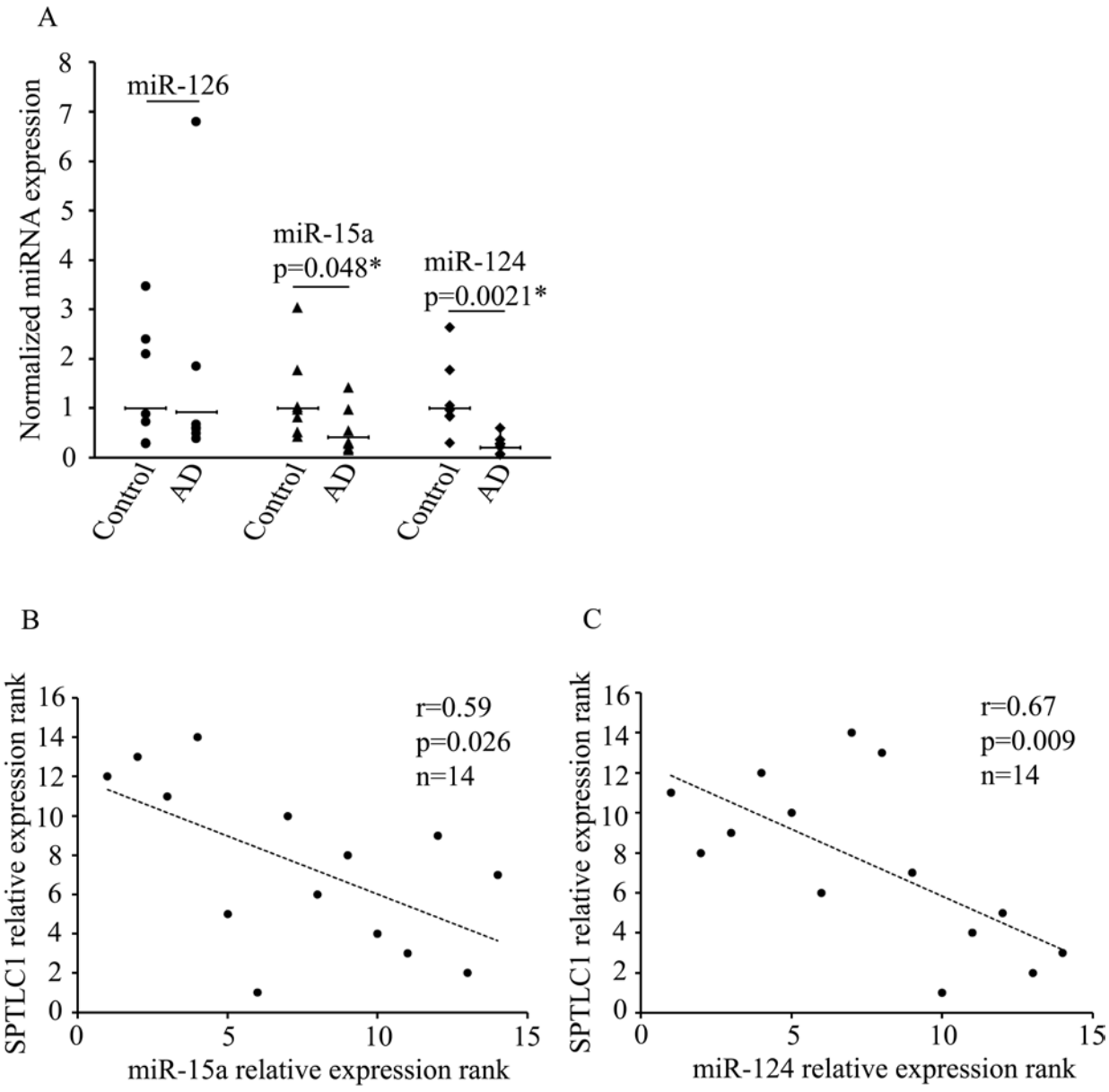

Figure 24: Misregulation of miR-15a and -124 in AD brain. (A) miR-15a and miR-124 expression levels were quantified by qRT-PCR in controls (n=7) and AD (n=7) frontal brain cortices. Relative expressions shown are normalized to RNU6B and average control brain expressions. The statistical significance between control and AD brains were determined by 2-tailed student *t* tests. **(B** and **C)** Spearman's correlation test demonstrates significant negative correlation between miR-15a,-124c and SPTLC1 expression in the entire sample set (control and

Figure 24 (cont'd)

(Figure 24 legend continues) AD) (n=14). The significance of the correlation was determined by two-tailed T distribution tests.

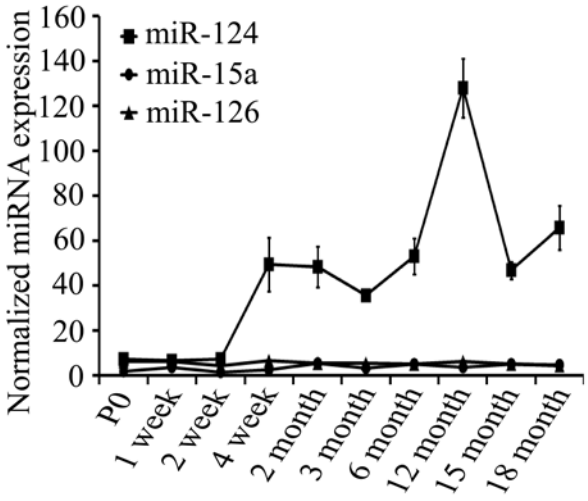

Figure 25: Developmental regulation of miR-124. Relative expression levels of miR-124 were measured by qRT-PCR in mouse brain cortices with RNU6B being used as the normalizing control.

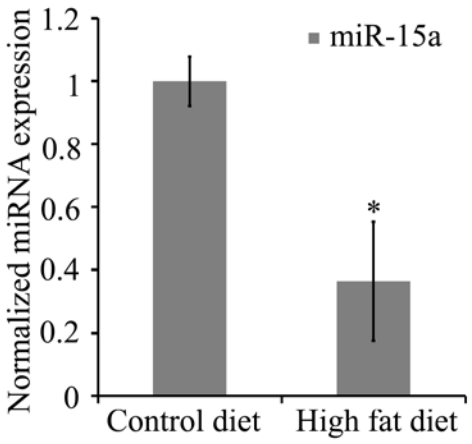

Figure 26: Regulation of miR-15a with diet. Wild-type mice were fed a 60%kcal diet for a period of 5 months starting at 4 months of age. The expression levels of miR-15a (*, P=0.01) in high-fat diet fed mice cortices were measured by qRT-PCR. Relative expressions shown are normalized to RNU6B and chow control diet expressions. The statistical significance between control chow diet and high-fat diet was determined by 2-tailed student *t* tests.

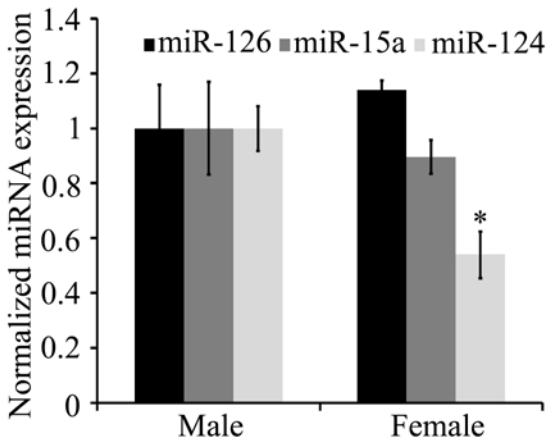

Figure 27: Gender specific differential regulation of miR-124. The expression levels of miR-124 (*, P=0.01) were measured by qRT-PCR. Relative expressions shown are normalized to RNU6B and average male expressions. The statistical significance between male and female expressions was determined by 2-tailed student *t* tests.

APPENDIX B

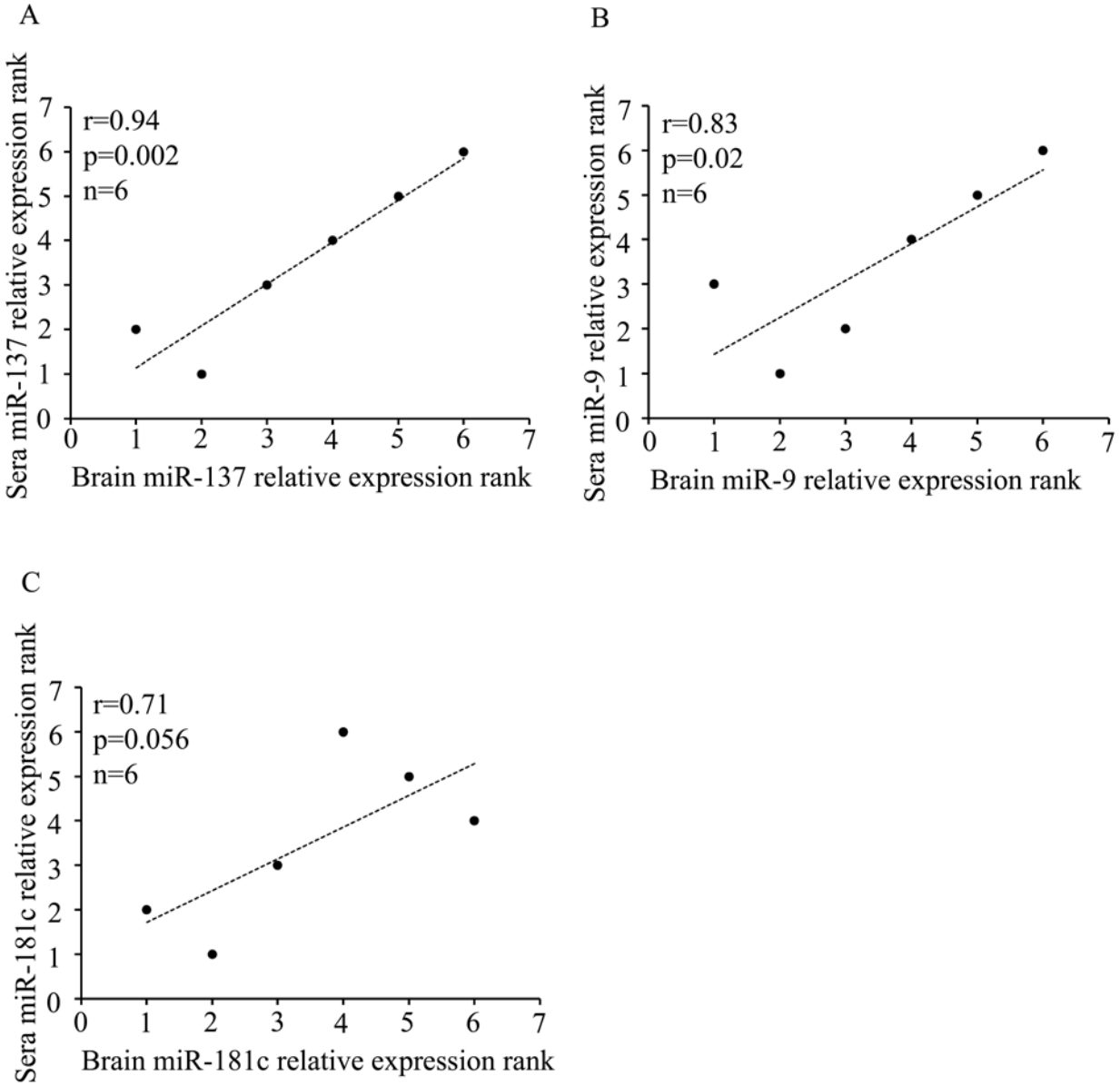

Figure 28: Misregulation of cortical miRNA levels correlate with sera miRNA levels. Spearman's correlation test demonstrated significant positive correlations between cortical and sera **(A)** miR-137, **(B)** miR-9 in control chow (n=3) and high-fat diet (n=3) fed mice. **(C)** Spearman's correlation test demonstrated positive correlations between cortical and sera miR-

Figure 28 (cont'd)

(Figure 28 legend continues) 181c in control chow (n=3) and high-fat diet (n=3) fed mice. The significance of the correlation was determined by two-tailed T distribution tests.

APPENDIX C

	Male	Female	Control chow diet	High-fat diet	LCS	Meloxicam at surgery (1-2 mg/kg)	Baytril (0.003% in 250 mL of H2O)
Control chow diet	7	5	X				
High-fat diet	5	8		X			
HFD + LCS	5	8		X	X	X	X

Table 3: Mouse nutrient information. Control chow diet category mice (7 males and 5 females) were fed control chow diet starting at 4 weeks of age and continued up to 4 months of age. High-fat diet category (5 males and 8 females) were fed a 60% kcal high-fat diet starting at 4 weeks of age and continued up to 4 months of age. HFD+LCS category (5 males and 8 females) were fed a 60% kcal high-fat diet starting at 4 weeks of age and continued up to 4 months of age. In addition, the HFD+LCS category was administered with LCS via a surgically implanted osmotic pump at 3 months of age that delivered LCS at a constant rate of 0.25 uL/hour for a period of 28 days, while being fed the 60% kcal high-fat diet stating at 4 weeks of age and continuing up to 4 months of age. The HFD+LCS category was administered a single dose of meloxicam (1-2 mg/kg) at surgery. The HFD+LCS category was administered Baytril (antibiotic) orally (0.003% dissolved in 250 mL of daily water consumption) starting from 2 days prior to surgery and continuing until euthanasia.

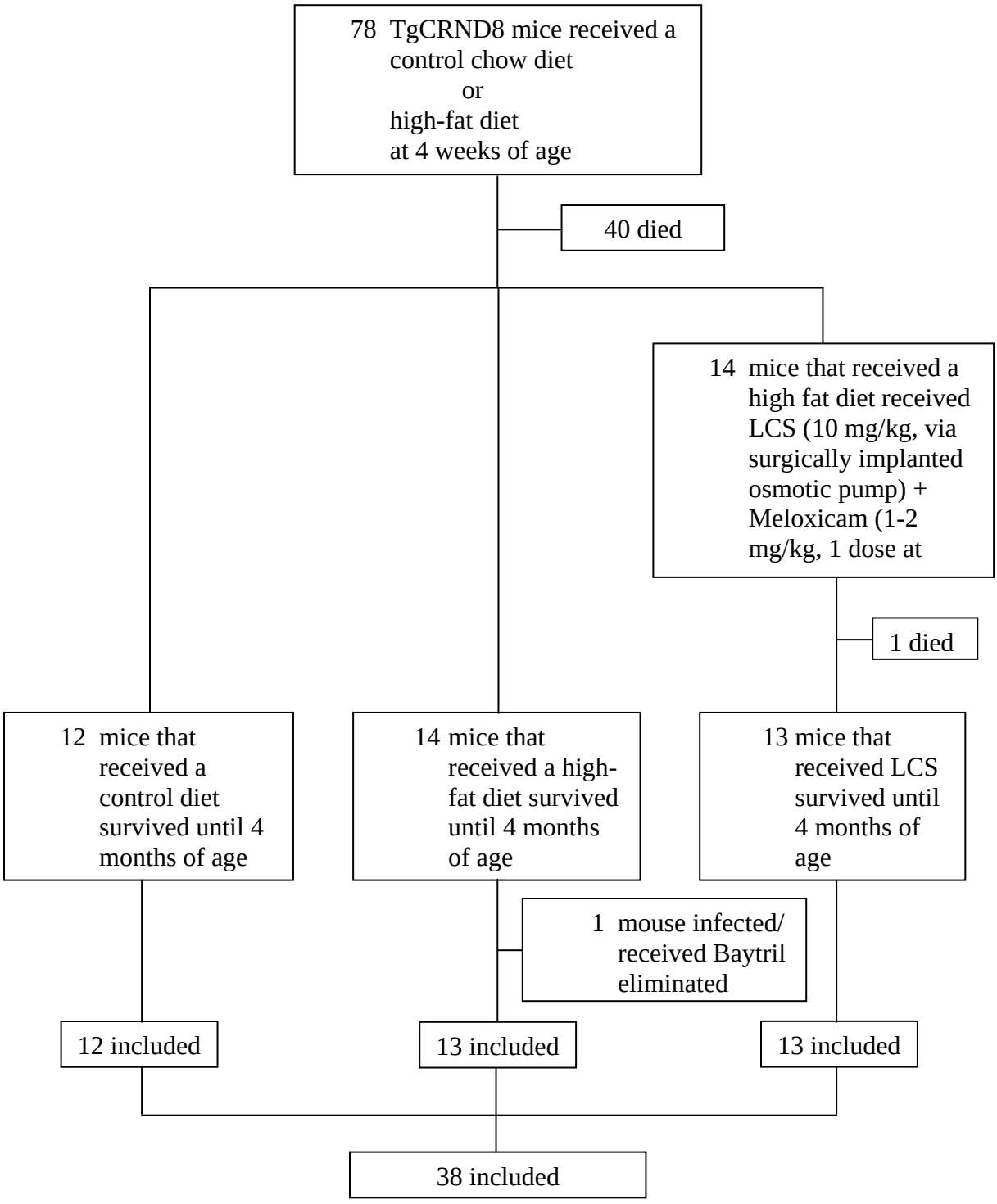

Figure 29: Random assignment to treatment. 78 mice, at 4 weeks of age, were incorporated in to the study and fed a control chow diet or a high-fat diet. At 3 months of age, 14 mice fed a

Figure 29 (cont'd)

(Figure 29 legend continues) high- fat diet, categorized in to LCS administered group, were administered 10 mg/kg of LCS subcutaneously via surgically implanted osmotic pumps that delivered LCS at a constant rate of 0.25 uL/hour for a period of 28 days. Out of the 14 mice administered with LCS, 13 mice survived to term (4 months of age) while 1 mouse died of the *Pasteurella pneumotropica* infection in the colony (survival rate of ~90% (13 out of 14) from the time of surgery to euthenasia (28 days)). 12 mice fed a control chow diet, categorized in to control chow diet group, and 14 mice fed a high-fat diet, categorized into the high-fat diet group, survived to term (4 months of age) (50% survival rate (39 out of 78 survived)). Out of the 14 mice that survided to term in the high-fat diet group, 1 mouse was administered Baytril to treat for an infection. This mouse was eliminated from the study to maintain homogeneity in the high-fat diet group (This mouse showed increased brain cortical ceramide levels by ~21% (d18:1; 16:0) - ~37% (d18:1; 18:0) compared with the average ceramide levels in the mice fed a control chow diet, possibly suggesting that the reduced ceramide and $A\beta_{42}$ observed in this study is due to inhibition of SPT and not the oral administration of Baytril).

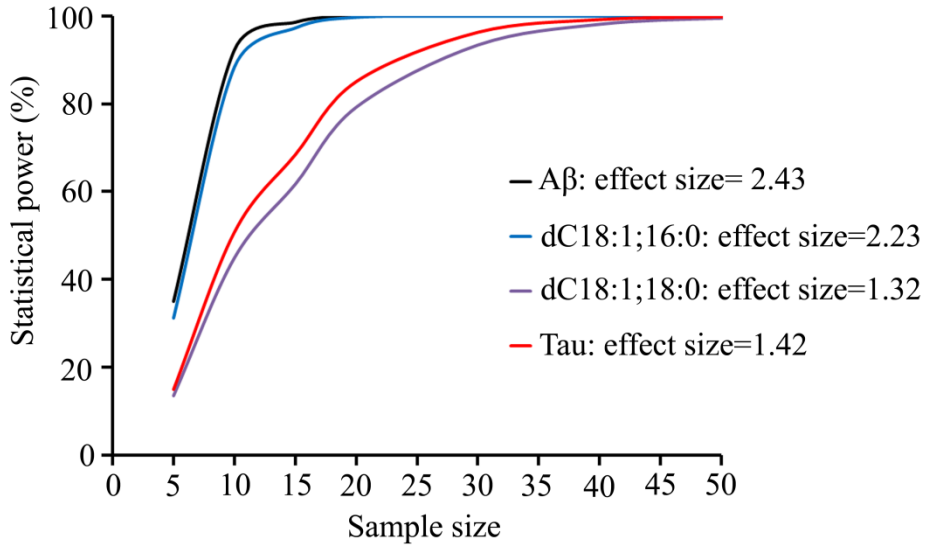

Figure 30: Post-hoc power analysis. Post-hoc statistical power analysis conducted on the 13 animals (sample size) administered with 10 mg/kg of the SPT inhibitor demonstrates that the reduction of $A\beta_{42}$ levels (~30% reduction) observed has a power of 97% to yield a significant effect with an effect size (Cohen's *d*) of 2.4. Post-hoc statistical power analysis conducted on the 13 animals (sample size) administered with 10 mg/kg of the SPT inhibitor demonstrates that the reduction of ceramide levels, d18:1; 16:0 (~38% reduction) and d18:1; 18:0 (~26% reduction) observed has a power of 94% and 54% respectively to yield a significant effect with an effect size (Cohen's *d*) of 2.3 and 1.32 respectively. A statistical power of 80% could be achieved for the reduction of d18:1; 18:0 (~26% reduction) levels with the use of 20 animals to yield a significant effect with an effect size (Cohen's *d*) of 1.32. Post-hoc statistical power analysis conducted on the 13 animals (sample size) administered with 10 mg/kg of the SPT inhibitor demonstrates that the reduction of hyperphosphorylated tau levels (~43% reduction) observed has a power of 60% to yield a significant effect with an effect size (Cohen's *d*) of 1.42. A statistical power of 85% could be achieved for the reduction of hyperphosphorylated tau (~43%

Figure 30 (cont'd)

(Figure 30 continues) reduction) levels with the use of 18 animals to yield a significant effect with an effect size (Cohen's *d*) of 1.42.

REFERENCES

REFERENCES

(1998) Consensus report of the Working Group on: "Molecular and Biochemical Markers of Alzheimer's Disease". The Ronald and Nancy Reagan Research Institute of the Alzheimer's Association and the National Institute on Aging Working Group. Neurobiol Aging 19:109-116.

Adams JM, 2nd, Pratipanawatr T, Berria R, Wang E, DeFronzo RA, Sullards MC, Mandarino LJ (2004) Ceramide content is increased in skeletal muscle from obese insulin-resistant humans. Diabetes 53:25-31.

Alberca R, Montes-Latorre E, Gil-Neciga E, Mir-Rivera P, Lozano-San Martin P (2002) [Alzheimer's disease and women]. Rev Neurol 35:571-579.

Almeida OP, Lautenschlager NT, Vasikaran S, Leedman P, Gelavis A, Flicker L (2006) A 20-week randomized controlled trial of estradiol replacement therapy for women aged 70 years and older: effect on mood, cognition and quality of life. Neurobiol Aging 27:141-149.

Altura BM, Shah NC, Li Z, Jiang XC, Perez-Albela JL, Altura BT Magnesium deficiency upregulates serine palmitoyl transferase (SPT 1 and SPT 2) in cardiovascular tissues: relationship to serum ionized Mg and cytochrome c. Am J Physiol Heart Circ Physiol 299:H932-938.

Alz.org (2010) Changing the trajectory of Alzheimer's disease. In: Alzheimer's Association.

Ambros V (2004) The functions of animal microRNAs. Nature 431:350-355.

An JH, Lee SY, Jeon JY, Cho KG, Kim SU, Lee MA (2009) Identification of gliotropic factors that induce human stem cell migration to malignant tumor. J Proteome Res 8:2873-2881.

Andorfer C, Kress Y, Espinoza M, de Silva R, Tucker KL, Barde YA, Duff K, Davies P (2003) Hyperphosphorylation and aggregation of tau in mice expressing normal human tau isoforms. J Neurochem 86:582-590.

Androulidaki A, Iliopoulos D, Arranz A, Doxaki C, Schworer S, Zacharioudaki V, Margioris AN, Tsichlis PN, Tsatsanis C (2009) The kinase Akt1 controls macrophage response to lipopolysaccharide by regulating microRNAs. Immunity 31:220-231.

Arendash GW, King DL (2002) Intra- and intertask relationships in a behavioral test battery given to Tg2576 transgenic mice and controls. Physiol Behav 75:643-652.

Arendash GW, Gordon MN, Diamond DM, Austin LA, Hatcher JM, Jantzen P, DiCarlo G, Wilcock D, Morgan D (2001) Behavioral assessment of Alzheimer's transgenic mice

following long-term Abeta vaccination: task specificity and correlations between Abeta deposition and spatial memory. DNA Cell Biol 20:737-744.

Arroyo JD, Chevillet JR, Kroh EM, Ruf IK, Pritchard CC, Gibson DF, Mitchell PS, Bennett CF, Pogosova-Agadjanyan EL, Stirewalt DL, Tait JF, Tewari M (2011) Argonaute2 complexes carry a population of circulating microRNAs independent of vesicles in human plasma. Proceedings of the National Academy of Sciences of the United States of America 108:5003-5008.

Asante EA, Gowland I, Linehan JM, Mahal SP, Collinge J (2002) Expression pattern of a mini human PrP gene promoter in transgenic mice. Neurobiol Dis 10:1-7.

Ashford JW (2008) Screening for memory disorder, dementia, and Alzheimer's disease Aging Health 4:399-432

Asthana S, Craft S, Baker LD, Raskind MA, Birnbaum RS, Lofgreen CP, Veith RC, Plymate SR (1999) Cognitive and neuroendocrine response to transdermal estrogen in postmenopausal women with Alzheimer's disease: results of a placebo-controlled, double-blind, pilot study. Psychoneuroendocrinology 24:657-677.

Bachman DL, Wolf PA, Linn R, Knoefel JE, Cobb J, Belanger A, D'Agostino RB, White LR (1992) Prevalence of dementia and probable senile dementia of the Alzheimer type in the Framingham Study. Neurology 42:115-119.

Baek D, Villen J, Shin C, Camargo FD, Gygi SP, Bartel DP (2008) The impact of microRNAs on protein output. Nature 455:64-71.

Bailey SA, Zidell RH, Perry RW (2004) Relationships between organ weight and body/brain weight in the rat: what is the best analytical endpoint? Toxicol Pathol 32:448-466.

Baker LD, Bayer-Carter JL, Skinner J, Montine TJ, Cholerton BA, Callaghan M, Leverenz J, Walter BK, Tsai E, Postupna N, Lampe J, Craft S (2011) High-Intensity Physical Activity Modulates Diet Effects on Cerebrospinal Amyloid-beta Levels in Normal Aging and Mild Cognitive Impairment. J Alzheimers Dis.

Ballard C, Howard R (2006) Neuroleptic drugs in dementia: benefits and harm. Nat Rev Neurosci 7:492-500.

Ballard C, Gauthier S, Corbett A, Brayne C, Aarsland D, Jones E (2011) Alzheimer's disease. Lancet 377:1019-1031.

Ballard C, Hanney ML, Theodoulou M, Douglas S, McShane R, Kossakowski K, Gill R, Juszczak E, Yu LM, Jacoby R (2009a) The dementia antipsychotic withdrawal trial (DART-AD): long-term follow-up of a randomised placebo-controlled trial. Lancet Neurol 8:151-157.

Ballard CG, Gauthier S, Cummings JL, Brodaty H, Grossberg GT, Robert P, Lyketsos CG (2009b) Management of agitation and aggression associated with Alzheimer disease. Nat Rev Neurol 5:245-255.

Bandaru VV, Troncoso J, Wheeler D, Pletnikova O, Wang J, Conant K, Haughey NJ (2009) ApoE4 disrupts sterol and sphingolipid metabolism in Alzheimer's but not normal brain. Neurobiol Aging 30:591-599.

Barbato C, Ruberti F, Cogoni C (2009) Searching for MIND: microRNAs in neurodegenerative diseases. Journal of biomedicine & biotechnology 2009:871313.

Barber RC Biomarkers for early detection of Alzheimer disease. J Am Osteopath Assoc 110:S10-15.

Bartel DP (2004) MicroRNAs: genomics, biogenesis, mechanism, and function. Cell 116:281-297.

Bayer-Carter JL, Green PS, Montine TJ, VanFossen B, Baker LD, Watson GS, Bonner LM, Callaghan M, Leverenz JB, Walter BK, Tsai E, Plymate SR, Postupna N, Wilkinson CW, Zhang J, Lampe J, Kahn SE, Craft S (2011) Diet intervention and cerebrospinal fluid biomarkers in amnestic mild cognitive impairment. Arch Neurol 68:743-752.

Becker I, Wang-Eckhardt L, Yaghootfam A, Gieselmann V, Eckhardt M (2008) Differential expression of (dihydro)ceramide synthases in mouse brain: oligodendrocyte-specific expression of CerS2/Lass2. Histochem Cell Biol 129:233-241.

Beeri MS, Ravona-Springer R, Silverman JM, Haroutunian V (2009) The effects of cardiovascular risk factors on cognitive compromise. Dialogues Clin Neurosci 11:201-212.

Bejaoui K, Wu C, Scheffler MD, Haan G, Ashby P, Wu L, de Jong P, Brown RH, Jr. (2001) SPTLC1 is mutated in hereditary sensory neuropathy, type 1. Nature genetics 27:261-262.

Bertram L, McQueen MB, Mullin K, Blacker D, Tanzi RE (2007) Systematic meta-analyses of Alzheimer disease genetic association studies: the AlzGene database. Nat Genet 39:17-23.

Betel D, Wilson M, Gabow A, Marks DS, Sander C (2008) The microRNA.org resource: targets and expression. Nucleic Acids Res 36:D149-153.

Billings LM, Oddo S, Green KN, McGaugh JL, LaFerla FM (2005) Intraneuronal Abeta causes the onset of early Alzheimer's disease-related cognitive deficits in transgenic mice. Neuron 45:675-688.

Binder EF, Schechtman KB, Birge SJ, Williams DB, Kohrt WM (2001) Effects of hormone replacement therapy on cognitive performance in elderly women. Maturitas 38:137-146.

Birks J, Grimley Evans J, Iakovidou V, Tsolaki M, Holt FE (2009) Rivastigmine for Alzheimer's disease. Cochrane Database Syst Rev:CD001191.

Blennow K, de Leon MJ, Zetterberg H (2006) Alzheimer's disease. Lancet 368:387-403.

Blennow K, Hampel H, Weiner M, Zetterberg H (2010) Cerebrospinal fluid and plasma biomarkers in Alzheimer disease. Nat Rev Neurol 6:131-144.

Bligh EG, Dyer WJ (1959) A rapid method of total lipid extraction and purification. Can J Biochem Physiol 37:911-917.

Borel C, Antonarakis SE (2008) Functional genetic variation of human miRNAs and phenotypic consequences. Mamm Genome 19:503-509.

Boy J, Leergaard TB, Schmidt T, Odeh F, Bichelmeier U, Nuber S, Holzmann C, Wree A, Prusiner SB, Bujard H, Riess O, Bjaalie JG (2006) Expression mapping of tetracycline-responsive prion protein promoter: digital atlasing for generating cell-specific disease models. Neuroimage 33:449-462.

Brookmeyer R, Gray S, Kawas C (1998) Projections of Alzheimer's disease in the United States and the public health impact of delaying disease onset. Am J Public Health 88:1337-1342.

Burns A, Zaudig M (2002) Mild cognitive impairment in older people. Lancet 360:1963-1965.

Butler AW, Ng MY, Hamshere ML, Forabosco P, Wroe R, Al-Chalabi A, Lewis CM, Powell JF (2009) Meta-analysis of linkage studies for Alzheimer's disease--a web resource. Neurobiol Aging 30:1037-1047.

Calhoun ME, Wiederhold KH, Abramowski D, Phinney AL, Probst A, Sturchler-Pierrat C, Staufenbiel M, Sommer B, Jucker M (1998) Neuron loss in APP transgenic mice. Nature 395:755-756.

Camper-Kirby D, Welch S, Walker A, Shiraishi I, Setchell KD, Schaefer E, Kajstura J, Anversa P, Sussman MA (2001) Myocardial Akt activation and gender: increased nuclear activity in females versus males. Circ Res 88:1020-1027.

Carlsson CM (2010) Type 2 diabetes mellitus, dyslipidemia, and Alzheimer's disease. J Alzheimers Dis 20:711-722.

Carrillo MC, Blackwell A, Hampel H, Lindborg J, Sperling R, Schenk D, Sevigny JJ, Ferris S, Bennett DA, Craft S, Hsu T, Klunk W (2009) Early risk assessment for Alzheimer's disease. Alzheimers Dement 5:182-196.

Caselli RJ, Dueck AC, Locke DE, Sabbagh MN, Ahern GL, Rapcsak SZ, Baxter LC, Yaari R, Woodruff BK, Hoffman-Snyder C, Rademakers R, Findley S, Reiman EM (2011) Cerebrovascular risk factors and preclinical memory decline in healthy APOE epsilon4 homozygotes. Neurology 76:1078-1084.

Chang ZQ, Lee SY, Kim HJ, Kim JR, Kim SJ, Hong IK, Oh BC, Choi CS, Goldberg IJ, Park TS (2011) Endotoxin activates de novo sphingolipid biosynthesis via nuclear factor kappa B-mediated upregulation of Sptlc2. Prostaglandins Other Lipid Mediat.

Chartier-Harlin MC, Crawford F, Houlden H, Warren A, Hughes D, Fidani L, Goate A, Rossor M, Roques P, Hardy J, et al. (1991) Early-onset Alzheimer's disease caused by mutations at codon 717 of the beta-amyloid precursor protein gene. Nature 353:844-846.

Chekulaeva M, Filipowicz W (2009) Mechanisms of miRNA-mediated post-transcriptional regulation in animal cells. Current opinion in cell biology 21:452-460.

Chen G, Chen KS, Knox J, Inglis J, Bernard A, Martin SJ, Justice A, McConlogue L, Games D, Freedman SB, Morris RG (2000) A learning deficit related to age and beta-amyloid plaques in a mouse model of Alzheimer's disease. Nature 408:975-979.

Chen K, Rajewsky N (2007) The evolution of gene regulation by transcription factors and microRNAs. Nature reviews 8:93-103.

Chishti MA et al. (2001) Early-onset amyloid deposition and cognitive deficits in transgenic mice expressing a double mutant form of amyloid precursor protein 695. The Journal of biological chemistry 276:21562-21570.

Choi MD (2006) The regulation of ceramide content and insulin resistance in skeletal muscle. In: Ball State University.

Chu FS, Li GY (1994) Simultaneous occurrence of fumonisin B1 and other mycotoxins in moldy corn collected from the People's Republic of China in regions with high incidences of esophageal cancer. Appl Environ Microbiol 60:847-852.

Citron M, Oltersdorf T, Haass C, McConlogue L, Hung AY, Seubert P, Vigo-Pelfrey C, Lieberburg I, Selkoe DJ (1992) Mutation of the beta-amyloid precursor protein in familial Alzheimer's disease increases beta-protein production. Nature 360:672-674.

Cogswell JP, Ward J, Taylor IA, Waters M, Shi Y, Cannon B, Kelnar K, Kemppainen J, Brown D, Chen C, Prinjha RK, Richardson JC, Saunders AM, Roses AD, Richards CA (2008) Identification of miRNA changes in Alzheimer's disease brain and CSF yields putative biomarkers and insights into disease pathways. J Alzheimers Dis 14:27-41.

Coolen M, Bally-Cuif L (2009) MicroRNAs in brain development and physiology. Curr Opin Neurobiol 19:461-470.

Cordy JM, Hussain I, Dingwall C, Hooper NM, Turner AJ (2003) Exclusively targeting beta-secretase to lipid rafts by GPI-anchor addition up-regulates beta-site processing of the amyloid precursor protein. Proceedings of the National Academy of Sciences of the United States of America 100:11735-11740.

Cortez MA, Nicoloso MS, Shimizu M, Rossi S, Gopisetty G, Molina JR, Carlotti C, Jr., Tirapelli D, Neder L, Brassesco MS, Scrideli CA, Tone LG, Georgescu MM, Zhang W, Puduvalli V, Calin GA (2010) miR-29b and miR-125a regulate podoplanin and suppress invasion in glioblastoma. Genes Chromosomes Cancer 49:981-990.

Costantini C, Ko MH, Jonas MC, Puglielli L (2007) A reversible form of lysine acetylation in the ER and Golgi lumen controls the molecular stabilization of BACE1. The Biochemical journal 407:383-395.

Craig MC, Murphy DG (2010) Estrogen therapy and Alzheimer's dementia. Ann N Y Acad Sci 1205:245-253.

Crum RM, Anthony JC, Bassett SS, Folstein MF (1993) Population-based norms for the Mini-Mental State Examination by age and educational level. JAMA 269:2386-2391.

Cruts M, Van Broeckhoven C (1998) Molecular genetics of Alzheimer's disease. Ann Med 30:560-565.

Cuellar TL, Davis TH, Nelson PT, Loeb GB, Harfe BD, Ullian E, McManus MT (2008) Dicer loss in striatal neurons produces behavioral and neuroanatomical phenotypes in the absence of neurodegeneration. Proceedings of the National Academy of Sciences of the United States of America 105:5614-5619.

Cutler RG, Pedersen WA, Camandola S, Rothstein JD, Mattson MP (2002) Evidence that accumulation of ceramides and cholesterol esters mediates oxidative stress-induced death of motor neurons in amyotrophic lateral sclerosis. Ann Neurol 52:448-457.

Cutler RG, Kelly J, Storie K, Pedersen WA, Tammara A, Hatanpaa K, Troncoso JC, Mattson MP (2004) Involvement of oxidative stress-induced abnormalities in ceramide and cholesterol metabolism in brain aging and Alzheimer's disease. Proceedings of the National Academy of Sciences of the United States of America 101:2070-2075.

Davis TH, Cuellar TL, Koch SM, Barker AJ, Harfe BD, McManus MT, Ullian EM (2008) Conditional loss of Dicer disrupts cellular and tissue morphogenesis in the cortex and hippocampus. J Neurosci 28:4322-4330.

Dawkins JL, Hulme DJ, Brahmbhatt SB, Auer-Grumbach M, Nicholson GA (2001) Mutations in SPTLC1, encoding serine palmitoyltransferase, long chain base subunit-1, cause hereditary sensory neuropathy type I. Nat Genet 27:309-312.

de Mena L, Cardo LF, Coto E, Miar A, Diaz M, Corao AI, Alonso B, Ribacoba R, Salvador C, Menendez M, Moris G, Alvarez V (2010) FGF20 rs12720208 SNP and microRNA-433 variation: no association with Parkinson's disease in Spanish patients. Neurosci Lett 479:22-25.

de Souza LC, Chupin M, Lamari F, Jardel C, Leclercq D, Colliot O, Lehericy S, Dubois B, Sarazin M (2011) CSF tau markers are correlated with hippocampal volume in Alzheimer's disease. Neurobiol Aging.

Delay C, Mandemakers W, Hebert SS (2012) MicroRNAs in Alzheimer's disease. Neurobiol Dis 46:285-290.

Delay C, Calon F, Mathews P, Hebert SS (2011) Alzheimer-specific variants in the 3'UTR of Amyloid precursor protein affect microRNA function. Mol Neurodegener 6:70.

Dougall NJ, Bruggink S, Ebmeier KP (2004) Systematic review of the diagnostic accuracy of 99mTc-HMPAO-SPECT in dementia. Am J Geriatr Psychiatry 12:554-570.

DrugBank (2012) DrugBAnk: Open data drug and drug target database. In, 3 Edition.

Ebina M, Futai E, Tanabe C, Sasagawa N, Kiso Y, Ishiura S (2009) Inhibition by KMI-574 leads to dislocalization of BACE1 from lipid rafts. J Neurosci Res 87:360-368.

Ehehalt R, Keller P, Haass C, Thiele C, Simons K (2003) Amyloidogenic processing of the Alzheimer beta-amyloid precursor protein depends on lipid rafts. J Cell Biol 160:113-123.

Elmen J, Lindow M, Silahtaroglu A, Bak M, Christensen M, Lind-Thomsen A, Hedtjarn M, Hansen JB, Hansen HF, Straarup EM, McCullagh K, Kearney P, Kauppinen S (2008a) Antagonism of microRNA-122 in mice by systemically administered LNA-antimiR leads to up-regulation of a large set of predicted target mRNAs in the liver. Nucleic Acids Res 36:1153-1162.

Elmen J, Lindow M, Schutz S, Lawrence M, Petri A, Obad S, Lindholm M, Hedtjarn M, Hansen HF, Berger U, Gullans S, Kearney P, Sarnow P, Straarup EM, Kauppinen S (2008b) LNA-mediated microRNA silencing in non-human primates. Nature 452:896-899.

Engelhart MJ, Geerlings MI, Ruitenberg A, Van Swieten JC, Hofman A, Witteman JC, Breteler MM (2002) Diet and risk of dementia: Does fat matter?: The Rotterdam Study. Neurology 59:1915-1921.

Eskelinen MH, Ngandu T, Helkala EL, Tuomilehto J, Nissinen A, Soininen H, Kivipelto M (2008) Fat intake at midlife and cognitive impairment later in life: a population-based CAIDE study. Int J Geriatr Psychiatry 23:741-747.

Ettorre E, Cerra E, Marigliano B, Vigliotta M, Vulcano A, Fossati C, De Benedetto G, Servello A, Andreozzi P, Marigliano V (2011) Role of cardiovascular risk factors (CRF) in the patients with mild cognitive impairment (MCI). Arch Gerontol Geriatr.

Ewers M, Mielke MM, Hampel H (2010) Blood-based biomarkers of microvascular pathology in Alzheimer's disease. Exp Gerontol 45:75-79.

Fassbender K, Simons M, Bergmann C, Stroick M, Lutjohann D, Keller P, Runz H, Kuhl S, Bertsch T, von Bergmann K, Hennerici M, Beyreuther K, Hartmann T (2001) Simvastatin strongly reduces levels of Alzheimer's disease beta -amyloid peptides Abeta 42 and Abeta 40 in vitro and in vivo. Proceedings of the National Academy of Sciences of the United States of America 98:5856-5861.

Fenn TD, Stamper GF, Morollo AA, Ringe D (2003) A side reaction of alanine racemase: transamination of cycloserine. Biochemistry 42:5775-5783.

Ferri CP, Prince M, Brayne C, Brodaty H, Fratiglioni L, Ganguli M, Hall K, Hasegawa K, Hendrie H, Huang Y, Jorm A, Mathers C, Menezes PR, Rimmer E, Scazufca M (2005) Global prevalence of dementia: a Delphi consensus study. Lancet 366:2112-2117.

Filipowicz W, Bhattacharyya SN, Sonenberg N (2008) Mechanisms of post-transcriptional regulation by microRNAs: are the answers in sight? Nature reviews 9:102-114.

Fillit H, Weinreb H, Cholst I, Luine V, McEwen B, Amador R, Zabriskie J (1986) Observations in a preliminary open trial of estradiol therapy for senile dementia-Alzheimer's type. Psychoneuroendocrinology 11:337-345.

Forlenza OV, Diniz BS, Gattaz WF (2010) Diagnosis and biomarkers of predementia in Alzheimer's disease. BMC medicine 8:89.

Freund-Levi Y, Eriksdotter-Jonhagen M, Cederholm T, Basun H, Faxen-Irving G, Garlind A, Vedin I, Vessby B, Wahlund LO, Palmblad J (2006) Omega-3 fatty acid treatment in 174 patients with mild to moderate Alzheimer disease: OmegAD study: a randomized double-blind trial. Arch Neurol 63:1402-1408.

Gable K, Slife H, Bacikova D, Monaghan E, Dunn TM (2000) Tsc3p is an 80-amino acid protein associated with serine palmitoyltransferase and required for optimal enzyme activity. The Journal of biological chemistry 275:7597-7603.

Gao FB Context-dependent functions of specific microRNAs in neuronal development. Neural Dev 5:25.

Geekiyanage H, Chan C (2011) MicroRNA-137/181c Regulates Serine Palmitoyltransferase and In Turn Amyloid {beta}, Novel Targets in Sporadic Alzheimer's Disease. J Neurosci 31:14820-14830.

Geekiyanage H, Jicha GA, Nelson PT, Chan C (2012) Blood serum miRNA: non-invasive biomarkers for Alzheimer's disease. Exp Neurol 235:491-496.

George AJ, Holsinger RM, McLean CA, Laughton KM, Beyreuther K, Evin G, Masters CL, Li QX (2004) APP intracellular domain is increased and soluble Abeta is reduced with diet-induced hypercholesterolemia in a transgenic mouse model of Alzheimer disease. Neurobiology of disease 16:124-132.

Gilad S, Meiri E, Yogev Y, Benjamin S, Lebanony D, Yerushalmi N, Benjamin H, Kushnir M, Cholakh H, Melamed N, Bentwich Z, Hod M, Goren Y, Chajut A (2008) Serum microRNAs are promising novel biomarkers. PloS one 3:e3148.

Gotz J, Streffer JR, David D, Schild A, Hoerndli F, Pennanen L, Kurosinski P, Chen F (2004) Transgenic animal models of Alzheimer's disease and related disorders: histopathology, behavior and therapy. Molecular psychiatry 9:664-683.

Grady D, Yaffe K, Kristof M, Lin F, Richards C, Barrett-Connor E (2002) Effect of postmenopausal hormone therapy on cognitive function: the Heart and Estrogen/progestin Replacement Study. Am J Med 113:543-548.

Graff-Radford NR, Crook JE, Lucas J, Boeve BF, Knopman DS, Ivnik RJ, Smith GE, Younkin LH, Petersen RC, Younkin SG (2007) Association of low plasma Abeta42/Abeta40 ratios with increased imminent risk for mild cognitive impairment and Alzheimer disease. Arch Neurol 64:354-362.

Grant WB (1999) Dietary links to Alzheimer's disease: 1999 update. J Alzheimers Dis 1:197-201.

Green RC, Schneider LS, Amato DA, Beelen AP, Wilcock G, Swabb EA, Zavitz KH (2009) Effect of tarenflurbil on cognitive decline and activities of daily living in patients with mild Alzheimer disease: a randomized controlled trial. JAMA 302:2557-2564.

Griffiths-Jones S, Saini HK, van Dongen S, Enright AJ (2008) miRBase: tools for microRNA genomics. Nucleic Acids Res 36:D154-158.

Gu HF, Alvarsson A, Efendic S, Brismar K (2009) SOX2 has gender-specific genetic effects on diabetic nephropathy in samples from patients with type 1 diabetes mellitus in the GoKinD study. Gend Med 6:555-564.

Gulbins E, Kolesnick R (2003) Raft ceramide in molecular medicine. Oncogene 22:7070-7077.

Haas RH, Rice MA, Trauner DA, Merritt TA (1986) Therapeutic effects of a ketogenic diet in Rett syndrome. Am J Med Genet Suppl 1:225-246.

Hall AM, Roberson ED (2012) Mouse models of Alzheimer's disease. Brain research bulletin 88:3-12.

Hampel H, Shen Y, Walsh DM, Aisen P, Shaw LM, Zetterberg H, Trojanowski JQ, Blennow K (2010) Biological markers of amyloid beta-related mechanisms in Alzheimer's disease. Exp Neurol 223:334-346.

Han X, D MH, McKeel DW, Jr., Kelley J, Morris JC (2002) Substantial sulfatide deficiency and ceramide elevation in very early Alzheimer's disease: potential role in disease pathogenesis. J Neurochem 82:809-818.

Hanada K (2003) Serine palmitoyltransferase, a key enzyme of sphingolipid metabolism. Biochimica et biophysica acta 1632:16-30.

Hanada K, Hara T, Nishijima M (2000) Purification of the serine palmitoyltransferase complex responsible for sphingoid base synthesis by using affinity peptide chromatography techniques. The Journal of biological chemistry 275:8409-8415.

Hanada K, Hara T, Nishijima M, Kuge O, Dickson RC, Nagiec MM (1997) A mammalian homolog of the yeast LCB1 encodes a component of serine palmitoyltransferase, the enzyme catalyzing the first step in sphingolipid synthesis. The Journal of biological chemistry 272:32108-32114.

Hannun YA, Obeid LM (2002) The Ceramide-centric universe of lipid-mediated cell regulation: stress encounters of the lipid kind. The Journal of biological chemistry 277:25847-25850.

Hannun YA, Obeid LM (2008) Principles of bioactive lipid signalling: lessons from sphingolipids. Nature reviews 9:139-150.

Hansson O, Stomrud E, Vanmechelen E, Ostling S, Gustafson DR, Zetterberg H, Blennow K, Skoog I (2011) Evaluation of Plasma Abeta as Predictor of Alzheimer's Disease in Older Individuals Without Dementia: A Population-Based Study. J Alzheimers Dis.

Hardy J (2006) Has the amyloid cascade hypothesis for Alzheimer's disease been proved? Curr Alzheimer Res 3:71-73.

Harold D et al. (2009) Genome-wide association study identifies variants at CLU and PICALM associated with Alzheimer's disease. Nat Genet 41:1088-1093.

Haughey NJ, Bandaru VV, Bae M, Mattson MP (2010) Roles for dysfunctional sphingolipid metabolism in Alzheimer's disease neuropathogenesis. Biochimica et biophysica acta 1801:878-886.

He L, Hannon GJ (2004) MicroRNAs: small RNAs with a big role in gene regulation. Nat Rev Genet 5:522-531.

He X, Huang Y, Li B, Gong CX, Schuchman EH (2010) Deregulation of sphingolipid metabolism in Alzheimer's disease. Neurobiol Aging 31:398-408.

Hebert LE, Scherr PA, Beckett LA, Albert MS, Pilgrim DM, Chown MJ, Funkenstein HH, Evans DA (1995) Age-specific incidence of Alzheimer's disease in a community population. JAMA 273:1354-1359.

Hebert SS, Horre K, Nicolai L, Papadopoulou AS, Mandemakers W, Silahtaroglu AN, Kauppinen S, Delacourte A, De Strooper B (2008) Loss of microRNA cluster miR-29a/b-1 in sporadic Alzheimer's disease correlates with increased BACE1/beta-secretase expression. Proceedings of the National Academy of Sciences of the United States of America 105:6415-6420.

Hebert SS, Papadopoulou AS, Smith P, Galas MC, Planel E, Silahtaroglu AN, Sergeant N, Buee L, De Strooper B (2010) Genetic ablation of Dicer in adult forebrain neurons results in abnormal tau hyperphosphorylation and neurodegeneration. Hum Mol Genet 19:3959-3969.

Henderson VW, Buckwalter JG (1994) Cognitive deficits of men and women with Alzheimer's disease. Neurology 44:90-96.

Hendrie HC, Osuntokun BO, Hall KS, Ogunniyi AO, Hui SL, Unverzagt FW, Gureje O, Rodenberg CA, Baiyewu O, Musick BS (1995) Prevalence of Alzheimer's disease and dementia in two communities: Nigerian Africans and African Americans. The American journal of psychiatry 152:1485-1492.

Henry MS, Passmore AP, Todd S, McGuinness B, Craig D, Johnston JA (2012) The development of effective biomarkers for Alzheimer's disease: a review. Int J Geriatr Psychiatry.

Herget T, Esdar C, Oehrlein SA, Heinrich M, Schutze S, Maelicke A, van Echten-Deckert G (2000) Production of ceramides causes apoptosis during early neural differentiation in vitro. The Journal of biological chemistry 275:30344-30354.

Ho L, Qin W, Pompl PN, Xiang Z, Wang J, Zhao Z, Peng Y, Cambareri G, Rocher A, Mobbs CV, Hof PR, Pasinetti GM (2004) Diet-induced insulin resistance promotes amyloidosis in a transgenic mouse model of Alzheimer's disease. FASEB J 18:902-904.

Hojjati MR, Li Z, Jiang XC (2005a) Serine palmitoyl-CoA transferase (SPT) deficiency and sphingolipid levels in mice. Biochimica et biophysica acta 1737:44-51.

Hojjati MR, Li Z, Zhou H, Tang S, Huan C, Ooi E, Lu S, Jiang XC (2005b) Effect of myriocin on plasma sphingolipid metabolism and atherosclerosis in apoE-deficient mice. The Journal of biological chemistry 280:10284-10289.

Holland WL, Brozinick JT, Wang LP, Hawkins ED, Sargent KM, Liu Y, Narra K, Hoehn KL, Knotts TA, Siesky A, Nelson DH, Karathanasis SK, Fontenot GK, Birnbaum MJ, Summers SA (2007) Inhibition of ceramide synthesis ameliorates glucocorticoid-, saturated-fat-, and obesity-induced insulin resistance. Cell Metab 5:167-179.

Holmes C, Boche D, Wilkinson D, Yadegarfar G, Hopkins V, Bayer A, Jones RW, Bullock R, Love S, Neal JW, Zotova E, Nicoll JA (2008) Long-term effects of Abeta42 immunisation in Alzheimer's disease: follow-up of a randomised, placebo-controlled phase I trial. Lancet 372:216-223.

Hooijmans CR, Kiliaan AJ (2008) Fatty acids, lipid metabolism and Alzheimer pathology. European journal of pharmacology 585:176-196.

Hornemann T, Richard S, Rutti MF, Wei Y, von Eckardstein A (2006) Cloning and initial characterization of a new subunit for mammalian serine-palmitoyltransferase. The Journal of biological chemistry 281:37275-37281.

Howland DS, Trusko SP, Savage MJ, Reaume AG, Lang DM, Hirsch JD, Maeda N, Siman R, Greenberg BD, Scott RW, Flood DG (1998) Modulation of secreted beta-amyloid precursor protein and amyloid beta-peptide in brain by cholesterol. The Journal of biological chemistry 273:16576-16582.

Hu W, Bielawski J, Samad F, Merrill AH, Jr., Cowart LA (2009) Palmitate increases sphingosine-1-phosphate in C2C12 myotubes via upregulation of sphingosine kinase message and activity. Journal of lipid research.

Huang Y (2006) Apolipoprotein E and Alzheimer disease. Neurology 66:S79-85.

Hur JY, Welander H, Behbahani H, Aoki M, Franberg J, Winblad B, Frykman S, Tjernberg LO (2008) Active gamma-secretase is localized to detergent-resistant membranes in human brain. The FEBS journal 275:1174-1187.

Ichi I, Nakahara K, Kiso K, Kojo S (2007) Effect of dietary cholesterol and high fat on ceramide concentration in rat tissues. Nutrition 23:570-574.

Imbimbo BP, Hutter-Paier B, Villetti G, Facchinetti F, Cenacchi V, Volta R, Lanzillotta A, Pizzi M, Windisch M (2009) CHF5074, a novel gamma-secretase modulator, attenuates brain beta-amyloid pathology and learning deficit in a mouse model of Alzheimer's disease. Br J Pharmacol 156:982-993.

Inoue M, Ohtake T, Motomura W, Takahashi N, Hosoki Y, Miyoshi S, Suzuki Y, Saito H, Kohgo Y, Okumura T (2005) Increased expression of PPARgamma in high fat diet-induced liver steatosis in mice. Biochem Biophys Res Commun 336:215-222.

Irizarry MC (2004) Biomarkers of Alzheimer disease in plasma. NeuroRx 1:226-234.

Jana A, Pahan K (2010) Fibrillar amyloid-beta-activated human astroglia kill primary human neurons via neutral sphingomyelinase: implications for Alzheimer's disease. J Neurosci 30:12676-12689.

Jankowsky JL, Fadale DJ, Anderson J, Xu GM, Gonzales V, Jenkins NA, Copeland NG, Lee MK, Younkin LH, Wagner SL, Younkin SG, Borchelt DR (2004) Mutant presenilins

specifically elevate the levels of the 42 residue beta-amyloid peptide in vivo: evidence for augmentation of a 42-specific gamma secretase. Hum Mol Genet 13:159-170.

Jellinger KA (2004) Head injury and dementia. Curr Opin Neurol 17:719-723.

Jicha GA, Abner EL, Schmitt FA, Kryscio RJ, Riley KP, Cooper GE, Stiles N, Mendiondo MS, Smith CD, Van Eldik LJ, Nelson PT (2011) Preclinical AD Workgroup staging: pathological correlates and potential challenges. Neurobiol Aging.

Julien C, Tremblay C, Phivilay A, Berthiaume L, Emond V, Julien P, Calon F (2010) High-fat diet aggravates amyloid-beta and tau pathologies in the 3xTg-AD mouse model. Neurobiol Aging 31:1516-1531.

Kalmijn S, Launer LJ, Ott A, Witteman JC, Hofman A, Breteler MM (1997) Dietary fat intake and the risk of incident dementia in the Rotterdam Study. Annals of neurology 42:776-782.

Kalvodova L, Kahya N, Schwille P, Ehehalt R, Verkade P, Drechsel D, Simons K (2005) Lipids as modulators of proteolytic activity of BACE: involvement of cholesterol, glycosphingolipids, and anionic phospholipids in vitro. The Journal of biological chemistry 280:36815-36823.

Kawase-Koga Y, Low R, Otaegi G, Pollock A, Deng H, Eisenhaber F, Maurer-Stroh S, Sun T (2010) RNAase-III enzyme Dicer maintains signaling pathways for differentiation and survival in mouse cortical neural stem cells. J Cell Sci 123:586-594.

Kim B, Backus C, Oh S, Hayes JM, Feldman EL (2009) Increased tau phosphorylation and cleavage in mouse models of type 1 and type 2 diabetes. Endocrinology 150:5294-5301.

Kim J, Inoue K, Ishii J, Vanti WB, Voronov SV, Murchison E, Hannon G, Abeliovich A (2007) A MicroRNA feedback circuit in midbrain dopamine neurons. Science 317:1220-1224.

Kimura R, Ohno M (2009) Impairments in remote memory stabilization precede hippocampal synaptic and cognitive failures in 5XFAD Alzheimer mouse model. Neurobiol Dis 33:229-235.

Klatt EC (1994-2012) The internet pathology laboatory for medical eductaion. In. Savannah: University of Utah eccles health sciences library.

Kluepfel D, Bagli J, Baker H, Charest MP, Kudelski A (1972) Myriocin, a new antifungal antibiotic from Myriococcum albomyces. J Antibiot (Tokyo) 25:109-115.

Ko MH, Puglielli L (2009) Two endoplasmic reticulum (ER)/ER Golgi intermediate compartment-based lysine acetyltransferases post-translationally regulate BACE1 levels. The Journal of biological chemistry 284:2482-2492.

Kohjima M, Sun Y, Chan L (2010) Increased food intake leads to obesity and insulin resistance in the tg2576 Alzheimer's disease mouse model. Endocrinology 151:1532-1540.

Kosaka N, Iguchi H, Yoshioka Y, Takeshita F, Matsuki Y, Ochiya T (2010) Secretory mechanisms and intercellular transfer of microRNAs in living cells. The Journal of biological chemistry 285:17442-17452.

Koturbash I, Zemp F, Kolb B, Kovalchuk O (2011) Sex-specific radiation-induced microRNAome responses in the hippocampus, cerebellum and frontal cortex in a mouse model. Mutat Res.

Kramer AF, Hahn S, Cohen NJ, Banich MT, McAuley E, Harrison CR, Chason J, Vakil E, Bardell L, Boileau RA, Colcombe A (1999) Ageing, fitness and neurocognitive function. Nature 400:418-419.

Krek A, Grun D, Poy MN, Wolf R, Rosenberg L, Epstein EJ, MacMenamin P, da Piedade I, Gunsalus KC, Stoffel M, Rajewsky N (2005) Combinatorial microRNA target predictions. Nat Genet 37:495-500.

Kroh EM, Parkin RK, Mitchell PS, Tewari M (2010) Analysis of circulating microRNA biomarkers in plasma and serum using quantitative reverse transcription-PCR (qRT-PCR). Methods 50:298-301.

Kwok JB, Loy CT, Hamilton G, Lau E, Hallupp M, Williams J, Owen MJ, Broe GA, Tang N, Lam L, Powell JF, Lovestone S, Schofield PR (2008) Glycogen synthase kinase-3beta and tau genes interact in Alzheimer's disease. Ann Neurol 64:446-454.

Ladisch S, Li R, Olson E (1994) Ceramide structure predicts tumor ganglioside immunosuppressive activity. Proceedings of the National Academy of Sciences of the United States of America 91:1974-1978.

Lagos-Quintana M, Rauhut R, Lendeckel W, Tuschl T (2001) Identification of novel genes coding for small expressed RNAs. Science 294:853-858.

Laneve P, Gioia U, Andriotto A, Moretti F, Bozzoni I, Caffarelli E (2010) A minicircuitry involving REST and CREB controls miR-9-2 expression during human neuronal differentiation. Nucleic Acids Res 38:6895-6905.

Lanford RE, Hildebrandt-Eriksen ES, Petri A, Persson R, Lindow M, Munk ME, Kauppinen S, Orum H (2010) Therapeutic silencing of microRNA-122 in primates with chronic hepatitis C virus infection. Science 327:198-201.

Langevin SM, Stone RA, Bunker CH, Grandis JR, Sobol RW, Taioli E (2010) MicroRNA-137 promoter methylation in oral rinses from patients with squamous cell carcinoma of the head and neck is associated with gender and body mass index. Carcinogenesis 31:864-870.

Lannfelt L, Blennow K, Zetterberg H, Batsman S, Ames D, Harrison J, Masters CL, Targum S, Bush AI, Murdoch R, Wilson J, Ritchie CW (2008) Safety, efficacy, and biomarker findings of PBT2 in targeting Abeta as a modifying therapy for Alzheimer's disease: a phase IIa, double-blind, randomised, placebo-controlled trial. Lancet Neurol 7:779-786.

Lanzillotta A, Sarnico I, Benarese M, Branca C, Baiguera C, Hutter-Paier B, Windisch M, Spano P, Imbimbo BP, Pizzi M The gamma-secretase modulator CHF5074 reduces the accumulation of native hyperphosphorylated tau in a transgenic mouse model of Alzheimer's disease. J Mol Neurosci 45:22-31.

Lee SJ, Liyanage U, Bickel PE, Xia W, Lansbury PT, Jr., Kosik KS (1998) A detergent-insoluble membrane compartment contains A beta in vivo. Nature medicine 4:730-734.

Leroy K, Ando K, Heraud C, Yilmaz Z, Authelet M, Boeynaems JM, Buee L, De Decker R, Brion JP (2010) Lithium treatment arrests the development of neurofibrillary tangles in mutant tau transgenic mice with advanced neurofibrillary pathology. J Alzheimers Dis 19:705-719.

Lewis BP, Burge CB, Bartel DP (2005) Conserved seed pairing, often flanked by adenosines, indicates that thousands of human genes are microRNA targets. Cell 120:15-20.

Lewis J, Dickson DW, Lin WL, Chisholm L, Corral A, Jones G, Yen SH, Sahara N, Skipper L, Yager D, Eckman C, Hardy J, Hutton M, McGowan E (2001) Enhanced neurofibrillary degeneration in transgenic mice expressing mutant tau and APP. Science 293:1487-1491.

Li ZG, Zhang W, Sima AA (2007) Alzheimer-like changes in rat models of spontaneous diabetes. Diabetes 56:1817-1824.

Liebhaber GM, Riemann E, Baumeister FA (2003) Ketogenic diet in Rett syndrome. J Child Neurol 18:74-75.

Linn SC, Kim HS, Keane EM, Andras LM, Wang E, Merrill AH, Jr. (2001) Regulation of de novo sphingolipid biosynthesis and the toxic consequences of its disruption. Biochemical Society transactions 29:831-835.

Liu F, Liang Z, Wegiel J, Hwang YW, Iqbal K, Grundke-Iqbal I, Ramakrishna N, Gong CX (2008) Overexpression of Dyrk1A contributes to neurofibrillary degeneration in Down syndrome. FASEB J 22:3224-3233.

Lowther J, Yard BA, Johnson KA, Carter LG, Bhat VT, Raman MC, Clarke DJ, Ramakers B, McMahon SA, Naismith JH, Campopiano DJ (2010) Inhibition of the PLP-dependent enzyme serine palmitoyltransferase by cycloserine: evidence for a novel decarboxylative mechanism of inactivation. Mol Biosyst 6:1682-1693.

Loy C, Schneider L (2006) Galantamine for Alzheimer's disease and mild cognitive impairment. Cochrane Database Syst Rev:CD001747.

Luchsinger JA, Tang MX, Shea S, Mayeux R (2002) Caloric intake and the risk of Alzheimer disease. Arch Neurol 59:1258-1263.

Lukiw WJ (2007) Micro-RNA speciation in fetal, adult and Alzheimer's disease hippocampus. Neuroreport 18:297-300.

Maki PM, Sundermann E (2009) Hormone therapy and cognitive function. Hum Reprod Update 15:667-681.

Malashkevich VN, Strop P, Keller JW, Jansonius JN, Toney MD (1999) Crystal structures of dialkylglycine decarboxylase inhibitor complexes. J Mol Biol 294:193-200.

Mangialasche F, Solomon A, Winblad B, Mecocci P, Kivipelto M (2010) Alzheimer's disease: clinical trials and drug development. Lancet Neurol 9:702-716.

Massi F, Klimov D, Thirumalai D, Straub JE (2002) Charge states rather than propensity for beta-structure determine enhanced fibrillogenesis in wild-type Alzheimer's beta-amyloid peptide compared to E22Q Dutch mutant. Protein Sci 11:1639-1647.

Mattson MP (2000) Neuroprotective signaling and the aging brain: take away my food and let me run. Brain research 886:47-53.

Mattson MP, Cutler RG, Jo DG (2005) Alzheimer peptides perturb lipid-regulating enzymes. Nat Cell Biol 7:1045-1047.

Mayeux R (2003) Epidemiology of neurodegeneration. Annu Rev Neurosci 26:81-104.

McClean PL, Parthsarathy V, Faivre E, Holscher C (2011) The diabetes drug liraglutide prevents degenerative processes in a mouse model of Alzheimer's disease. J Neurosci 31:6587-6594.

McGowan E, Pickford F, Kim J, Onstead L, Eriksen J, Yu C, Skipper L, Murphy MP, Beard J, Das P, Jansen K, Delucia M, Lin WL, Dolios G, Wang R, Eckman CB, Dickson DW, Hutton M, Hardy J, Golde T (2005) Abeta42 is essential for parenchymal and vascular amyloid deposition in mice. Neuron 47:191-199.

McKhann G, Drachman D, Folstein M, Katzman R, Price D, Stadlan EM (1984) Clinical diagnosis of Alzheimer's disease: report of the NINCDS-ADRDA Work Group under the auspices of Department of Health and Human Services Task Force on Alzheimer's Disease. Neurology 34:939-944.

McNaughton D, Knight W, Guerreiro R, Ryan N, Lowe J, Poulter M, Nicholl DJ, Hardy J, Revesz T, Rossor M, Collinge J, Mead S (2012) Duplication of amyloid precursor protein (APP), but not prion protein (PRNP) gene is a significant cause of early onset dementia in a large UK series. Neurobiol Aging 33:426 e413-421.

McPherson S, Back C, Buckwalter JG, Cummings JL (1999) Gender-related cognitive deficits in Alzheimer's disease. Int Psychogeriatr 11:117-122.

McShane R, Areosa Sastre A, Minakaran N (2006) Memantine for dementia. Cochrane Database Syst Rev:CD003154.

Mehler MF, Mattick JS (2006) Non-coding RNAs in the nervous system. The Journal of physiology 575:333-341.

Memon RA, Holleran WM, Uchida Y, Moser AH, Grunfeld C, Feingold KR (2001) Regulation of sphingolipid and glycosphingolipid metabolism in extrahepatic tissues by endotoxin. J Lipid Res 42:452-459.

Merrill AH, Jr., Nixon DW, Williams RD (1985) Activities of serine palmitoyltransferase (3-ketosphinganine synthase) in microsomes from different rat tissues. J Lipid Res 26:617-622.

Migliore L, Coppede F (2009) Genetics, environmental factors and the emerging role of epigenetics in neurodegenerative diseases. Mutation research 667:82-97.

mirbase.org (2012) In: Manchester.

Mishra PJ, Banerjee D, Bertino JR (2008) MiRSNPs or MiR-polymorphisms, new players in microRNA mediated regulation of the cell: Introducing microRNA pharmacogenomics. Cell Cycle 7:853-858.

Morris MC, Evans DA, Bienias JL, Tangney CC, Wilson RS (2004) Dietary fat intake and 6-year cognitive change in an older biracial community population. Neurology 62:1573-1579.

Mott JL, Kurita S, Cazanave SC, Bronk SF, Werneburg NW, Fernandez-Zapico ME (2010) Transcriptional suppression of mir-29b-1/mir-29a promoter by c-Myc, hedgehog, and NF-kappaB. J Cell Biochem 110:1155-1164.

Mucke L, Masliah E, Yu GQ, Mallory M, Rockenstein EM, Tatsuno G, Hu K, Kholodenko D, Johnson-Wood K, McConlogue L (2000) High-level neuronal expression of abeta 1-42 in wild-type human amyloid protein precursor transgenic mice: synaptotoxicity without plaque formation. J Neurosci 20:4050-4058.

Mungas D, Reed BR, Jagust WJ, DeCarli C, Mack WJ, Kramer JH, Weiner MW, Schuff N, Chui HC (2002) Volumetric MRI predicts rate of cognitive decline related to AD and cerebrovascular disease. Neurology 59:867-873.

Nelson PT, Wang WX (2010) MiR-107 is reduced in Alzheimer's disease brain neocortex: validation study. J Alzheimers Dis 21:75-79.

Ng TP, Niti M, Chiam PC, Kua EH (2007) Ethnic and educational differences in cognitive test performance on mini-mental state examination in Asians. Am J Geriatr Psychiatry 15:130-139.

Ngandu T, von Strauss E, Helkala EL, Winblad B, Nissinen A, Tuomilehto J, Soininen H, Kivipelto M (2007) Education and dementia: what lies behind the association? Neurology 69:1442-1450.

Nilsberth C, Westlind-Danielsson A, Eckman CB, Condron MM, Axelman K, Forsell C, Stenh C, Luthman J, Teplow DB, Younkin SG, Naslund J, Lannfelt L (2001) The 'Arctic' APP mutation (E693G) causes Alzheimer's disease by enhanced Abeta protofibril formation. Nat Neurosci 4:887-893.

Nilsen TW (2007) Mechanisms of microRNA-mediated gene regulation in animal cells. Trends Genet 23:243-249.

Niwa R, Zhou F, Li C, Slack FJ (2008) The expression of the Alzheimer's amyloid precursor protein-like gene is regulated by developmental timing microRNAs and their targets in Caenorhabditis elegans. Dev Biol 315:418-425.

Noland BW, Newman JM, Hendle J, Badger J, Christopher JA, Tresser J, Buchanan MD, Wright TA, Rutter ME, Sanderson WE, Muller-Dieckmann HJ, Gajiwala KS, Buchanan SG (2002) Structural studies of Salmonella typhimurium ArnB (PmrH) aminotransferase: a 4-amino-4-deoxy-L-arabinose lipopolysaccharide-modifying enzyme. Structure 10:1569-1580.

Nunez-Iglesias J, Liu CC, Morgan TE, Finch CE, Zhou XJ (2010) Joint genome-wide profiling of miRNA and mRNA expression in Alzheimer's disease cortex reveals altered miRNA regulation. PloS one 5:e8898.

Ohkura T, Isse K, Akazawa K, Hamamoto M, Yaoi Y, Hagino N (1994) Evaluation of estrogen treatment in female patients with dementia of the Alzheimer type. Endocr J 41:361-371.

Oksman M, Iivonen H, Hogyes E, Amtul Z, Penke B, Leenders I, Broersen L, Lutjohann D, Hartmann T, Tanila H (2006) Impact of different saturated fatty acid, polyunsaturated fatty acid and cholesterol containing diets on beta-amyloid accumulation in APP/PS1 transgenic mice. Neurobiol Dis 23:563-572.

Park SA A common pathogenic mechanism linking type-2 diabetes and Alzheimer's disease: evidence from animal models. J Clin Neurol 7:10-18.

Patil S, Melrose J, Chan C (2007) Involvement of astroglial ceramide in palmitic acid-induced Alzheimer-like changes in primary neurons. Eur J Neurosci 26:2131-2141.

Patwardhan MB, McCrory DC, Matchar DB, Samsa GP, Rutschmann OT (2004) Alzheimer disease: operating characteristics of PET--a meta-analysis. Radiology 231:73-80.

Pedrini S, Thomas C, Brautigam H, Schmeidler J, Ho L, Fraser P, Westaway D, Hyslop PS, Martins RN, Buxbaum JD, Pasinetti GM, Dickstein DL, Hof PR, Ehrlich ME, Gandy S (2009) Dietary composition modulates brain mass and solubilizable Abeta levels in a mouse model of aggressive Alzheimer's amyloid pathology. Mol Neurodegener 4:40.

Perry DK, Carton J, Shah AK, Meredith F, Uhlinger DJ, Hannun YA (2000) Serine palmitoyltransferase regulates de novo ceramide generation during etoposide-induced apoptosis. The Journal of biological chemistry 275:9078-9084.

Petersen RC, Thomas RG, Grundman M, Bennett D, Doody R, Ferris S, Galasko D, Jin S, Kaye J, Levey A, Pfeiffer E, Sano M, van Dyck CH, Thal LJ (2005) Vitamin E and donepezil for the treatment of mild cognitive impairment. N Engl J Med 352:2379-2388.

Pettegrew JW, Panchalingam K, Hamilton RL, McClure RJ (2001) Brain membrane phospholipid alterations in Alzheimer's disease. Neurochem Res 26:771-782.

Planel E, Tatebayashi Y, Miyasaka T, Liu L, Wang L, Herman M, Yu WH, Luchsinger JA, Wadzinski B, Duff KE, Takashima A (2007) Insulin dysfunction induces in vivo tau hyperphosphorylation through distinct mechanisms. J Neurosci 27:13635-13648.

Podlisny MB, Lee G, Selkoe DJ (1987) Gene dosage of the amyloid beta precursor protein in Alzheimer's disease. Science 238:669-671.

Pogribny IP, Starlard-Davenport A, Tryndyak VP, Han T, Ross SA, Rusyn I, Beland FA (2010) Difference in expression of hepatic microRNAs miR-29c, miR-34a, miR-155, and miR-200b is associated with strain-specific susceptibility to dietary nonalcoholic steatohepatitis in mice. Lab Invest 90:1437-1446.

Psaltopoulou T, Kyrozis A, Stathopoulos P, Trichopoulos D, Vassilopoulos D, Trichopoulou A (2008) Diet, physical activity and cognitive impairment among elders: the EPIC-Greece cohort (European Prospective Investigation into Cancer and Nutrition). Public Health Nutr 11:1054-1062.

Puglielli L, Ellis BC, Saunders AJ, Kovacs DM (2003) Ceramide stabilizes beta-site amyloid precursor protein-cleaving enzyme 1 and promotes amyloid beta-peptide biogenesis. The Journal of biological chemistry 278:19777-19783.

Qiagen (2011) Profiling miRNA in Serum and Plasma: Perils and Pitfalls on the Road to Biomarker Development. In.

Rademakers R et al. (2008) Common variation in the miR-659 binding-site of GRN is a major risk factor for TDP43-positive frontotemporal dementia. Hum Mol Genet 17:3631-3642.

Refolo LM, Malester B, LaFrancois J, Bryant-Thomas T, Wang R, Tint GS, Sambamurti K, Duff K, Pappolla MA (2000) Hypercholesterolemia accelerates the Alzheimer's amyloid pathology in a transgenic mouse model. Neurobiol Dis 7:321-331.

Resnick SM, Maki PM, Rapp SR, Espeland MA, Brunner R, Coker LH, Granek IA, Hogan P, Ockene JK, Shumaker SA (2006) Effects of combination estrogen plus progestin hormone treatment on cognition and affect. J Clin Endocrinol Metab 91:1802-1810.

Ripich DN, Petrill SA, Whitehouse PJ, Ziol EW (1995) Gender differences in language of AD patients: a longitudinal study. Neurology 45:299-302.

Roberts GW, Gentleman SM, Lynch A, Murray L, Landon M, Graham DI (1994) Beta amyloid protein deposition in the brain after severe head injury: implications for the pathogenesis of Alzheimer's disease. J Neurol Neurosurg Psychiatry 57:419-425.

Rocchi A, Pellegrini S, Siciliano G, Murri L (2003) Causative and susceptibility genes for Alzheimer's disease: a review. Brain research bulletin 61:1-24.

Rockenstein E, Crews L, Masliah E (2007) Transgenic animal models of neurodegenerative diseases and their application to treatment development. Advanced drug delivery reviews 59:1093-1102.

Rockenstein E, Mallory M, Mante M, Sisk A, Masliaha E (2001) Early formation of mature amyloid-beta protein deposits in a mutant APP transgenic model depends on levels of Abeta(1-42). J Neurosci Res 66:573-582.

Rockwood K, Fay S, Song X, MacKnight C, Gorman M (2006) Attainment of treatment goals by people with Alzheimer's disease receiving galantamine: a randomized controlled trial. CMAJ 174:1099-1105.

Roses AD (2010) An inherited variable poly-T repeat genotype in TOMM40 in Alzheimer disease. Arch Neurol 67:536-541.

Rotthier A, Baets J, De Vriendt E, Jacobs A, Auer-Grumbach M, Levy N, Bonello-Palot N, Kilic SS, Weis J, Nascimento A, Swinkels M, Kruyt MC, Jordanova A, De Jonghe P, Timmerman V (2009) Genes for hereditary sensory and autonomic neuropathies: a genotype-phenotype correlation. Brain 132:2699-2711.

Rotthier A, Auer-Grumbach M, Janssens K, Baets J, Penno A, Almeida-Souza L, Van Hoof K, Jacobs A, De Vriendt E, Schlotter-Weigel B, Loscher W, Vondracek P, Seeman P, De Jonghe P, Van Dijck P, Jordanova A, Hornemann T, Timmerman V (2010) Mutations in the SPTLC2 subunit of serine palmitoyltransferase cause hereditary sensory and autonomic neuropathy type I. Am J Hum Genet 87:513-522.

Rovelet-Lecrux A, Hannequin D, Raux G, Le Meur N, Laquerriere A, Vital A, Dumanchin C, Feuillette S, Brice A, Vercelletto M, Dubas F, Frebourg T, Campion D (2006) APP locus duplication causes autosomal dominant early-onset Alzheimer disease with cerebral amyloid angiopathy. Nat Genet 38:24-26.

Samaco RC, Nagarajan RP, Braunschweig D, LaSalle JM (2004) Multiple pathways regulate MeCP2 expression in normal brain development and exhibit defects in autism-spectrum disorders. Hum Mol Genet 13:629-639.

Samad F, Hester KD, Yang G, Hannun YA, Bielawski J (2006) Altered adipose and plasma sphingolipid metabolism in obesity: a potential mechanism for cardiovascular and metabolic risk. Diabetes 55:2579-2587.

Satoi H, Tomimoto H, Ohtani R, Kitano T, Kondo T, Watanabe M, Oka N, Akiguchi I, Furuya S, Hirabayashi Y, Okazaki T (2005) Astroglial expression of ceramide in Alzheimer's disease brains: a role during neuronal apoptosis. Neuroscience 130:657-666.

Sawamura N, Ko M, Yu W, Zou K, Hanada K, Suzuki T, Gong JS, Yanagisawa K, Michikawa M (2004) Modulation of amyloid precursor protein cleavage by cellular sphingolipids. The Journal of biological chemistry 279:11984-11991.

Scarlatti F, Sala G, Somenzi G, Signorelli P, Sacchi N, Ghidoni R (2003) Resveratrol induces growth inhibition and apoptosis in metastatic breast cancer cells via de novo ceramide signaling. FASEB J 17:2339-2341.

Schaefer A, O'Carroll D, Tan CL, Hillman D, Sugimori M, Llinas R, Greengard P (2007) Cerebellar neurodegeneration in the absence of microRNAs. J Exp Med 204:1553-1558.

Scheltens P, Fox N, Barkhof F, De Carli C (2002) Structural magnetic resonance imaging in the practical assessment of dementia: beyond exclusion. Lancet Neurol 1:13-21.

Schenk D et al. (1999) Immunization with amyloid-beta attenuates Alzheimer-disease-like pathology in the PDAPP mouse. Nature 400:173-177.

Schilling S, Zeitschel U, Hoffmann T, Heiser U, Francke M, Kehlen A, Holzer M, Hutter-Paier B, Prokesch M, Windisch M, Jagla W, Schlenzig D, Lindner C, Rudolph T, Reuter G, Cynis H, Montag D, Demuth HU, Rossner S (2008) Glutaminyl cyclase inhibition attenuates pyroglutamate Abeta and Alzheimer's disease-like pathology. Nature medicine 14:1106-1111.

Schipper HM, Maes OC, Chertkow HM, Wang E (2007) MicroRNA expression in Alzheimer blood mononuclear cells. Gene Regul Syst Bio 1:263-274.

Schmelz EM, Dombrink-Kurtzman MA, Roberts PC, Kozutsumi Y, Kawasaki T, Merrill AH, Jr. (1998) Induction of apoptosis by fumonisin B1 in HT29 cells is mediated by the accumulation of endogenous free sphingoid bases. Toxicol Appl Pharmacol 148:252-260.

Schonrock N, Ke YD, Humphreys D, Staufenbiel M, Ittner LM, Preiss T, Gotz J (2010) Neuronal microRNA deregulation in response to Alzheimer's disease amyloid-beta. PloS one 5:e11070.

Schratt GM, Tuebing F, Nigh EA, Kane CG, Sabatini ME, Kiebler M, Greenberg ME (2006) A brain-specific microRNA regulates dendritic spine development. Nature 439:283-289.

Schupf N, Tang MX, Fukuyama H, Manly J, Andrews H, Mehta P, Ravetch J, Mayeux R (2008) Peripheral Abeta subspecies as risk biomarkers of Alzheimer's disease. Proceedings of the National Academy of Sciences of the United States of America 105:14052-14057.

Selbach M, Schwanhausser B, Thierfelder N, Fang Z, Khanin R, Rajewsky N (2008) Widespread changes in protein synthesis induced by microRNAs. Nature 455:58-63.

Sempere LF, Freemantle S, Pitha-Rowe I, Moss E, Dmitrovsky E, Ambros V (2004) Expression profiling of mammalian microRNAs uncovers a subset of brain-expressed microRNAs with possible roles in murine and human neuronal differentiation. Genome biology 5:R13.

Seshadri S et al. Genome-wide analysis of genetic loci associated with Alzheimer disease. JAMA 303:1832-1840.

Sethupathy P, Collins FS (2008) MicroRNA target site polymorphisms and human disease. Trends Genet 24:489-497.

Shah C, Yang G, Lee I, Bielawski J, Hannun YA, Samad F (2008) Protection from high fat diet-induced increase in ceramide in mice lacking plasminogen activator inhibitor 1. The Journal of biological chemistry 283:13538-13548.

Sheehan DCaH, B. B., ed (1980) Theory and practice of histotechnology, 2nd Edition: Battelle press.

Shioya M, Obayashi S, Tabunoki H, Arima K, Saito Y, Ishida T, Satoh J (2010) Aberrant microRNA expression in the brains of neurodegenerative diseases: miR-29a decreased in Alzheimer disease brains targets neurone navigator 3. Neuropathol Appl Neurobiol 36:320-330.

Sisodia SS (1992) Beta-amyloid precursor protein cleavage by a membrane-bound protease. Proceedings of the National Academy of Sciences of the United States of America 89:6075-6079.

Sjogren M, Davidsson P, Wallin A, Granerus AK, Grundstrom E, Askmark H, Vanmechelen E, Blennow K (2002) Decreased CSF-beta-amyloid 42 in Alzheimer's disease and amyotrophic lateral sclerosis may reflect mismetabolism of beta-amyloid induced by disparate mechanisms. Dement Geriatr Cogn Disord 13:112-118.

Slevin M, Krupinski J (2009) A role for monomeric C-reactive protein in regulation of angiogenesis, endothelial cell inflammation and thrombus formation in cardiovascular/cerebrovascular disease? Histol Histopathol 24:1473-1478.

Solfrizzi V, Panza F, Frisardi V, Seripa D, Logroscino G, Imbimbo BP, Pilotto A (2011) Diet and Alzheimer's disease risk factors or prevention: the current evidence. Expert Rev Neurother 11:677-708.

Solfrizzi V, Capurso C, D'Introno A, Colacicco AM, Santamato A, Ranieri M, Fiore P, Capurso A, Panza F (2008) Lifestyle-related factors in predementia and dementia syndromes. Expert Rev Neurother 8:133-158.

Sparks DL, Kuo YM, Roher A, Martin T, Lukas RJ (2000) Alterations of Alzheimer's disease in the cholesterol-fed rabbit, including vascular inflammation. Preliminary observations. Annals of the New York Academy of Sciences 903:335-344.

Stephan A, Phillips AG (2005) A case for a non-transgenic animal model of Alzheimer's disease. Genes, brain, and behavior 4:157-172.

Strettoi E, Gargini C, Novelli E, Sala G, Piano I, Gasco P, Ghidoni R (2010) Inhibition of ceramide biosynthesis preserves photoreceptor structure and function in a mouse model of retinitis pigmentosa. Proceedings of the National Academy of Sciences of the United States of America 107:18706-18711.

Sulkava R (1998) [Anti-inflammatory drug therapy for prevention of Alzheimer's Disease?]. Duodecim; laaketieteellinen aikakauskirja 114:2025, 2027.

Sundaram KS, Lev M (1984a) L-cycloserine inhibition of sphingolipid synthesis in the anaerobic bacterium Bacteroides levii. Biochem Biophys Res Commun 119:814-819.

Sundaram KS, Lev M (1984b) Inhibition of sphingolipid synthesis by cycloserine in vitro and in vivo. J Neurochem 42:577-581.

Sundaram KS, Lev M (1985) Inhibition of cerebroside synthesis in the brains of mice treated with L-cycloserine. J Lipid Res 26:473-477.

Sundaram KS, Lev M (1989) The long-term administration of L-cycloserine to mice: specific reduction of cerebroside level. Neurochem Res 14:245-248.

Suzuki N, Cheung TT, Cai XD, Odaka A, Otvos L, Jr., Eckman C, Golde TE, Younkin SG (1994) An increased percentage of long amyloid beta protein secreted by familial amyloid beta protein precursor (beta APP717) mutants. Science 264:1336-1340.

Szulwach KE, Li X, Smrt RD, Li Y, Luo Y, Lin L, Santistevan NJ, Li W, Zhao X, Jin P (2010) Cross talk between microRNA and epigenetic regulation in adult neurogenesis. J Cell Biol 189:127-141.

Takeda S, Sato N, Uchio-Yamada K, Sawada K, Kunieda T, Takeuchi D, Kurinami H, Shinohara M, Rakugi H, Morishita R (2010) Diabetes-accelerated memory dysfunction via cerebrovascular inflammation and Abeta deposition in an Alzheimer mouse model with

diabetes. Proceedings of the National Academy of Sciences of the United States of America 107:7036-7041.

Tao J, Wu H, Lin Q, Wei W, Lu XH, Cantle JP, Ao Y, Olsen RW, Yang XW, Mody I, Sofroniew MV, Sun YE (2011) Deletion of astroglial Dicer causes non-cell-autonomous neuronal dysfunction and degeneration. J Neurosci 31:8306-8319.

Theuns J, Brouwers N, Engelborghs S, Sleegers K, Bogaerts V, Corsmit E, De Pooter T, van Duijn CM, De Deyn PP, Van Broeckhoven C (2006) Promoter mutations that increase amyloid precursor-protein expression are associated with Alzheimer disease. Am J Hum Genet 78:936-946.

Tran HT, LaFerla FM, Holtzman DM, Brody DL (2011) Controlled cortical impact traumatic brain injury in 3xTg-AD mice causes acute intra-axonal amyloid-beta accumulation and independently accelerates the development of tau abnormalities. J Neurosci 31:9513-9525.

Tremblay F, Lavigne C, Jacques H, Marette A (2001) Defective insulin-induced GLUT4 translocation in skeletal muscle of high fat-fed rats is associated with alterations in both Akt/protein kinase B and atypical protein kinase C (zeta/lambda) activities. Diabetes 50:1901-1910.

Turchinovich A, Weiz L, Langheinz A, Burwinkel B (2011) Characterization of extracellular circulating microRNA. Nucleic Acids Res 39:7223-7233.

Turinsky J, Bayly BP, O'Sullivan DM (1990) 1,2-Diacylglycerol and ceramide levels in rat skeletal muscle and liver in vivo. Studies with insulin, exercise, muscle denervation, and vasopressin. The Journal of biological chemistry 265:7933-7938.

Unger RH, Orci L (2001) Diseases of liporegulation: new perspective on obesity and related disorders. FASEB J 15:312-321.

Valsecchi M, Mauri L, Casellato R, Prioni S, Loberto N, Prinetti A, Chigorno V, Sonnino S (2007) Ceramide and sphingomyelin species of fibroblasts and neurons in culture. J Lipid Res 48:417-424.

Van der Auwera I, Wera S, Van Leuven F, Henderson ST (2005) A ketogenic diet reduces amyloid beta 40 and 42 in a mouse model of Alzheimer's disease. Nutrition & metabolism 2:28.

van Oijen M, Hofman A, Soares HD, Koudstaal PJ, Breteler MM (2006) Plasma Abeta(1-40) and Abeta(1-42) and the risk of dementia: a prospective case-cohort study. Lancet Neurol 5:655-660.

Vetrivel KS, Cheng H, Kim SH, Chen Y, Barnes NY, Parent AT, Sisodia SS, Thinakaran G (2005) Spatial segregation of gamma-secretase and substrates in distinct membrane domains. The Journal of biological chemistry 280:25892-25900.

Vetrivel KS, Cheng H, Lin W, Sakurai T, Li T, Nukina N, Wong PC, Xu H, Thinakaran G (2004) Association of gamma-secretase with lipid rafts in post-Golgi and endosome membranes. The Journal of biological chemistry 279:44945-44954.

Vickers KC, Palmisano BT, Shoucri BM, Shamburek RD, Remaley AT (2011) MicroRNAs are transported in plasma and delivered to recipient cells by high-density lipoproteins. Nat Cell Biol 13:423-433.

Wada S, Morishima-Kawashima M, Qi Y, Misono H, Shimada Y, Ohno-Iwashita Y, Ihara Y (2003) Gamma-secretase activity is present in rafts but is not cholesterol-dependent. Biochemistry 42:13977-13986.

Wagner JA (2008) Strategic approach to fit-for-purpose biomarkers in drug development. Annu Rev Pharmacol Toxicol 48:631-651.

Wahlund LO, Julin P, Johansson SE, Scheltens P (2000) Visual rating and volumetry of the medial temporal lobe on magnetic resonance imaging in dementia: a comparative study. J Neurol Neurosurg Psychiatry 69:630-635.

Wahrle S, Das P, Nyborg AC, McLendon C, Shoji M, Kawarabayashi T, Younkin LH, Younkin SG, Golde TE (2002) Cholesterol-dependent gamma-secretase activity in buoyant cholesterol-rich membrane microdomains. Neurobiol Dis 9:11-23.

Waldemar G, Dubois B, Emre M, Georges J, McKeith IG, Rossor M, Scheltens P, Tariska P, Winblad B (2007) Recommendations for the diagnosis and management of Alzheimer's disease and other disorders associated with dementia: EFNS guideline. Eur J Neurol 14:e1-26.

Waldemar G, Gauthier S, Jones R, Wilkinson D, Cummings J, Lopez O, Zhang R, Xu Y, Sun Y, Knox S, Richardson S, Mackell J (2011) Effect of donepezil on emergence of apathy in mild to moderate Alzheimer's disease. Int J Geriatr Psychiatry 26:150-157.

Wang G, Dinkins M, He Q, Zhu G, Poirier C, Campbell A, Mayer-Proschel M, Bieberich E (2012) Astrocytes Secrete Exosomes Enriched with Proapoptotic Ceramide and Prostate Apoptosis Response 4 (PAR-4): POTENTIAL MECHANISM OF APOPTOSIS INDUCTION IN ALZHEIMER DISEASE (AD). The Journal of biological chemistry 287:21384-21395.

Wang GK, Zhu JQ, Zhang JT, Li Q, Li Y, He J, Qin YW, Jing Q (2010a) Circulating microRNA: a novel potential biomarker for early diagnosis of acute myocardial infarction in humans. Eur Heart J 31:659-666.

Wang K, Long B, Zhou J, Li PF (2010b) miR-9 and NFATc3 regulate myocardin in cardiac hypertrophy. The Journal of biological chemistry 285:11903-11912.

Wang PN, Liao SQ, Liu RS, Liu CY, Chao HT, Lu SR, Yu HY, Wang SJ, Liu HC (2000) Effects of estrogen on cognition, mood, and cerebral blood flow in AD: a controlled study. Neurology 54:2061-2066.

Wang WX, Rajeev BW, Stromberg AJ, Ren N, Tang G, Huang Q, Rigoutsos I, Nelson PT (2008) The expression of microRNA miR-107 decreases early in Alzheimer's disease and may accelerate disease progression through regulation of beta-site amyloid precursor protein-cleaving enzyme 1. J Neurosci 28:1213-1223.

Weinmann S, Roll S, Schwarzbach C, Vauth C, Willich SN (2010) Effects of Ginkgo biloba in dementia: systematic review and meta-analysis. BMC Geriatr 10:14.

Weintraub D, Rosenberg PB, Drye LT, Martin BK, Frangakis C, Mintzer JE, Porsteinsson AP, Schneider LS, Rabins PV, Munro CA, Meinert CL, Lyketsos CG (2010) Sertraline for the treatment of depression in Alzheimer disease: week-24 outcomes. Am J Geriatr Psychiatry 18:332-340.

Weiss B, Stoffel W (1997) Human and murine serine-palmitoyl-CoA transferase--cloning, expression and characterization of the key enzyme in sphingolipid synthesis. Eur J Biochem 249:239-247.

Wen Y, Yang S, Liu R, Perez E, Yi KD, Koulen P, Simpkins JW (2004) Estrogen attenuates nuclear factor-kappa B activation induced by transient cerebral ischemia. Brain Res 1008:147-154.

Wiggins JF, Ruffino L, Kelnar K, Omotola M, Patrawala L, Brown D, Bader AG (2010) Development of a lung cancer therapeutic based on the tumor suppressor microRNA-34. Cancer Res 70:5923-5930.

Williams RD, Sgoutas DS, Zaatari GS, Santoianni RA (1987) Inhibition of serine palmitoyltransferase activity in rabbit aorta by L-cycloserine. J Lipid Res 28:1478-1481.

Wolf OT, Kudielka BM, Hellhammer DH, Torber S, McEwen BS, Kirschbaum C (1999) Two weeks of transdermal estradiol treatment in postmenopausal elderly women and its effect on memory and mood: verbal memory changes are associated with the treatment induced estradiol levels. Psychoneuroendocrinology 24:727-741.

Won JS, Im YB, Khan M, Contreras M, Singh AK, Singh I (2008) Lovastatin inhibits amyloid precursor protein (APP) beta-cleavage through reduction of APP distribution in Lubrol WX extractable low density lipid rafts. J Neurochem 105:1536-1549.

Wu D, Hu T, Zhang L, Chen J, Du J, Ding J, Jiang H, Shen X (2008) Residues Asp164 and Glu165 at the substrate entryway function potently in substrate orientation of alanine racemase from E. coli: Enzymatic characterization with crystal structure analysis. Protein Sci 17:1066-1076.

Yasuda S, Nishijima M, Hanada K (2003) Localization, topology, and function of the LCB1 subunit of serine palmitoyltransferase in mammalian cells. The Journal of biological chemistry 278:4176-4183.

Yoshizawa T, Yamashita A, Luo Y (1994) Fumonisin occurrence in corn from high- and low-risk areas for human esophageal cancer in China. Appl Environ Microbiol 60:1626-1629.

Zahs KR, Ashe KH (2010) 'Too much good news' - are Alzheimer mouse models trying to tell us how to prevent, not cure, Alzheimer's disease? Trends Neurosci 33:381-389.

Zendzian-Piotrowska M, Baranowski M, Zabielski P, Gorski J (2006) Effects of pioglitazone and high-fat diet on ceramide metabolism in rat skeletal muscles. J Physiol Pharmacol 57 Suppl 10:101-114.

Zeng L, Liu J, Wang Y, Wang L, Weng S, Tang Y, Zheng C, Cheng Q, Chen S, Yang GY (2011) MicroRNA-210 as a novel blood biomarker in acute cerebral ischemia. Front Biosci (Elite Ed) 3:1265-1272.

Zha Q, Ruan Y, Hartmann T, Beyreuther K, Zhang D (2004) GM1 ganglioside regulates the proteolysis of amyloid precursor protein. Mol Psychiatry 9:946-952.

Zhang J, Zhang F, Didelot X, Bruce KD, Cagampang FR, Vatish M, Hanson M, Lehnert H, Ceriello A, Byrne CD (2009) Maternal high fat diet during pregnancy and lactation alters hepatic expression of insulin like growth factor-2 and key microRNAs in the adult offspring. BMC Genomics 10:478.

Zhang X, Dong F, Ren J, Driscoll MJ, Culver B (2005) High dietary fat induces NADPH oxidase-associated oxidative stress and inflammation in rat cerebral cortex. Exp Neurol 191:318-325.

Zhu CW, Sano M (2006) Economic considerations in the management of Alzheimer's disease. Clin Interv Aging 1:143-154.